THE INTERNATIONAL HYDROGRAPHIC REVIEW

INTERNATIONAL HYDROGRAPHIC BUREAU
MONACO

No. 4

November 2010

Page intentionally left blank

Contents

Editorial

Articles

Notes

Page intentionally left blank

Editorial

The time has come for me to pass the task of Editor on and the IHO has decided that Ian Halls from Australia, will take on the work. Knowing him from long ago days of ECDIS developments I am sure that you are in good hands. I want to take this opportunity to thank the Members of the Editorial board, particularly those who have been with us for a long time, both when the Review was published by GITC and in the last two years when it has again been published by the IHB. The job of finding good reviewers is not easy but good reviews contribute substantially to the quality of a publication. Others have also kept this publication going to reflect the progress of hydrography. There can be no doubt in my mind that hydrography as a profession needs a scholarly record of its progress both to bring attention to a relatively narrow discipline and to provide an historical record.

During the last year I should once again like to thank The Hydrographic Society of America for its strong support in helping me as the editor find interesting material. The papers in this issue reflect the continuing strong interest of developing the technology of multibeam echo sounders and LIDAR. Hydrographic surveying has been revolutionized by this technology and the papers in this issue discuss a number of approaches to evaluate its quality, make use of the irregular density structure of the sea and other technology in order that the measurements truly reflect the true shape of the sea floor. It is appropriate that we include in this issue a historic paper on the contributions of the British Admiralty Hydrographers, who over many years added so much to our knowledge of the oceans. It is also something of a coincidence that there should be a paper noting how differences between this historical hydrography and hydrography measured by modern means can be used to assist in understanding environmental processes. This use of hydrography for a much wider use than straightforward navigation is being increasingly realised by Hydrographic Offices. I can only encourage the incoming editor to continue to monitor the new and exciting developments of our profession and see that world at large knows of the very existence of hydrography.

Adam J. Kerr
Editor

Page intentionally left blank

Article

FOUNDATIONS FOR "INTERNATIONAL COOPERATION IN THE FIELD OF HYDROGRAPHY": SOME CONTRIBUTIONS BY BRITISH ADMIRALTY HYDROGRAPHERS, 1795-1855

By Adrian Webb[1]

Abstract

Great Britain established its Hydrographic Office in 1795 with a remit to produce charts for the use of its Navy. As time progressed and Hydrographers to the Admiralty Board changed so did the remit of the Hydrographic Office. As a facet of the steady development of Office activities there was an underlying theme of international cooperation, which resulted in British Hydrographers entering into correspondence and agreements with their international counterparts. Some of those activities are examined in this paper to hopefully redefine the International Hydrographic Bureau's statement that 'International cooperation in the field of hydrography began with a Conference held in Washington in 1899[2].

Résumé

La Grande-Bretagne a établi son Service hydrographique en 1795 avec pour mission de produire des cartes devant être utilisées par sa Marine. Par la suite, cette mission se modifia à mesure que les hydrographes du Conseil de l'Amirauté se renouvelèrent. L'une des facettes du développement régulier des activités du Service hydrographique fut le thème fondamental de la coopération internationale qui incita les hydrographes britanniques à entrer en correspondance et à passer des accords avec leurs homologues internationaux. Quelques unes de ces activités sont passées en revue dans l'article qui suit, avec pour dessein de redéfinir la déclaration du Bureau hydrographique international d'après laquelle la coopération internationale dans le domaine de l'hydrographie a commencé lors de la conférence tenue à Washington, en 1899[2].

Resumen

Gran Bretaña fundó su Servicio Hidrográfico en 1795 con un mandato para producir cartas para su uso por la Marina. El tiempo ha pasado y del mismo modo que los Hidrógrafos del Consejo del Almirantazgo han cambiado, así ha sucedido con el mandato del Servicio Hidrográfico. Como faceta del desarrollo estable de las actividades del Servicio había un tema fundamental de cooperación internacional, cuyo resultado fue que los Hidrógrafos Británicos iniciaron un intercambio de correspondencia y acuerdos con sus homólogos internacionales. En este artículo se examinan algunas de esas actividades, esperando definir de nuevo la declaración del Bureau Hidrográfico Internacional según la cual 'la cooperación internacional en el campo de la hidrografía empezó con una Conferencia celebrada en Washington en 1899[2].

Alexander Dalrymple F.R.S. (1737-1808)

Alexander Dalrymple

Britain was already behind the times, in international terms, when it decided to establish a government hydrographic office, as both France and Denmark had already done so in 1720 and 1785 respectively. Sitting alongside those two government offices were similar institutions established by the mighty trading companies, such as that of the Honourable East India Company (H.E.I.C.) whose own Hydrographer was also appointed to the newly formed post of Hydrographer to the British Admiralty in 1795. Britain was exceptionally fortunate in appointing Dalrymple for three particular reasons. First, as he was not a naval officer and a military figure he did not come with the limitations of such trappings when dealing with foreign institutions. Secondly, he was already very well connected in the world of charting, science and exploration, having been elected as a Fellow of the Royal Society of London; he was also the Society's candidate to lead an expedition to record a transit of Venus in 1768, although he did not go and Lieutenant (later Captain) James Cook R.N. did. As well as being a close friend of Sir Joseph Banks he was supported in his election to a fellowship by Benjamin Franklin, natural philosopher, writer, and revolutionary politician in America, and Nevil Maskelyne, astronomer and mathematician. Thirdly, he had corresponded with French hydrographers Jean Baptiste Nicolas Denis d'Après de Mannevillette through the 1770s and Charles Pierre Claret (later comte de Fleurieu), as well as employing Elisabeth-Paul Edouard, chevalier de Rossel (who later become French Hydrographer).[3]

Dalrymple epitomised the fundamental strands of international co-operation, those of science, cordial international relations and a desire to put hydrography before military gains. He even proposed to the Admiralty Board in 1807 how British 'Ministers and Consuls in Foreign parts' could be used to obtain foreign charts and subsequently improve international relations.[4] However, many factors worked against expanding Dalrymple's collaborative endeavours, the main one being the state of conflict between the major European powers.

Matters came to a head for Dalrymple when he put his international values up against those of the British Admiralty, forcing his employers to pension him off. Thankfully all his good work was not undone, as the benefits from international collaboration became more deeply ensconced within the mind sets of hydrographers, not only in France and Britain but in other nations over succeeding decades.

Captain Hurd R.N. (*c*.1747-1823)

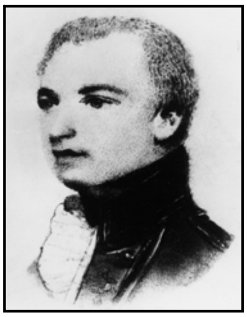

Thomas Hurd

After Dalrymple's departure from the Hydrographic Office in 1808, the Admiralty appointed Thomas Hurd, an experienced hydrographic surveyor and captain in the Royal Navy as Hydrographer. The shift from a civilian to a naval appointment, coupled with the fact that Britain was at war with France and Hurd was not a Fellow of the Royal Society (unlike Dalrymple), could have been a disaster for international relations. However, the ethos of co-operation may have been curtailed but it was certainly not gone. Hurd was very interested in science and was on very good terms with Sir Joseph Banks, and could count amongst his fellow hydrographic specialists many men who were much more scientifically orientated. Men like Captain Matthew Flinders, Captain Francis Beaufort and Captain John Franklin, had all proved their worth by the time Hurd was in post. All three men collaborated internationally despite negative experiences with foreign powers; Flinders had been incarcerated by the French for years, Beaufort nearly killed in the Mediterranean and Franklin served at the Battle of Copenhagen when only 14 years old.[5] Despite all of this potential animosity, when the American 'Hydrographer' found himself in England at the time the war of 1812 was declared, far from being treated harshly as a foreign national, he was granted a passport with the caveat that 'the British government makes no wars on science'.[6] After the peace of 1815 the situation was very different and it was in everyone's interests to co-operate.

With relationships with France restored and Dalrymple's openness to cooperation with Rossel bearing fruit as the latter was now French Hydrographer, it was only natural Britain should look elsewhere to strengthen its position in international hydrographic affairs. Subsequently it fell to Hurd to make an approach to Spain. Thus in 1817 he sent a collection of 42 Admiralty charts to the Depósito Hidrografico[7] in an attempt to open up a reciprocal arrangement for the mutual supply of charts. He did not stop with contacting just Spain, as two years later he opened up communications with the second oldest government hydrographic office, which belonged to Denmark.[8] Fortunately for Hurd the Danish Hydrographic Office, or what was properly known as the Royal Danish Sea Chart Office, was in the capable hands of Rear Admiral Poul Löwenörn. Löwenörn was also someone with international experience as he had served in the French Navy from 1776 to 1782 and was inspired by the organisation of the French Dépôt to establish a similar one in his own country.[9] He was a man with all the right hydrographic experience in both science and navigation, being responsible for erecting numerous lighthouses on the Danish coast, backing a proposal for a portable log watch and involved with the Royal Society of Sciences at Copenhagen, amongst other things. [10]

Towards the end of 1819 Hurd managed, through assistance from the British Ambassador at the Court of Denmark, to open up communications with the Danish royal family.[11] His thinking behind this can be seen in his obtaining from the Admiralty Board permission for a mutual exchange of sea charts and 'useful maritime knowledge'. He wrote to Löwenörn stating: Ever since the year 1808, in which I succeeded the late Mr. Dalrymple in this office, my increasing endeavours have been exerted to accomplish so desirable and liberal an object as an interchange of Hydrographical charts and knowledge with all the maritime nations in Europe – and I cannot but offer you my very sincere congratulations on the success attendant on our joint efforts towards the producing this effect between Denmark and Great Britain.[12]

Why Hurd left it until 1819 was most likely due to the pressure of war upon his office, preparations for the Arctic voyages and the opportunity of peace that had only materialised during the previous few years. Hurd certainly needed Danish charts of the Baltic, but the hatred many Danes had for the British after Copenhagen meant they were closer to the Russians, making a contact in 1819 between the two Hydrographers a landmark event.[13] Nevertheless an important ally and source of maritime information was quickly established. To seal what was most likely Hurd's first (and possibly only) bilateral arrangement he sent Löwenörn a copy of every chart he had published, as well as pointing out the shortcomings of many other charts published outside the Admiralty in England. Subsequently two packages of charts arrived at the Admiralty from Copenhagen in 1820 and another in June the following year.[14] Another consignment of charts (under Hurd's mutual exchange system) was sent to the Danish court in 1822,[15] but after his death in April 1823 the arrangement temporarily stagnated.

At sea, one officer, Commander William Henry Smyth R.N., epitomised the spirit of international collaboration and science through hydrography. After peace was declared in Europe in 1815 he found himself in the Mediterranean having to survey areas of interest to numerous European nations with a hydrographic capability, without the shackles of conflict. Whilst Smyth was on Malta in 1816 he found Captain Gauttier, a French naval officer, had arrived on the island with the intention to measure meridian distances. Smyth offered Captain Gauttier every assistance and even showed him the spot he had used to obtain his own observations, hoping the Frenchmen would use the same place so their data could be compared. Their collaboration in the field was a seminal moment in the history of relationships between the two countries surveying officers, as the two men went on to meet up in the following years exchanging and comparing further information. Great faith was placed in Smyth by the Admiralty as he was sent to Paris to sort out further survey planning arrangements between the two nations, when the French agreed to concentrate on the Greek Archipelago leaving Smyth to work in the western Mediterranean and the north coast of Africa.[16] Smyth also went to Naples in 1818 to undertake negotiations with the Austrian and Neapolitan governments for a joint survey of the Adriatic. Consequently four Austrian surveyors were attached to Smyth's survey vessel, *Aid*, and the Austrian sloop *Velox* was put under his direct command.[17] Further international relations were fostered by Smyth, when he became great friends with Baron von Zach (1754-1832) the German astronomer and Colonel Visconti, Director of the Officio Topografico of Naples. To add to his list of international contacts he could also count Marshall Koller (an Austrian general and diplomat), Count Nugent (Commander-in-Chief of the Bourbon army) and Baron Poiter (of the Austrian staff).[18]

Outside of formal channels between hydrographic offices there was a great reliance on a small group of countries to undertake hydrographic surveys in waters of countries who lacked such a function. Britain, France, Spain, Denmark and Russia had all established themselves as capable of undertaking such surveys, even though the territorial waters they surveyed in were owned, in some cases, by countries whom possessed their own naval vessels. .

For example, the British had sent two survey vessels in 1821, the *Leven* and *Barracouta*, to survey the coast from the Cape of Good Hope to Cape Gardafui. The commanding officer, W.F.W. Owen, had been involved in anti-slaving operations as well as numerous international incidents. He took the decision to annexe Portuguese territories around Delagoa Bay and parts of the northern coast of east Africa, as well as purchasing Clarence Town (on Fernando Po) apparently overlooking Spanish interests in the area, which caused some consternation back in England as well as in Spain. Also, at the port of Mombasa, to ensure its management under British rule, he installed one of his own officers as governor.[19] Owen's work extended into east Africa, but it was not all controversy, as relationships were strengthened between the Sultan of Oman and Britain when the two men met at Muscat. Owen was belligerent towards the slavers but established good relations with the native population, even though the diplomatic fall-out caused some embarrassment to the British Government.[20]

Captain William Edward Parry R.N. (1790-1855)

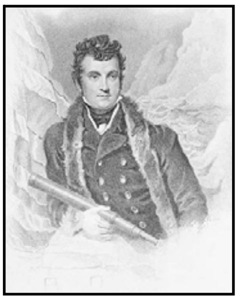

William Edward Parry

After Hurd's death in April 1823 there was a hiatus as his successor, the noted Arctic explorer, Captain Parry, was not appointed until the end of the year. Parry like Dalrymple was a man of science, who (additionally) had exhibited great leadership skills during his first command to the Arctic. However, he appears not to have been fully aware of the arrangement Hurd had set up with Löwenörn, as in 1825 it appeared nothing had been sent to Copenhagen since 1822.[21] Parry soon put matters straight and the charts were eagerly expected at the Royal Danish Sea Chart Archives.[22] Unfortunately by the time they arrived, two and a half months later, Löwenörn had passed away and his temporary replacement, Commodore Fabricius, wrote to Parry stating:

It is not without the most sensible regret, that at the same time I have to mention the decease of our highly deserving and respectable Admiral Löwenörn, who departed this life the 16th of March. I have nothing to add to the kind praises, where with you have been pleased to speak of a man whose death may be said to be a loss not only to his family and friends, but to the whole country whose ornament he was.[23]

Fabricius was also very conducive towards the reciprocal arrangement entered into by his predecessor and the charts the Admiralty received from the Danes Parry found especially worthy of further supply to the British navy. [24]

Parry, like Hurd, found himself administering British surveys in foreign waters, such as those off north Africa (an area of former Anglo-French rivalry)[25] where Smyth continued to expand his contacts and, as a result of co-operation with France, was able to concentrate on further surveys. By 1824 Smyth had orchestrated surveys from Tripoli (modern Tarabulus) across to Alexandria (modern Al Iskandariyah), whilst Lieutenant F.W. Beechey R.N. and his brother (dressed in Arab clothing) sketched the coastline from Tripoli to Derna. Lieutenant Boteler's survey of Morocco, which received one of the most detailed set of geographical instructions from Parry [26], saw him in 1829 in a difficult position when the local authority, the Emperor of Morocco, did not grant him permission to survey his waters. That decision was due to the position of the European powers as a whole rather than any action Boteler had taken. At the same time Smyth was at work, the French were undertaking clandestine surveys of the north African and eastern Mediterranean coasts. [27]

When it came to science during the 1820s the position the Admiralty Board took can be seen in the instructions given to one surveyor for his voyage to the Pacific, as he was: not on any account to commit any hostile act whatsoever; the vessel you command being sent out only for the purpose of discovery and science, and it being the practice of all civilised nations to consider vessels so employed as excluded from the operations of war: and, confiding in this general feeling, we should trust that you would receive every assistance from the ships or subjects of any foreign power you may fall in with.[28]

Such then were the terms of engagement between most advanced maritime nations when it came to hydrography, whereby safety and science were often put before war, on more occasions than not, with Flinders being unfortunate to have been incarcerated whilst undertaking such duties. Fortunately for Parry, science and such an enlightened attitude by the British government to hydrography paved the way for more international cooperation.

Parry was fortunate when it came to establishing relations with Spain, as on his return from his third Arctic voyage in 1825, he met with the exiled Spanish Hydrographer Felipe Bauzá y Cañas in London.

As the two men shared similar interests in surveying, science and astronomy they became good friends and through Bauzá a line of communication was opened up with the Madrid Office. Parry was able to inform the Admiralty Board how Bauzá had 'given us several, and but (for copying) a great number of the best Spanish surveys, and has been very attentive and obliging in immediately communicating any recent information of this nature'. [29] It was not just a one way exchange as Parry gave Bauzá a set of the latest Admiralty charts in return for his benevolent act. Bauzá also arranged for a large number of charts to be sent to His Royal Highness the Duke of Clarence[30] during his term as Lord High Admiral, thus making every effort to put in place the firm foundations of formal international relations. Bauzá was also invited to attend the annual visit to the Greenwich Observatory as a member of the examining board, where he met Sir John Herschel,[31] which subsequently led to the Spanish astronomer, Sánchez Cerquero, visiting both Greenwich and the home of Captain Smyth.[32] This led to an association with the Royal Society, which resulted in contact with one of, if not the most, prominent men of science (internationally speaking), Baron Alexander von Humboldt. It was through Humboldt that Bauzá subsequently met Jabbo Oltmanns, the astronomer who worked for Humboldt in Paris and Baron Franz Xaver von Zach at the Seeberg Observatory.[33] This was a classic example of international collaboration through science facilitated by hydrography.

If Parry thought he was fortunate in fostering beneficial links with Spain, then how he must of felt when an opportunity came along to collaborate with France it can only be speculated. Such an opportunity occurred through the preparations Parry made for Commander Foster's voyage in H.M.S. *Chanticleer*,[34] which undertook a cruise around the Atlantic. The enthusiasm for joint cooperation was shared with his French counterpart, as when Parry asked Rossel for any longitudinal observations that he held in his office, he replied: It is with eagerness that I send you the information that you have requested concerning the geographical determinations which result from the astronomical observations made in various parts of the globe by the French Naval Officers. [36]

The two men exchanged letters and a great deal of information in the spirit of *entente cordiale*. This was all despite differences in some of the geographical positions the two men had exchanged, which Rossel determined were only negligible and the product of better chronometrical readings.[37]

Parry used Rossel's information to institutionalise international co-operation when he placed them before the Council of the Duke of Clarence, Lord High Admiral. In response to the generosity of the French the Council ordered a complete copy of the survey of the coasts of Africa and Madagascar, containing two atlases, to be sent to France. Parry subsequently wrote to Rossel stating: how much satisfaction it will afford me to maintain between our respective Departments a constant communication, which cannot fail to be equally beneficial to both, which it tends to the promotion and improvement of that department of science to which we more particularly belong.[38]

Rossel was delighted with this news and in his letter of reply explained the terms under which he was instructed in his duties:

I am very flattered, Sir, that the communications maintained by the two establishments that we run have the suffrage of an authority so respectable. Myself, I only execute the kind intentions of His Majesty the King of France whose care extends not only to his subjects but to the sailors and navigators of all nations.[39]

This clearly showed how the French, like the British, were operating a like-minded policy of supporting navigational science and safety of life at sea, no matter what nationality was involved. This was an important era in Franco-British relationships, which secured a much closer working relationship than had ever been enjoyed before in the nineteenth century, but Parry did not stop there.

With Spanish and French cooperation secured, Parry turned his attention to the remaining hydrographic nations. His underlying agenda was to try to improve the supply of foreign government charts to the Admiralty, as during the 1820s there was a 'limited and irregular' supply of charts from other governments. This was much to the embarrassment of the Hydrographic Office because the London chart sellers had better supply arrangements than the Admiralty. Therefore Parry proposed a complete exchange of all those published by each department during the last (seven?) years; and, at the same time come to some decided and explicit understanding, as to a similar exchange being made in future, at regular stated intervals, (say at the end of every half year).[40]

His scheme was limited to the major players in the world of government hydrography, only including the French, Spanish, Russian, Danish, Swedish and Neapolitan nations. He even included with his proposals a pro-forma letter when he sent this to the Admiralty Board on 18 January 1828, in which he further suggested that exchanges should be made every six months. He did not stipulate that it should only be new or amended publications that should be exchanged, rather than a complete package of everything, once every six months.[41]

However, Parry's proposal was not taken up and he suggested to John Wilson Croker, First Secretary of the Admiralty, that the Netherlands should be included along with the other nations. This second proposal was accepted but then stopped when it came to light that the problem was the concept of reciprocal exchange and the method of approach to the foreign countries. A revised scheme involved working through established diplomatic channels via the Foreign Office, who would use the appropriate ambassador or consul to obtain catalogues of charts and sailing directions published by government hydrographic offices, as well as any by private chart sellers. The Hydrographer would then use those catalogues to identify any charts or sailing directions he needed, then order the ambassadors to purchase them, also checking once a quarter for any new catalogues. This revised proposal was taken up[42] and some 24 works were identified by Parry as being needed in the Hydrographic Office,[43] including charts received by the consuls at Hamburg and Elsinore which arrived at the Admiralty in July 1828.[44] Krusenstern also presented Parry with a copy of his atlas covering the Pacific, which arrived in the Hydrographic Office in October 1828.[45]

Not taking up the idea for reciprocal exchange was a great opportunity missed, especially as it was cost and protocol which prevented it happening. This was a reflection of the lack of understanding Croker (an administrator) had over the advantages reciprocal exchange could lead to, rather than any shortcomings by Parry (a surveyor and Hydrographer). The days of keeping charts for the sole use of the British Navy were long gone as Admiralty charts were easily available through selected chart sellers, so there was little to be gained from not exchanging them with foreign hydrographic offices.

Captain Francis Beaufort R.N. (1774-1857)

Francis Beaufort

By the time Beaufort was appointed Hydrographer in May of 1829 the precedent for international cooperation through hydrographic offices, as well as through surveyors at sea, had been well and truly set. The die was cast and Beaufort did not break it. As a man who both privately and professionally was greatly involved in science and hydrography, this naturally led to spin-offs for international collaboration. Beaufort wasted no time in cashing in on such a profitable position by sending a copy of the first issue of the *Nautical Magazine* to Russia in 1832 in an effort to open up more formal relations. He was indirectly assisted with his dealings with Russia by his old friend Franklin, who had travelled to Russia as a guest of Tsar Nicholas I in 1828, where he met the celebrated navigators Otto Kotzebue and Admiral Krusentern.[46] Krusenstern eagerly entered into a very friendly relationship with Beaufort, which saw the exchange of charts and surveys, with copies of the *Nautical Magazine* being translated for the use of Russian officers.[47] Krusenstern thought highly of Beaufort, stating in one letter accompanying some Japanese surveys obtained at great risk, how 'no better use can be made of it than to lodge them in your and Captain Beechey's hands'.[48] Krusenstern became great friends with Sir John Ross, Franklin and Beaufort.

However, Krusenstern passed away in 1846 and by 1850 Beaufort was receiving little encouragement in return for his efforts, and matters made even worse after Britain found itself at war with Russia soon after. He did manage to continue the good work Parry had undertaken with the French and Spanish, as well as open up communications with the Norwegians,[49] Prussians,[50] Neapolitans[51] and the Americans.[52] Of those final four America was the last to join in Beaufort's circle of international collaborators, when in 1845 Mr Lewis sent 'the first fruits of our coast triangulation and survey commenced by Mr Hassler' who had passed away the year before.[53] A mutual exchange followed shortly afterwards[54] and the relationship grew even stronger when W.F. Maury, who had been appointed as head of the Depot of Charts and Instruments in Washington, made an appeal in Brussels for climatological observations over the oceans. This naturally caught Beaufort's interest and that of the British parliament.[55] Rear Admiral F.W. Beechey represented British interests at the Brussels conference of 1853,[56] where he argued successfully for the adoption of the Beaufort Scale on an international basis.[57]

For Beaufort the opportunities he was involved with in scientific circles gave him contacts with a legion of scientists, hydrographers and surveyors. With the arrangements and relationships put in place by Beaufort's predecessors, Hurd and Parry, his role in the field of international cooperation whilst Hydrographer was more one of consolidation than innovation. He certainly took advantage of his position as Hydrographer to expand British scientific interests in the international arena, especially through his support of the work of scientists like Dr Whewell and his agenda of worldwide tidal data collection.

Beaufort was also involved with numerous scientific organisations, such as the Royal Society (of which he held a fellowship), the Royal Astronomical Society (of which he was vice-president), Royal Irish Academy, Institut de France, United States Naval Lyceum and the American Philosophical Society.

Conclusion

Dalrymple had led the way for the British in international cooperation in the field of hydrography with Mannevillette, which certainly had the potential for greater things had not factors beyond his control, such as conflict between Britain and France, worked against him. During times of peace, Hurd's effort to formulate a mutual exchange of charting products with Denmark was more than admirable. Had ill health not deprived him of the strength and time to undertake similar arrangements with 'all the maritime nations in Europe', then further nations across Europe could have benefited from his idea. Who knows what might have materialised as a result of Hurd's idea for international collaboration across Europe? A lack of interaction with Russia, which 'had been identified as Britain's main security concern after Waterloo', and also with Portugal were notable absentees before Beaufort's efforts tried to resolve the issue. However, a Russian decree of 28 September 1821, claiming rights to an exclusive use of the Siberian and Alaskan seas,[58] was a direct threat to the plans for exploration being worked upon by John Barrow, Second Secretary to the Admiralty and his circle of friends. Clearly Russia must have felt there was little need for collaboration with Hurd or Parry, especially after Admiralty charts were offered for sale in 1821.

Beaufort's efforts were equally admirable and during his term as the longest serving British Hydrographer (since 1795) he dealt with all the main charting nations. However, despite good relations between such nations, principally with the aim of supplying each other with charts and collaborating to avoid the duplication of survey work, there were some problems with obtaining the right charts, especially those of areas that were poorly surveyed, if at all. Such deficiencies were well known by Hurd and Parry, and one such example caused Parry to write to the Admiralty Board, stating:

There is certainly great room for improvement in our charts of the eastern and north-eastern coasts of South America; a very small proportion of which has, until lately, been regularly surveyed. We now possess the means of compiling a very tolerable chart of that coast from Mahanham to the Island of St Catherine; having lately received from Paris the complete survey of Baron Roussin, comprehendible between those limits, accompanied by a book of sailing directions. In Baron Roussin's charts, there are a good many gaps left unsurveyed; but they seem to be faithfully marked, so that the attention of future surveyors may be directed to those particular parts.[59]

Parry was fortunate in being able to obtain copies of Roussin's charts and for them to have been so well compiled, enabling him to easily establish what further work needed to be done. Many hydrographic offices relied heavily on foreign government charts, as well as local contacts, at that time.

There were also problems with the rights needed to survey in foreign waters, even after Britain had secured the pre-eminent position as a world maritime power after the Peace of 1815. The situation was difficult for the British and on one occasion the Admiralty Board decided to avoid the issue rather than tackle it head on when, fortunately for them, the surveyor in question was deployed to a different area.[60] Permissions were sought, for example, from the Ambassador at Madrid to survey the Spanish West Indies and from the Emperor of Morocco to survey his territorial waters, of which the latter was refused. [61] Despite those setbacks the agenda for international cooperation was well and truly on the table, over half a century before the American Bureau of Navigation proposed a 'system of international hydrographic work' in 1879.[62] There may well have been other interactions and I am interested in corresponding with historians who have identified examples of international collaboration before 1899.[63]

The question of 'why they needed to cooperate?' is not easily answered. Indeed, should a much wider study be undertaken it may reveal how hydrography helped the Admiralty hide the main purpose of the exercise which was in fact military intelligence gathering. It was not only hydrographic information, essential for navigation and trade, that was required but strategic information on defences and military strength, which could be gathered quite easily by the mutual exchange of charts. Foreign charts were, for example, certainly used to the advantage of the British when they mounted their Baltic and Crimean campaigns in the mid-nineteenth century. Nevertheless, despite such drawbacks with mutual exchange, the International Hydrographic Bureau's statement that 'International cooperation in the field of hydrography began with a Conference held in Washington in 1899'[64] should perhaps be revised in the light that at least nine nations were undertaking such activity half a century earlier.

Acknowledgements

I wish to thank the following experts in the history of the Hydrographic Office and Surveying Service for their helpful comments on this paper: Dr A.S. Cook (British Library), Lt-Cdr A.C.F. David R.N., Professor Andrew Lambert and Cdr R. Wilson R.N. My thanks also go to all those who read through this paper (prior to its publication) for their helpful comments.

Websites

www.hidrografico.pt/cronologia.php
www.iho-ohi.net - www.lib.noaa.gov

References

1. United Kingdom Hydrographic Office, Admiralty Way, Taunton, Somerset, England, TA1 2DN, UK

2. http://www.iho-ohi.net/english/home/about-the-iho/about-the-iho.html (accessed 9 January 2010).

3. A.S. Cook, 'Dalrymple, Alexander (1737–1808)', *Oxford Dictionary of National Biography*, Oxford University Press, Sept 2004; online edn, Jan 2008.

4. The National Archives, Kew, England (TNA), ADM1/3522, Dalrymple to Pole, 10 October 1807.

5. A. Lambert, *Franklin tragic hero of Polar navigation* (London, 2009), 23.

6. http://www.lib.noaa.gov/noaainfo/heritage/coastsurveyvol1/HASSLER1.html (accessed 23 August 2008).

7. Lt-Cdr A.C.F. David, 'Anglo-Spanish cooperation in hydrography, navigation and nautical astronomy, 1788-1834' in L. Martín-Merás (ed.) *Navigarre necesse est estudios de historia marítima en honor de Lola Higueras* (Gijón, 2008), 161; Museo Naval, Madrid, MN, A-10395. The majority of the 42 charts are ones published by Hurd of the Americas and Africa, except for three published by Dalrymple.

8. H. Ravn, *Det Kongelige Danske Søkort-Arkiv 1784 to 1934* (Copenhagen, 1934), 8.

9. A.P. Niblack, 'Det Kongelige Søkort-arkiv (The Danish Royal Hydrographic Office)', *Hydrographic Review* (1927), 21; Ravn, *Kongelige Danske Søkort-Arkiv*, 9.

10. *The Annals of Philosophy*, new series 1 (January-June 1821), 113-15. That society was also involved with cartography (Ravn, *Kongelige Danske Søkort-Arkiv*, 18).

11.The United Kingdom Hydrographic Office, Taunton, England (UKHO), MB1 f.6, Schifter to the Admiralty Board, 4 January 1826.

12. UKHO, LB1 fos.261-2, Hurd to Löwenörn, 30 December 1819.

13. Ex inf Prof. Lambert, January 2010.

14. TNA, ADM17/28.

15. UKHO, LB1 f.488, Hurd to Spencer, 30 April 1822.

16. Cdr L.S. Dawson, *Memoirs of hydrography including brief biographies of the principal officers who have served in H.M. Naval Surveying Service between the years 1750 and 1885* (Eastbourne, 1885, reprinted London, 1969), 53-4, 72; A.C.F. David, *The rise of Great Britain as a major charting nation* (Portsmouth, 2008). The French were thought by Parry to have been working in the Archipelago in 1825 (UKHO, LB2 f.54, Parry to Copeland, 23 December 1825).

17. Dawson, *Memoirs*, 54.

18. E. Valerio, 'Landscapes and Charting in the 19th Century. Neapolitan-Austrian and English cooperation in the Adriatic Sea' in *Mappæ Antiquæ. Liber Amicorum Günter Schilder* (2007), 469-70, 472-3.

19. R.T. Brown, 'Fernando Po and the Anti-Sierra Leonean campaign: 1826-1834', *The International Journal of African Historical Studies* 6:2 (1973), 253-62.

20. E.H. Burrows, *Captain Owen of the African survey. The hydrographic surveys of Admiral W.F.W. Owen on the coast of Africa and the Great Lakes of Canada. His fight against the African slave trade. His life in Campobello Island, New Brunswick 1774-1857* (Rotterdam, 1978), 78-48. Some embarrassment was avoided. When the *Leven* was carrying a number of pigs that were used as fresh meat and as His Highness was a Moslem a decision was taken to load the pigs into the ship's boats and take them away where they could not be seen.

21. UKHO, MB1 fos.8-9, minutes 4-7 January 1826.

22. UKHO, LP1857 F239, Fabricius to Parry, 15 March 1826.

23. UKHO, LP1857 F240, Fabricius to Parry, 17 June 1826.

24. UKHO, MLP5/3ii f.9, Report on the Hydrographic Office by Parry, 1 February 1827.

25. C.R. Middleton, *The administration of British foreign policy, 1782-1846* (Durham N.C., 1977), 8.

26. UKHO, LB1, fos 120-4, Parry to the Admiralty Board, 3 November 1827.

27. UKHO, Ritchie Papers box P.

28. F.W. Beechey, *Narrative of a voyage to the Pacific and Beering's Strait. To co-operate with the Polar expeditions: performed in His Majesty's Ship Blossom, under the command of Captain F.W. Beechey, R.N. in the years 1825, 26, 27, 28* 2 vols (repr. London, 1968), vol.1, xii.

29. UKHO, MB1 f.42 Parry to the Admiralty Board, 31 May 1826. See also Chapter Three for details of his supply of data to Parry.

30. U. Lamb, 'The London years of Felipe Bauzá: Spanish Hydrographer in exile, 1823-34', *The Journal of Navigation* 34:3 (September 1981), 326.

31. Lamb, 'The London years of Felipe Bauzá', 324. The Admiralty accepted the administration of the Royal Observatory in 1818 (Vice-Admiral Sir A. Day, *The Admiralty Hydrographic Service 1795-1919* (London, 1967), 33).

32. Lamb, 'The London years of Felipe Bauzá', 324.

33. Lamb, 'The London years of Felipe Bauzá', 329.

34. See A.J. Webb, 'The Hydrographer, science and international relations: Captain Parry's contribution to the cruise of HMS *Chanticleer*, 1828-9' in *The Mariner's Mirror* 6:1 (London, 2010), 62-71. See also J.N. Pasquay, *La cooperation Franco-Britannique en hydrographie* (Brest, 1996), 1-4 for a very brief and selected account of relations involving Rossel and others with the Admiralty.

35. For Parry's letter to Rossel see UKHO, LB2 fos 88-9, 11 January 1828.

36.UKHO, LP1857 M481, Rossel to Parry, 23 February 1828.

37. UKHO, LP1857 M481, Rossel to Parry, 23 February 1828.
38. UKHO, LB2 fos.129-32, Parry to Rossel, 19 April 1828.
39. UKHO, LP1857, M480 Rossel to Parry, 8 August 1828.
40. UKHO, MB1 fos.130-1, Parry to the Admiralty Board, 18 January 1828. There were other charts that remained unpublished, which the Admiralty and its Hydrographer did not wish to fall into the hands of their enemies, but they were predominantly of interest to operations in or adjacent to American waters.
41. UKHO, MB1 fos.130-2, Parry to the Admiralty Board, 18 January 1828.
42. UKHO, MB1 fos.140-1, Parry to the Admiralty Board, 14 February 1828.
43. UKHO, MB1 f.190, Parry to Owen, 28 May 1828.
44. UKHO, Accession ledger book 1, E626-E631.
45. UKHO, LP1857 B369, Booth to Parry, 29 October 1828.
46. A. Lambert, *Franklin tragic hero of Polar navigation* (London, 2009), 44, 163.
47. UKHO, LP1857 K150, Krusenstern to Beaufort, 20 April 1834.
48. UKHO, LP1857 K148, Krusenstern to Beaufort, 15 September 1834.
49. UKHO, LP1857 H128, Hausteen to Beaufort, 4 May 1835.
50. UKHO, LP1857 H272, Hebeler to Beaufort, 28 March 1839.
51. UKHO, LP1857 V78, Visconti to Beaufort, 17 August 1844.
52. Day, *Hydrographic Service*, 49.
53. UKHO, LP1857 L152, Lewis to Beaufort, 31 January 1845.
54. UKHO, LP1857 L515, Lewis to Beaufort, 25 March 1845.
55. Day, *Hydrographic Service*, 57.
56. TNA, ADM 12/577, Admiralty Digest 1853, cut 90a, 'System of Meteorological Observations Congress of Brussels', 27 July 1853.
57. A. Friendly, *Beaufort of the Admiralty. The life of Sir Francis Beaufort 1774-1857* (London, 1977), 147.
58. Lambert, *Franklin*, 36.
59. UKHO, MB1 fos.206-7, Minutes on charts of South America, 14 August 1828.
60. UKHO, MB1 f.34, Parry to Melville, 10 April 1826. See also UKHO, MB1 fos.32-4.
61. Day, *Hydrographic Service*, 61.
62. UKHO, MLP85.
63. The address for correspondence is 19 Kirke Grove, Taunton, Somerset, England, TA2 8SB, email aj.webb@virgin.net.
64. http://www.iho-ohi.net/english/home/about-the-iho/about-the-iho.html (accessed 9 January 2010).

Biography of the author

Dr Adrian Webb is Archive Services Manager at the UKHO. He joined the United Kingdom Hydrographic in 1988. He is Convener of the Historical Military Mapping Group for the British Cartographic Society and holds a Fellowship of that organisation. His qualifications include a Masters and a PhD in Naval History from the University of Exeter. His PhD studies concentrated on the expansion of the British Hydrographic Office during the period 1808 to 1829.
Email adrian.webb@ukho.gov.uk.

Article

FROM 19th CENTURY TO PRESENT: CHANGES IN HYDROGRAPHIC SURVEYING TECHNIQUES AND DETERMINATION OF SOUNDING ACCURACY

By Katherine CRONIN (THE NETHERLANDS) and Robert DEVOY (IRELAND)
DELTARES, Rotterdamseweg 185, Delft, The Netherlands
Geography Department, University College Cork, Co. Cork, Ireland

Abstract

Calculation of morphological change between hydrographic surveys is marred by uncertainties, in particular when methods have changed. When examining estuarine evolution, an approximation of measurement errors is needed. An overview of the changing approaches since the 19th century is given to aid error estimation and subsequent comparison with modern surveys. Changes and errors in horizontal positioning, soundings and datums need to be considered when interpreting sediment gains and losses. As a case study, the derivation of error estimates for an 1845 and modern hydrographic dataset on the south-west coast of Ireland is described.

Résumé

Les calculs du changement morphologique entre les levés hydrographiques sont faussés par les incertitudes, en particulier, lorsque les méthodes changent. Lorsqu'on examine l'évolution des estuaires, il est nécessaire d'avoir une estimation des erreurs de mesurage. Une vue d'ensemble du changement d'approches depuis le 19ème siècle est présentée aux fins d'appuyer l'estimation des erreurs et la comparaison ultérieure avec les levés modernes. Les changements et les erreurs dans le positionnement horizontal, les sondes et les systèmes de référence doivent être pris en compte pour interpréter les gains et les pertes en sédiments. Comme étude de cas, l'évolution des estimations d'erreurs pour une série de données de 1845 et pour un ensemble de données hydrographiques modernes sur la côte sud-ouest de l'Irlande est décrite.

Resumen

El cálculo del cambio morfológico entre los levantamientos hidrográficos está deformado por incertidumbres, en particular cuando los métodos han cambiado. Al examinar la evolución de los estuarios, se requiere una aproximación de los errores de medida. Se proporciona una visión general de los aproches cambiantes desde el siglo 19, para ayudar a efectuar la estimación de errores y la consiguiente comparación con los estudios modernos. Tienen que considerarse los cambios y errores en el posicionamiento horizontal, en las sondas y los datums, al interpretar los aumentos y las pérdidas de sedimentos. Como estudio de un caso, se describe la derivación de las estimaciones de errores para una colección de datos hidrográficos de 1845 y una colección moderna en la costa suroccidental de Irlanda.

Introduction

Hydrographic and topographic surveys of estuarine channels and intertidal flats provide a source of data for quantifying volume changes over time. The integration of these datasets is important for a wide range of coastal applications e.g. channel maintenance, infrastructure development and restoration of habitats, as well as research into the sedimentation and erosion rates. The net movement of sediment in and out of the study area can be calculated, and longer term trends may be determined using historical datasets (Van der Waal and Pye, 2003; Byrnes *et al*., 2002). With growing evidence of climate change and the predicted effects on storminess, sea level and hydrological balances, there is an increasing need to understand the evolution of estuaries to determine past changes in order to predict future trends
This paper provides an overview of historical survey methods and the uncertainties to be considered when comparing modern and historical surveys. A case study is presented describing the determination of error in hydrographic surveys, of different time periods, from the Argideen Estuary on the south west coast of Ireland.

There have been large improvements in the accuracy and precision of soundings and positioning over time, therefore the error associated with measurements may be different between historical and modern surveys and between two modern surveys. In the 19th century soundings were acquired using a lead line, Rude-Fisher pressure tube or a graduated pole in shallow areas. The collection of elevation and depth data now includes the use of accurate GPS systems, echo sounders and remote techniques such as LIDAR. However determination of the accuracy and total error associated between two bathymetric datasets is difficult. When comparing survey data an assessment of the differences, whether real, as a result of differences in the methodology between the two surveys, and/or errors within the survey itself, should be performed.

The accuracy of soundings is dependent on many random and systematic errors in the measurement process. The amount of real versus apparent change can only be determined by quantifying the total error in the comparison of two surveys so that the apparent changes can be removed from the calculation of the overall change.
Measurement error is defined as the difference between a measured value and the true value and it can be categorized as a blatant error, systematic error or random error (e.g. Byrnes and Hiland, 1994; Kraus and Rosati, 1998; Ministry of Defence, 1987). Blatant errors (human) can be eliminated with adequate quality control procedures. Systematic errors follow a regular pattern and if identified can be measured or estimated through calibration and removed from the survey data. Random errors are typically small errors resulting from the limitation of measuring devices or from the inability to calculate and remove systematic errors exactly. They do not include the errors associated with the measurement of tides and datum (Van der Waal & Pye, 2003). These errors change rapidly with time and are governed by the laws of probability. Some authors argue that even blatant errors are difficult to detect as the bottom elevation being measured is not visible. Langeraar, (1984) claims that giving an error estimate on a value that isn't known in the first place is quite pointless. What can be measured clearly however, are the fluctuations that the depth measurements are exposed to. These include changes in sea water parameters, irregularities in machinery and fluctuations in bottom reflection processes i.e. - the systematic errors.

Horizontal uncertainties

The accurate comparison of the position of soundings from historical and modern charts depends on the accuracy of the positioning method and knowledge of the reference datum it refers to. Horizontal datums on different charts may not be the same. A number of datums and associated spheroids have been used for charting worldwide and there are differences in geodetic latitudes and longitudes, albeit small, between different charting systems. In the past these differences had very little effect on the day to day navigation of ships, particularly because the errors inherent in astronomical observations were larger than any inconsistency in charted latitude and longitude (Ministry of Defence, 1987). See Alymer and White (1914), Ministry of Defence, (1987) and Langeraar, (1984) for more detail on geodesy, projections, grids and the creation of different coordinate systems.

The worldwide 3D reference system (WGS84) was defined in the 1960s with the advent of extremely accurate satellite techniques. It was then possible to establish the relationships between previously unconnected datums and to convert them to the world datum (Ministry of Defence, 1987). The development of satellite navigation systems has also shown discrepancies in the horizontal datums of many charts. Differences have resulted from errors in the astronomical fixes used for early surveys that were computed on local geographical datums. The reference spheroid of a local datums is a best fit for that particular area, whereas the ellipsoid used by WGS84 adjusts to the earth surface as a whole. This creates a datum shift, which can be in the order of a few hundred metres. The datum shift needed to relate older charts to current GPS datums is outlined on charts and in the "User's Handbook on Datum Transformations involving WGS84" (IHO, 2003).

In addition to datum errors, the survey data from which the chart was compiled may contain errors in geographical positions (Ministry of Defence, 1987).

These errors are the inaccuracy of the plotted soundings on charts relative to the horizontal datum. Historical surveys used transects and horizontal angles, measured against coastal features, to determine position through geometry. The precision of these positions was often affected by adverse sea conditions (Bale et al., 2007). The position error will decrease with decreasing chart scale but the affect on the soundings will depend on the slope of the seabed (Sallenger et al., 1975). See Aylmer and White, (1914) for details on historical navigation and positioning and the errors involved. In the latest IHO standards for hydrographic surveys, the horizontal position of soundings should have a 95% probability that the true position lies within a defined radius (IHO, 2008).

Vertical uncertainties

Changes in vertical datums

Vertical datums can be either orthometric (based on the geoid), tidal (a tidally-derived surface of high or low water), or ellipsoid (used by e.g. GPS). In the case of historical charts (early 20th century and previous), the accuracy of the vertical datums must be considered, especially when comparing depths with modern surveys. The level that was used to construct an historical survey is often unknown. It may be related to a tide gauge or mainland benchmark that is not retrievable today (Van der Waal & Pye, 2003).

The first task for surveyors on arriving in an area was to start observing the tide (Edgell, 1948). Chart datum for 19th century surveys was Mean Low Water Ordinary Springs (Aylmer and White, 1914). Now, Chart Datum is the level of the lowest possible water level (LAT). The accuracy of tidal information gathered depended on how long the surveyors were in any particular location and their focus was on tidal observations for the reduction of soundings rather than scientific investigation (Wharton, 1882). The main requirement was knowledge of low-water springs and the time of high water at full and new moon. Therefore tidal levels were usually only recorded during the duration of the survey and the results extrapolated, unlike today where tidal datums are averaged over an 18.6 year period. Despite the short nature of the tidal surveys, surveyors were cautious when carrying out the reductions. Even on a small scale chart, accuracy in reduction was regarded as being very important. If the surveyors were not in an area during the spring tide they had to note the high-water mark on the shore, measure how far it is above the high tide of the day, and subtract the same amount from the low-water mark measured on that day. This level was taken as the low water spring datum. Often a foot or two extra was subtracted to be on the safe side. A description of how tidal observations were taken and calculated in the late 19th century is outlined in Wharton, (1882).

The relative datum difference between two survey periods, especially when the period is long, could also have been influenced by decadal tidal variations, eustatic sea level rise and tectonic movement (Sallenger et al., 1975; List et al., 1997; Gibbs and Gelfenbaum, 1999).

Modern depth measurement uncertainties

All acoustic depth readings are dependent on the sea state, water temperature and salinity, transducer beam width, bottom sediment type, surface irregularity and vessel heave-pitch-roll motions, among other things. Vessel position and elevation may be measured separately and would have uncertainties independent of those associated with the positioning and orientation systems. International Hydrographic Office standards are applicable around the world. For shallow water surveys (<40m), random errors in depth measurement should not exceed 25cm with a 95% probability, depending the survey order (IHO, 2008). There are several sources of error that need to be taken into consideration when comparing two *modern* bathymetric sets. These are:

- The errors associated with the different measurement techniques and instrumentation. The accuracy of the soundings will be affected by the precision of the equipment used and the survey conditions at the time i.e. wave height, vessel velocity and the type of sediment on the seabed.
- The errors associated with the post-processing of the data such as tidal corrections, speed of sound adjustments and vessel draft corrections, if the resolution of the corrections is not higher than the resolution of the measurements themselves.
- The potential movement of the datums to which the soundings and positions have been reduced to.
- The errors associated with the digitisation (in a GIS) of the positions and depths.
- The effect of data density on the accuracy of the interpolation between survey lines.

Measurement of depths relative to still-water level. This measurement is more difficult in small boats due to waves, course and speed changes, and variations in load distribution affecting the vertical position and the tilt of the transducer. The difference between the still water level and the mean water level in the presence of waves of just 0.5m high would hide bedforms and bars of similar or smaller amplitude. Furthermore, in estuaries the speed of sound may vary significantly during the tidal cycle and in space which may result in an error (Gibeaut et al., 1998).

Historical depth measurement uncertainties

In addition to the errors in comparing two modern surveys, even larger errors may be associated with comparing modern and historical charts.

Undoubtedly, the random error of depth measurements from the 19th century is likely to be greater than in modern surveys. Historical surveys were undertaken manually and for navigational purposes, so they were mainly interested in recording the shallowest point (Thomas et al., 2002; Van der Waal & Pye, 2003; Aylmer and White, 1914). Sea state and equipment limitations played a major role in the accuracy of readings. No instructions explicitly defining accuracy limits were found in the historical literature for British hydrographers. Quality control requirements for depth measurements were detailed nonetheless. The hydrographic surveyors of the time went to extreme lengths to ensure the quality of the data (Shipman and Laughton, 2000; Wharton, 1882). It is assumed that each sounding was recorded as accurately as possible in the circumstances.

According to Wharton (1882), a good hydrographer should *"have a quick eye...but above all he must have a boundless capacity for taking pains in details at all times and seasons…nothing may appear that is not known to be correct*". This opinion is borne out in further descriptions given in Wharton, (1882), emphasising the importance of checking and testing all instruments to *"ascertain their errors"*. He was very much aware of all the potential errors involved in hydrographic surveying and wrote that *"no instrument, not even engine-divided protractors can be assumed to be without error…no work can be deemed satisfactory without the knowledge of how much correction should be applied…machines are more liable to error than a trained man, under most circumstances"*

At that time new instrumentation was being developed to ease the procedure of sounding, like the Massey's, Lucas's machine. The "small boat" sounding machine was used in shallower waters and the boat had to be stopped in order to allow the soundings to be taken correctly (Edgell, 1948; Cook and Carleton, 2000). Another type of sounding machine, the Kelvin Mark IV, used by the Royal Navy at the start of the 20th century, enabled soundings to be taken from the main ship while it was moving.

Lead lines were the main method of acquiring soundings until about 1935 when the echosounder came into more general use, but the lead line continued to be used for inshore work until the 1950s (Ministry of Defence, 1987; Shipman and Laughton, 2000). It was essential that the rope or wire was vertical from the surface to the seabed and that the weight was in contact with the seabed (Shipman and Laughton, 2000). Lead line measurements only cover the few centimetres actually struck by the lead and features less than a metre away from each sounding can remained undetected. Therefore, although each line of soundings may be miles in length, it only represents a few centimetres in width (Aylmer and White, 1914; Shipman and Laughton, 2000) and depending on the scale of the chart a single figure may occupy several hectares of ground (Ministry of Defence, 1987; Aylmer and White, 1914).

As with modern surveys the density of depth measurements will have an important effect on the overall interpolation of depth. The density of soundings taken in any particular area depended on how rapidly the slope of the seabed changed and whether or not there were unexpected readings. A shoal patch between lines could easily have been missed (Aylmer and White, 1982).

Potential instrumental errors would have included a stretch in the line and curvature of the line due to currents or ship movement. By the middle of the 19th century the use of wire lines greatly reduced the amount of stretch. Sounding lines for manual use were still made from rope but had a wire core. If the correct tension was maintained on the line it was assumed not to stretch more than 1-2%. Surveyors were instructed to measure the lead lines on return to the main ship and to note whether the length of the lead line didn't exceed the 1-2% tolerance (Wharton, 1882, Shipman and Laughton, 2000). Operational errors may also have occurred where the boundary between the seawater and the seabed was unclear, especially where the bottom was muddy. The point at which the bottom was thought to have been reached depended on the density of the material on the bed and on the shape and weight of the weight attached to the wire (Shipman and Laughton, 2000).

Unlike modern survey equipment that records to several decimal places, soundings using leadlines were recorded to the nearest half or quarter fathom. How much the halves and quarters were recorded depended on the scale of the chart. Therefore the accuracy of a chart is often dependent on the scale that the original survey was made on (Aylmer and White, 1914). In general, fractions were retained up to 6 fathoms and above that depth the fathoms were rounded down to the nearest even fathom. For safety, depth values are usually rounded down, especially if low water at spring tide was not measured directly.

During the metrification of charts in the 1950's, further errors might have been included as a result of conversion and subsequent rounding down (Van der Waal & Pye, 2003). A description of the range of instrumentation used in surveys from the late 1800's to the early 1900's can be found in Wharton, (1882); Aylmer and White, (1914) and Shipman and Laughton, (2000). Although accuracies increased with the initial use of echo sounders, the determination of where the seabed began and where the water column ended still caused uncertainties. The first echo sounders were subsonic and at this frequency the signal penetrated into soft mud before being reflected.

These were replaced by sounders using ultrasonic frequencies which reflected the echo from the top of the fluid mud which still may have been mostly liquid (Van der Waal & Pye, 2003).

Determination of measurement error

A compilation of the magnitude of different error sources should be estimated to give better confidence in whether the changes calculated between two surveys are real or apparent. Estimation of error is easily obtained with modern survey equipment as the accuracy and precision capabilities of instrumentation, under optimum conditions, are clear. In addition systematic errors can be carefully monitored. The determination of RMS error provides a consistent means of combining biases and random errors for calculating the statistical error associated with depth observations (Byrnes et al., 2002). As an additional test, the relative precision of individual depth measurements can be checked by comparing measurements of survey lines that intersect.

The determination of the accuracy of historical surveys is more difficult given the nature of the measurements as outlined in the previous section. Gibbs and Gelfenbaum, (1999) used the survey accuracy standards of 1883 for United States surveys as a starting point for determining the error estimates in their comparison of historical datasets (Table 1). Although determination of RMS error is more rigorous for modern surveys, Byrnes et al., (2002) found that potential errors in water depth measurements for late 1800s and early 1900s surveys in the USA were approximately ± 1-1.3m. For mid-1900s surveys, the RMS error is about ± 0.6-1m.
No explicit standards have been found thus far in the literature associated with the surveys undertaken by the British Admiralty. It is assumed that errors in British surveys are of the same magnitude considering similar procedures would have been followed. What can be determined from the literature on British survey techniques from the 19th century is summarized as follows:

1. Soundings were recorded to the nearest ½ or ¼ fathom or foot;

2. Fractions were retained only up to 6 fathoms and for safety values were rounded down;

3. Further rounding down may have occurred during the metrification of charts; and

4. Tidal datum were only recorded over the survey period and so could have been influenced by meteorology and sea level changes. If surveyors were not present during the time of low water springs the value was estimated and a foot or two extra could have been subtracted from the depths as a precaution.

Water Depth	Depth resolution
Deep sea soundings	Nearest fathom (~2m)
Outside 15 fathom curve (27m)	Nearest half fathom (0.91m)
Between 15 and 10 fathom curves (27-8m)	Nearest foot (0.3m)
Between 10 and 4 fathom curves (18-7m)	Nearest half foot (0.15m)
Between 24 and 12 foot curves (7-3.6m)	Nearest quarter foot (0.08m)
Inside 12 foot curve (<3.6m)	Nearest tenth foot (0.03m)

Table 1
Late 19th century bathymetric survey accuracy standards in the USA (Gibbs and Gelfenbaum, (1999))

A summary of all potential errors, both vertical and horizontal, that must be considered when comparing and interpolating data from both modern and historical surveys is given in ***Table 2***.

Modern surveys	Historical surveys	Both
Speed of sound adjustments	Variations in line length	Terrain irregularity
Transducer movement/heave	Vertical datum changes	Data density
Effect of waves	Accurate positioning	Effect of seabed sediment on instrumentation
Dynamic draught	Rounding up or down of readings	Heave of boat
	Readings to nearest ½ or ¼ fathom	Vessel speed
		Accuracy of digitisation
		Water levels, tides, transducer elevation

Table 2
A range of vertical and horizontal error considerations to be taken into account when comparing surveys of either historical or modern origin

Volume change calculations

Data density, the magnitude and frequency of bottom irregularities and the orientation of survey tracklines relative to bathymetric features are the most important factors influencing the calculation of volume change between two bathymetric surveys. These issues must be considered when creating a grid or contours. The presence of these uncertainties can be checked by visually comparing surface characteristics at adjacent survey lines. The closer the survey lines are or the smaller the bottom irregularities between lines, the lower the uncertainty will be (Sallenger et al., 1975; Byrnes et al., 2002). The orientation of tracklines may also cause an error in interpolation. According to Sallenger et al., (1975) surveyors were told to orient tracklines along the supposed contours until 1878 so they may have missed deep or shallow points by not surveying across that particular contour resulting in extremes in bathymetric fluctuation.

There are a number of techniques that were used for making quantitative estimates of change; contour overlay, contour overlay-data point and grid point comparisons (Sallenger et al., 1975). These were standard practice up to the 1980's (Byrnes and Hiland, 1993). Now statistical techniques and surface modelling software, such as Surfer, and GIS packages can be used to calculate volume changes between two surfaces. Two common ways of representing bathymetric surfaces from hydrographic data are TIN and interpolating the data on a grid. Creation of a TIN surface is best suited where data are sparse or unevenly distributed throughout the survey area. Furthermore all data points are used directly as they form the vertices of triangles that comprise the modelled terrain. Where data density is higher, interpolating the data on a grid (e.g. krigging) provides a good representation of surface characteristics.

According to Gibeaut et al., (1998) detailed comparisons of repeated bathymetric surveys are commonly inconclusive because the magnitudes of potential errors are equal to or greater than the actual changes of seafloor morphology. For example, in a survey covering 2,500m of shoreline across a nearshore width of 400m, a systematic elevation error of just 5cm would translate into an error in sand volume of 50,000m^3.

Case Study: Argideen estuary, Ireland

The bathymetric surveying of Irish coastal waters was very limited until 1999 when the Irish National Seabed Survey (INSS) was launched by The Geological Survey of Ireland (GSI). Today it is amongst the largest marine mapping programme ever undertaken in the world, producing over 300 paper-based charts and a total of 5.5 Terabyte of digital information stored on the INSS database in GSI.

The main focus of the Irish National Seabed Survey was deep water mapping at the outer margins of Ireland's territorial seabed, moving shoreward as time went by. Now INFOMAR (INtegrated mapping FOr the sustainable development of Ireland's Marine Resource), the successor to INSS, concentrates on nearshore surveys (GSI, 2010).

In this study, the error estimates of historical sounding data (year 1845) and modern bathymetric and topographic surveys (years 1991 up to 2008), for the Argideen Estuary on the south west coast of Ireland, were estimated. These errors were used in the calculation of morphological changes that have occurred in the estuary over the last 163 years. In addition, the surveys were used as input and validation data for two numerical models of the estuary. Delft3D, a process-based model was used to simulate annual morphological change and ASMITA, a behavior orientated model, the longer-term volume changes (Cronin et al., 2007; Cronin et al., 2009). The interpolated depth profiles were compared rather than individual points, so the accuracy considerations for depth measurements were examined in more detail than position accuracies. An overview of the charts and survey data used in this analysis is given in *Table 3*.

Charts and maps in Ireland were related to the Irish Grid geodetic system. It was developed more than 200 years ago and is based on a rigorous adjustment of a carefully observed triangulation network. Since then there have been many changes and adjustments to the system. In 1994, OSI (Ordnance Survey Ireland) and OSNI (Ordnance Survey Northern Ireland) agreed to establish a new geodetic control network in Ireland based on ETRS89 (European Terrestrial Reference System 1989) and from this the IRENET95 network was developed. The IRENET95 network complies with international standards and provides high precision, distortion free control for GPS surveys. 79% of all Irish charts refer to this OSI datum. The most recent Admiralty chart of the Argideen estuary refers to this datum and has a gnomonic projection.

All depths and elevations in this analysis were referenced to the same vertical reference datum in order to be compared. In Ireland the current vertical datum is the Malin Head Vertical Datum. Earlier maps used the low water mark of the spring tide on the 8th of April 1837 at the Poolbeg Lighthouse, Dublin. Elevations above or below this datum were in feet. The Malin Head datum is approximately 2.7m above the Poolbeg Light house datum.

Map/Chart/Survey	Date	Source	Horizontal Datum	Vertical Datum
1845 Admiralty Soundings of Courtmacsherry Bay	1845	UKHO	digitised to Irish Grid	depths (in feet) at level of LWS
1846 Admiralty Chart of Courtmacsherry Bay	1846	UKHO	digitised to Irish Grid	depths reduced approx to MLWS
1977 Admiralty Chart of Courtmacsherry Bay	1846 & 1907 surveys	UKHO		depths to Chart Datum
Courtmacsherry Harbour sounding charts	1991 (25/05/1991 & 06/09/1991)	DJ Fitzgibbon & Company Ltd	Irish Grid	depths to Chart Datum
Courtmacsherry Harbour sounding charts	1992 (14/07/1992, 28/09/1992 & 02/10/1992)	DJ Fitzgibbon & Company Ltd	Irish Grid	depths to Chart Datum
Courtmacsherry Harbour bathymetric survey	2006	author	Irish National Grid	depths reduced to Chart Datum
XYZ GPS survey of the Argideen Estuary	2006	author	Irish Map Grid 1975	OD Malin
XYZ GPS survey of the Argideen Estuary	2007	author	Irish Map Grid 1975	OD Malin
XYZ GPS survey of the Argideen Estuary	2008	author	Irish Map Grid 1975	OD Malin

Table 3.
Hydrographic data available for analysis

Argideen Estuary bathymetric and topographic datasets

Determination of sediment losses and gains in the the Argideen estuary were computed in Surfer by calculating volume change between datasets. The error associated with measurement was first determined for each dataset.

1845 soundings dataset

There are large temporal gaps in the bathymetric data available for the Argideen estuary and Courtmacsherry bay. The first major survey of the estuary was in 1845 by Commander James Wolfe on the H.M.S. Tartarus, during a survey of the south coast of Ireland from the Old Head of Kinsale to Calley Head, on a scale of 6.9 inches to 1 nautical mile. The resulting Admiralty Chart (number 2081) of the area was published in 1851 (UKHO, 2008, personal communication). The original survey sheet was used in this analysis. The current Admiralty Chart, published in 1977, is based on the 1845 survey (except for the channel which was resurveyed in 1907). No survey material was found in the UKHO (United Kingdom Hydrographic Office) archives for the period 1930-1980. Only high resolution digital images of the original survey sheets could be obtained as they were too large for the copying or scanning equipment in the UKHO. These images were taken perpendicular to the sheet to avoid distortion, but some alteration is likely to have occurred.
Some deformation will also have occurred during the process of georeferencing the images to the Irish Grid in ArcMap. Care was taken to ensure the RMS error was small during the georeferencing process for each image by using several fixed reference points, such as slipways, piers, roads and bridges. A slight shift of sounding positions as result of georeferencing was considered acceptable (***Fig. 1***) as depth points were interpolated to create a profile, and the measure of the 1845 coastline may not be as accurate the current coastline.

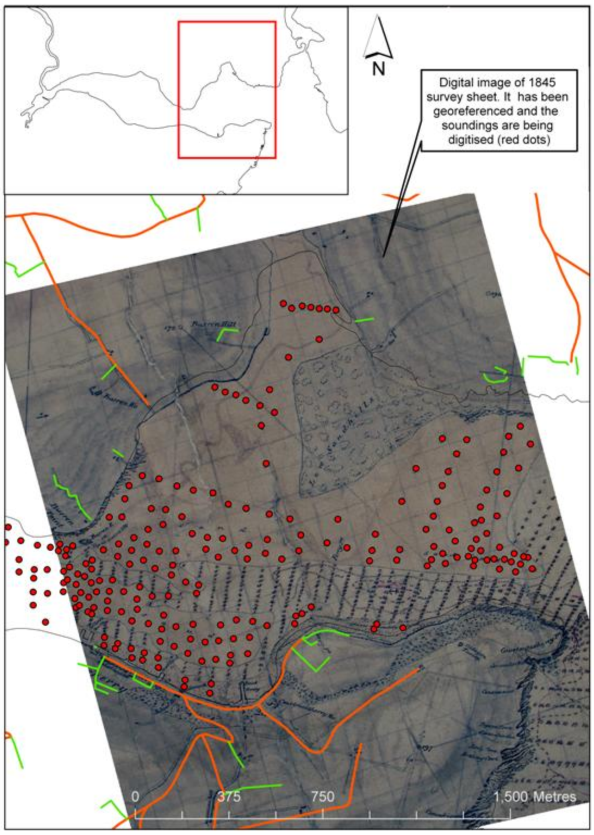

Figure 1
Georeferencing and digitisation of the 1845 survey sheet in ArcMap

The vertical datum for the 1845 soundings was the level of low water of ordinary spring tides. This level was recorded as 33 feet and 7.5 inches (10.25m) below the sill of the middle window (lower edge of the stone) of the school house in Courtmacsherry Village. The soundings were recorded in feet inside the harbour and in fathoms outside. Depths were recorded to the nearest quarter of a fathom and half foot. The depths were reduced to low water springs and the heights on the drying banks were reduced to high water ordinary springs.
In order to compare the depths recorded in 1845 to values from the modern surveys, the values were converted to metres and reduced to the current chart datum, lowest astronomical tide (10.70m below the sill of the middle window of the school). Very few records exist of datum adjustments in the Argideen Estuary.

However, there is a minute from Lt. Cdr. Powell, (1977) stating that 0.46m was subtracted from the soundings of 1845 to adjust them to LAT (UKHO, 2008, personal communication). This concurs with the difference between the two datums (0.45m) in relation to the benchmark at Courtmacsherry. Considering the tidal levels are only quoted to the nearest 0.1m, the additional 0.01m might have been subtracted for safety.

There are no available records of the mean tidal levels measured in the estuary during the survey in 1845. On the most recent publication of the chart, (1977) MLWS is 0.4m above LAT. The MLWS of 1845 was reduced by 0.46m to convert it to LAT so there is a 0.06m difference. From this it is assumed that the tidal ranges haven't changed significantly. The 0.06m difference is irrelevant in relation to the accuracy of tidal level recordings. This tidal information is required to calculate the level of MHWS on the 1845 sounding chart.
If tidal levels are assumed to be similar to today then the difference between MLWS and MHWS are also comparable. The heights on the drying banks were thus reduced to LAT using current tidal levels.

Using the information from the UKHO on the datum shift and the errors associated with historical sounding measurements outlined in the previous sections, the total error associated with these soundings could be estimated.

1845 error calculations

Based on the surveying methodology of the time, it is assumed the soundings of 1845 (measured in feet) were rounded down to the nearest half foot (0.153m). Therefore depths were underestimated by at most 0.153m. The accuracy of tidal readings and subsequent datum shifts must also be taken into account. It is not known whether the surveyors were present in Courtmacsherry during LWS. If it is assumed that they were not, the tidal levels would have been reduced by 1-2 feet (0.3-0.6m) for safety. A value of 0.3m is used here as the survey area analysed was within the estuary where depths are much shallower than the outer bay.

A total estimated error of +0.5m was calculated (rounding down of depths plus tidal levels and datum shift error margin). There is no negative error in this case because as the chart was produced for navigational safety all depths calculations have been rounded down.

1990s soundings dataset

Apart from a small survey of the main channel in Courtmacsherry Harbour in 1907 (data unavailable), the next bathymetric survey undertaken in the Argideen Estuary was in the early 1990s. The main channel was surveyed by Hydrographic Surveys Ltd for D.J. Fitzgibbon Company Ltd , both before and after dredging work.

These surveys were undertaken using rangefinders, digital echosounders and drawn up by hand. The accuracy of the echosounder used (Raytheon DE719D) is ±0.5% of the indicated depth. The soundings were measured directly from the paper records and the accuracy would have been to the nearest 5cm (Hydrographic Surveys Ltd, 2006, personal communication). Original survey sheets were obtained from Hydrographic Ltd., and the surveys dated May and September 1991 and July 1992 were used in the analysis. The surveys were scanned and georeferenced to Irish Grid in ArcMap in the same way as the 1845 survey images. Any slight distortion in the position of soundings as a result of the scanning or georeferencing was accepted, as depths between soundings were being interpolated. The total measurement error associated with these soundings is ±0.05m.

2006 bathymetric dataset

A complete resurvey of Courtmacsherry harbour, from the northern pier as far as Coolmain Point was undertaken in March 2006 with a single-beam echosounder by Irish Hydrodata Ltd. A Trimble NT300D DGPS was used to determine position and soundings were acquired using a Knudsen 320M dual frequency system (210kHz, 33kHz). The speed of sound profile in the water column was measured using an Odom Hydrographics Digibar and tide levels were measured using a Microtide self-recording tide gauge. Tide (and subsequently depth) levels were reduced to chart datum at Courtmacsherry. Due to the time of year that the survey was carried out the sea conditions were not ideal. Therefore, in order to allow for the effect of waves, the data was visually inspected by Hydrographics Ltd., to note the approximate period of the waves and a 'moving average' procedure was implemented to remove the effect of the waves. The accuracy of the echosounder system used was ±0.01m (Knudsen Engineering Ltd.). The presence of waves may have introduced a greater error but the total error in measuring depth, according to the 4th Edition of the IHO Standards should not exceed, with a probability of 90%, ±0.3m for depths less than 30m. Therefore based on this information a conservative error estimate of ±0.1m was assumed.

2006 -2008 topographic datasets

Three differential GPS surveys of the intertidal areas were undertaken annually by the author from 2006-2008 using the Trimble DGPS system with a ProXH receiver. This system provided real-time sub-metre accuracy with built-in SBAS, OmniSTAR and beacon capabilities. All areas reachable at low water were surveyed, including parts of the intertidal area that were surveyed during the bathymetric survey. This increased the resolution in those areas and provided a method of cross checking the bathymetric dataset.

Height and position readings (on Irish Grid) were taken along transect lines in these areas. The resolution varied in accordance with each location. In areas where there were significant changes in height over short distances the resolution was higher than in areas that were relatively flat and featureless. Elevations were corrected to Ordnance Datum Malin with RINEX base station data (Cork Station, ITM 563308.3 570435.3) downloaded from the Ordnance Survey Ireland website (http://www.osi.ie). The average vertical and horizontal error of the 2006 topographic dataset was a lot higher than desired and so the data was not used in the volumetric analysis.

The survey was repeated in 2007 and 2008 with more accurate results. The average vertical error of these surveys was ±0.16m and the average horizontal error ±0.16m, with some areas being more accurate than the average. ***Table 4*** presents the total vertical error estimation of each dataset used.

Hydrographic Data	Total vertical error estimation
1845 Admiralty Soundings of Courtmacsherry Bay	+0.5m
1991 and 1992 Courtmacsherry Harbour sounding charts	±0.05m
2006 Courtmacsherry Harbour bathymetric survey	±0.3m
2006 XYZ GPS survey of the Argideen Estuary	±0.62m
2007 XYZ GPS survey of the Argideen Estuary	±0.16m
2008 XYZ GPS survey of the Argideen Estuary	±0.16m

Table 4 Measurement error estimates of each dataset

Conclusions

Changes in hydrographic surveying methods over the last 150 years and sources of measurement error have been described. There are many uncertainties in both vertical and horizontal measurements and their respective datums which make the analysis of historical change challenging. The accuracy of historical data is often unknown, therefore when calculating morphological change in a coastal system, different sources of error need to be taken into account. Although the accuracy of modern survey methods is easier to determine, there are still uncertainties. This paper provides additional information on how to quantify the errors associated with historical surveys when comparing charts and analysing change. Quantification of these errors greatly helped in the determination of such change in the Argideen Estuary on the south coast of Ireland, where no meta-information of the first survey of the area in 1845 was available.

Acknowledgements

The authors would like to thank the United Kingdom Hydrographic Office (UKHO) for providing images of the original (1845) sounding sheets of the Argideen Estuary and Courtmacsherry Bay and for their helpfulness in searching for any additional information on those surveys. Thanks also to Hydrographic Surveys Ltd. (Cork) who provided the 1991-1992 survey sheets of Courtmacsherry Harbour.

References

- ALYMER, H. E. & WHITE, J, (1914). *Admiralty Manual of Navigation*. His Majesty's Stationary Office, London
- BALE, A.J., UNCLES, R.J., VILLENA-LINCOLN, A. & WIDDOWS, J., (2007). An assessment of the potential impact of dredging activity on the Tamar Estuary over the last century: Bathymetric and hydrodynamic changes. *Hydrobiologica,* 588, 83-95
- BYRNES, M. R., BAKER, J. & LI, F, (2002). Quantifying potential measurement errors and uncertainties associated with bathymetric change analysis. *ERDC/CHL CHETN-IV-50*, U.S. Army Engineer Research and Development Centre, Vicksburg, Mississippi, USA.
- BYRNES, M.R. & HILAND, M.W, (1994). Shoreline position and nearshore bathymetric change (Chapter 3). In: *Kings Bay Coastal and Estuarine Physical Monitoring and Evaluation Program: Coastal Studies. Tech. Rep., CERC-94-9*, Coastal Eng. Res. Cent., Vicksburg, Mississippi, USA , 61–144.
- BYRNES, M.R. AND HILAND, M.W, (1993). Regional seafloor change near St. Mary's entrance, Georgia/ Florida and its influence on shoreline response. In: *Large-Scale Coastal Behavior '93*, Ed. Jeffrey H. List. USGS, St Petersburg, Florida, USA, 17-20
- CRONIN, K.C., DEVOY, R.J.D. & GAULT, J., (2007). Modelling Estuarine Morphodynamics on the South Coast of Ireland, *Journal of Coastal Research*, SI 50, 474-479
- CRONIN, K.C., DEVOY, R.J.D. & GAULT, J., (2009). The value of different modelling approaches to investigate estuarine morphodynamics, *Journal of Coastal Research*, SI 56, 932-936
- EDGELL, VICE-ADMIRAL, J., (1948). *Sea Surveys – Britain's contribution to hydrography*. Longmans, Green and Co. Ltd. London, 29p
- GIBBS, A. E. & GELFENBAUM, G., (1999). Bathymetric change off the Washington-Oregon Coast. *In: 4th International Conference on Coastal Engineering and Coastal Sediment Processes*, June 20-24 1999, Long Island, NY. American Society of Civil Engineers.
- GIBEAUT, J. C., R., G. & KYSER, J. A., (1998). Increasing the accuracy and resolution of coastal bathymetric surveys. *Journal of Coastal Research,* 14**,** 1082-1098.
- GSI, (2010). Geological Survey of Ireland Website www.gsi.ie
- IHO, (2008); *IHO Standards for Hydrographic Surveys (5th edition)* Special Publication No. 44. Published by the International Hydrographic Bureau, Monaco, pp.36
- IHO, (2003). *User's handbook on datum transformations involving WSG84*. Monaco: International Hydrographic Bureau.

- KRAUS, N.C., & ROSATI, J.D., (1998). "Estimation of uncertainty in coastal-sediment budgets at inlets." U.S. Army Corps of Engineers, *Coastal Engineering Technical Note IV-16, 12p*
- LANE, A., (2004). Bathymetric evolution of the Mersey Estuary, UK, 1906-1997: causes and effects. *Estuarine, Coastal and Shelf Science,* 59**,** 249-263.
- LANGERAAR, W., (1984). *Surveying and charting of the seas, Elsevier Oceanography Series, Amsterdam, The Netherlands, 590p*
- LIST, J.H., JAFFE, B.E., SALLENGER, A.H. & HANSEN, M.E., (1997). Bathymetric comparisons adjacent to the Louisiana Barrier Islands: Processes of large-scale change. *Journal of Coastal Research*, 13, 670-678
- MINISTRY OF DEFENCE, (1987). *Admiralty Manual of Navigation*, Her Majesty's Stationary Office, London, England 80p
- OSI, (2008). Ordnance Survey Ireland website www.osi.ie
- SALLENGER, A. H. GOLDSMITH. V. &. SUTTON. C. H., (1975). *Bathymetric chart comparisons: A manual of methodology, error criteria and applications*. Virginia Institute of Marine Science, Virginia, USA.
- SHIPMAN, S. & LAUGHTON A., (2000). Historical methods of depth measurement. *In:* Carlton, C. & Cook, P. J. (eds.) *Continental Shelf Limits: The Scientific and Legal Interface.* Oxford University Press, Oxford, UK,
- THOMAS, C. G., SPEARMAN, J. R. & TURNBULL, M. J., (2002). Historical morphological change in the Mersey Estuary. *Continental Shelf Research,* 22**,** 1775-1794.
- UKHO, (2008), personal communication.
- VAN DER WAL, D. & PYE, K., (2003). The use of historical bathymetric charts in a GIS to assess morphological change in estuaries. *The Geographical Journal,* 169**,** 21-31.
- WHARTON, W.J.L., (1882). Hydrographical Surveying. A description of means and methods employed in constructing marine charts. John Murray, Albemarle Street, London, UK.

Biographies of the Authors

Dr Katherine Cronin graduated with a degree in Environmental Science from University College Cork (UCC), Ireland in 2004. She then began her PhD research in estuarine morphological modelling in the Department of Geography (UCC), during which time she worked part-time at the Coastal and Marine Resources Centre (UCC) on a variety of projects. In 2009 she began working in the Marine and Coastal Systems Unit of Deltares, in The Netherlands, where she works as a research/advisor in the field of hydrodynamics, water quality modelling and sediment transport modelling. (Email: katherine.cronin@deltares.nl)

Professor Robert Devoy graduated in the 1970s from Durham and Cambridge (UK) after completing PhD research on the analysis of sea-level changes and land subsidence in the Thames estuary. He moved to Cork, Ireland in 1977 to lecture in UCC. There, his research continued, on many aspects of sea-level changes, coastal processes and coastal management. In 1993 he founded the Coastal and Marine Resources Centre (CMRC). More recently he has worked on the prediction of the impacts of changes in storminess patterns on European Atlantic coasts and was a lead author of the Fourth Assessment Report on the IPCC.

Article

MULTIBEAM CROSSCHECK ANALYSIS
A Case Study

By Jørgen EEG (DENMARK)
Danish Maritime Safety Administration

Abstract

A new method for analyzing overlapping areas in multibeam surveys is introduced. The method requires that the velocity of sound in the water at the transducer is monitored during the survey. The method applies the principle of least squares to determine the vertical offset and the bias of the swaths caused by insufficient knowledge of the velocity of sound in the water column below the transducer. The precision and robustness of the method is demonstrated on a survey.

Résumé

Une nouvelle méthode d’analyse des zones de chevauchement dans les levés multifaisceaux est ici présentée. Cette méthode impose que la vitesse du son dans l’eau au transducteur soit surveillée pendant l’exécution du levé. Par ailleurs, le principe des moindres carrés est appliqué pour déterminer le décalage vertical et les biais des bandes couvertes que provoque un manque de connaissances de la vitesse du son dans la colonne d’eau sous le transducteur. La précision et la robustesse de la méthode sont démontrées pendant l’exécution du levé.

Resumen

Se presenta un nuevo método para analizar las zonas de solapamiento en los levantamientos multihaz. El método requiere que se controle la velocidad del sonido en el agua del transductor durante el levantamiento. Este método aplica el principio de los mínimos cuadrados para determinar el desfase vertical y las distorsiones de las zonas exploradas causadas por un conocimiento insuficiente de la velocidad del sonido en la columna de agua situada bajo el transductor. La precisión y la resistencia del método se demuestran durante un levantamiento.

Introduction

S-44 Annex A – Guidelines for Quality Control (S-44 2008) recommends that depth data integrity in multibeam surveys is controlled by check lines or overlapping swaths using a '*quality control procedure* (which) *should include statistical analysis of differences and the consideration of common errors to provide an indication of compliance of the survey with the standards given in* (Minimum Standards for Hydrographic Surveys)'. The present case study presents a modus operandi for a multibeam crosscheck analysis which has an impact on the planning of multibeam surveys in which the velocity of sound in the water at the transducer is measured continuously during the survey. The Cross-Section method, which is treated in detail below, takes advantage of the fact that detailed knowledge of the sound speed profile is not needed in order to correct soundings, by employing the principle of least squares to estimate corrections to measured profiles. This makes it possible to improve casts taken by traditional methods or, alternatively, to separate long periodic errors i.e. biases from the noise when the a posteriori error budget is put together.

Figure 1.
Distribution of cells in DTM of survey track (red) and check line (white).

The fact that the Minimum Standards for Hydrographic Surveys (S-44 2008) relate the soundings to the true position of the sea bed, forces the quality control of a multibeam survey to aim at verifying whether or not the different sensors entering into the multibeam equation adhere to the specs stated by the manufacturer. In case they do, the reasoning is that the a priori error budget of the survey then presents a true picture of the distribution of the soundings relative to the sea bed. It follows that approaches to disclose artefacts in the survey are at a premium. The author's method of choice is the following. For a given cell size, which, as a rule-of-thumb, may be as large as 10% of the depth, construct a DTM of the soundings which covers the intersection between the survey lines. Following a long tradition in hydrography, the smallest depth inside each cell determines the height of the cell, but for our purpose we shall be more interested in to which of the two tracks the sounding and therefore the cell belongs. A census of the number of cells belonging to the two tracks may be compared to the expected number using statistics, see (Eeg 2004). When the issue is disclosure of artefacts, ***Figure 1*** illustrates that this method of analysis cannot stand alone, but must be supplemented by an evaluation of the pattern of the blending of the cells belonging to the two tracks. ***Figure 2*** illustrates the power of this method. The eye catches the surplus of red cells to the right and of white cells at the bottom of the intersection which, together with the added information that the tracks were surveyed towards North and East respectively, causes the analyst to suspect a minor roll calibration error. This was confirmed by using the method in (Eeg 2008), changing the angle by 0.03°.

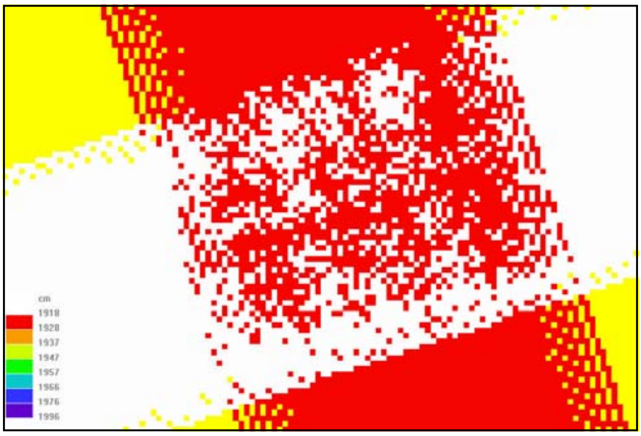

Figure 2
Small artefact from incorrect roll calibration of multibeam echo sounder

By the way, the two tracks depicted in ***Figure 1*** were randomly chosen from a RTK survey. For experimental purposes the ray tracing of the soundings was based only on the measured velocity of sound (s/v) at the transducer placed at the bottom of the vessel. The Cross-Section method yielded estimates of correction to the s/v profile and to the *vertical* displacement between the two tracks of -8.0m/s, -6.5m/s and 0.5cm respectively. Figure 2 depicts a DTM of the two tracks after the ray tracing was corrected by adding the estimated s/v's to the measured values in the profiles, starting just below the transducer.

The Cross-Section method

Following the layout of the ship lanes, most of the hydrographic surveying in Danish waters is conducted along parallel lines.

While this method is optimal only when the depth along the survey line is constant, the fringe benefit of varying depths is that the overlapping swaths between neighbouring lines may be used to assert the quality of the survey. Considering that the sea bed in general is smooth, the check up ought to be a piece of cake. It is not, however, because the s/v profile below the survey vessel as a rule is quickly changing from place to place. In order to establish some measure of control the Danish survey vessels have since 1999 measured the s/v at the transducer at all times during survey. It holds true that, if the s/v at the transducer is known, the vertical movement Δz of the soundings in a swath for small relative changes in the s/v to a linear approximation is governed by the formula

$$\Delta z \simeq d \cdot \overline{\rho} \cdot (1 - \tan^2 \theta) \qquad (1.1)$$

d being the (observed) depth difference between the sounding and the transducer, $\overline{\rho}$ the average relative change in the s/v in the water column and the launch angle θ is measured relative to the Nadir (Eeg 1999). The relation is (2.9) derived in the appendix. (Eisler 2000) demonstrates that the ray-path stability quickly deteriorates for launch angles beyond 60°, so as a rule of thumb we shall limit the Cross-Section method to data sampled within this angular sector and be wary of values of $\overline{\rho}$ exceeding 2%. In the shallow Danish waters these precautions will ensure the validity of (1.1), even for small perturbations of the s/v at the transducer, see (Eisler 2000).

In a region where swaths from two survey lines overlap, we may consider the average relative errors in the s/v profiles $\overline{\rho_1}$ and $\overline{\rho_2}$ together with the vertical displacement $\delta_{1,2}$ between the two lines, to be constant, but unknown, if the region is small enough. In order to fix the ideas, the reader may think of $\delta_{1,2}$ as representing errors in correction for tide, vessel settlement etc., but any slowly varying error in the direction of the plumb line, as for example displacements caused by unfavourable satellite constellations in RTK, will do. Suppose now that we construct two DTMs, one for the survey line and the other for the check line, both covering the intersection, in such a way that each cell i in the two DTMs covers the same area of the sea bed.

Suppose furthermore that the cell size is so small, that we can consider the (unknown) depth of the sea floor in a cell, D_i, to be constant. Then, for each of the two tracks, we find

$$d_{j,i} + d_{j,i}(1 - \tan^2 \theta_{j,i})\overline{\rho_j} + \Delta_{j,i} = D_i \qquad j = 1,2 \qquad (1.2)$$

where the (unknown) corrections $\Delta_{j,i}$ satisfy the relation

$$\Delta_{1,i} - \Delta_{2,i} = \delta_{1,2} + \varepsilon_i$$

The difference between the two equations in (1.2) yields at each cell in the region an observation equation

$$d_{1,i} \cdot (1 - \tan^2 \theta_{1,i}) \cdot \overline{\rho_1} - d_{2,i} \cdot (1 - \tan^2 \theta_{2,i}) \cdot \overline{\rho_2} + \delta_{1,2} = d_{2,i} - d_{1,i} + \varepsilon_i \qquad (1.3)$$

and it makes sense to fit the two surfaces together by seeking values of the unknowns, $\widehat{\rho_1}$, $\widehat{\rho_2}$ and $\widehat{\delta_{1,2}}$, which minimize the sum of the squared errors $\sum \varepsilon_i^2$.

Having ended up in a classical least squares adjustment, the inverse to the normal equation matrix, i.e. the variance-covariance matrix, is the key to the precision of the unknowns and indeed, being small-dimensional it can be readily evaluated in each particular case whenever data is available. In order to be able to take full advantage of the method, however, it is necessary to investigate how the precision of the unknowns depends on the angle between the survey line and the check line.

Design considerations in crosscheck analysis

Figure 2 may have seduced the reader into believing that the Cross-Section method is very precise and indeed its power is demonstrated on a survey below. However, an inspection of equation (1.3) reveals, other things being equal, that the solution breaks down if the check line is placed exactly on top and parallel to the survey line. In this case the coefficient to the first two unknowns in each of the observation equations become equal with opposite signs, i.e. the two unknowns can only be determined up to a common constant. Geometrically this means that the swaths in the two lines can be bended so that they coincide, leaving the correct common curvature undetermined. When the check line is placed parallel to the survey line so that the overlapping area only consists of the outermost set of beams, the situation is quite contrary. In order to see that, place a co-ordinate system with origin at the transducer, z-axis positive down along the plumb line and x-axis orthogonal to the z-axis so that the swath is spanned by the x-z plane.

In this co-ordinate system any change in the ray trace of the soundings, caused by a perturbation of a s/v profile which only depends on z, is an even function of x. We can change parameters in (1.1) by setting

$$x = d \cdot \tan\theta$$

yielding

$$\Delta z = (\overline{\rho}/d)(d^2 - x^2) \tag{1.4}$$

Suppose the centre of the overlap between the two parallel tracks has abscissa a, then in the parallel track its abscissae is $-a$ and we can determine the slopes of the two tracks such that they coincide at the intersection. In fact, for a given value of $\overline{\rho_1}$ we can determine $\overline{\rho_2}$ so that the equality

$$\frac{2a\overline{\rho_1}}{d_1} = -\frac{2a\overline{\rho_2}}{d_2}$$

holds, and then the observations in the overlapping zone only differ by a common vertical displacement. This displacement, however, depends on the choice of $\overline{\rho_1}$ In general, then, we should either have a relatively large overlap or reliable estimates of the s/v errors before we estimate a difference in level between neighbouring survey lines.

The Cross-Section method yields reliable estimates of the s/v errors if the control line is surveyed at right angles to the survey lines. The reason is that, at the area of intersection, all soundings in any given swath belonging to the control line are placed within the same small angular sector seen from the transducer when the survey line was measured, so that any s/v error in the control line is measured against the correct form of the sea bed, albeit shifted vertically by the s/v error in the survey line. For reasons of symmetry this argument holds true for the swaths of the survey line with respect to the control line too.

In the above discussion of the method it is understood that an adequate cell size is chosen. If the cell size is too large, the two DTMs lack the flexibility to react adequately to subtle changes in the curvature of the sea bed, resulting in poor estimates of the $\overline{\rho}$'s followed by a poor estimate of the standard deviation between the two data sets. On the other extreme, the cell size may become so small, that information is lost by reducing the set of cells with contributions from both data sets. The investigation below indicates that there is some robustness in the method as regards the choice of cell size and ways to safeguard against these extremes.

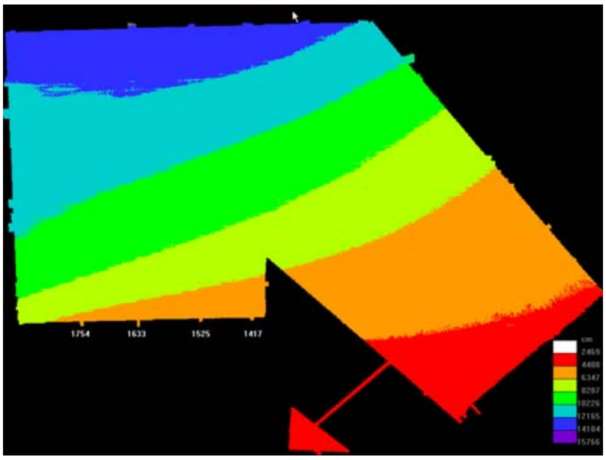

Figure 3
DTM of 00309, cell size 6m. Reson SeaBat 7125 200kHz

Survey 00309

00309 is the third compact area surveyed in 2009 by HDMS Jens Sørensen. The survey was RTK, the echo sounder a Reson SeaBat 7125 200 kHz with a SVP-70 to monitor the s/v at the transducer. Most of the s/v below the transducer was sampled as discrete profiles by an ASV5002, the ScanFish only being functional at the end of the survey. Figure 3 depicts the depth variation in the area.

Figure 4 depicts the lay out of the survey lines and check lines. Five parallel check lines were selected because of their lengths. Four of the check lines were surveyed at 28 August while the fifth, painted red in Figure 4, was surveyed at 1 September in bad weather, the vessel going into harbour after completing the line. The survey time for each of the four lines is depicted below each line in Figures 3 and 4. The common s/v profile used for the four check lines was sampled immediately before they were surveyed at 28 August 14:04. Below this profile is referred to as profile 14:04. Its position is indicated by the mouse cursor in form of an arrow near top of the image in both figures.

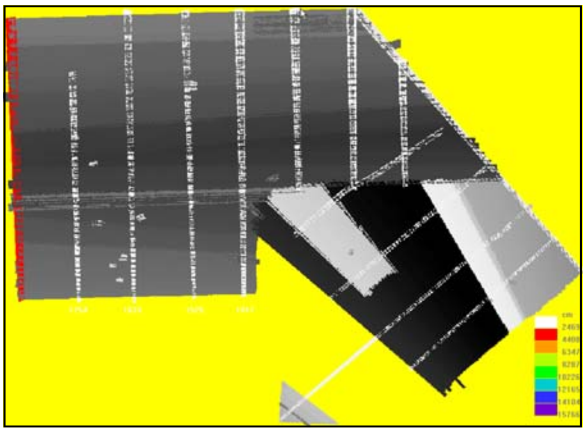

Figure 4
Layout of check lines in 00309

The Cross-Section method was employed on the intersections of 44 parallel survey lines with the five check lines. Throughout the cell size for the observations equations was 6m, using an average whenever more than one contribution fell into a cell. For reasons of presentation, the resulting estimates of the average relative error in the s/v profile were multiplied by 1465 m/s in order to convert them into quantities which could be related to the entries in the s/v profile. The normal variation of the s/v in Danish waters is between 1430m/s and 1500m/s, so the error in multiplying by 1465 is less than 3%.

Figure 5 depicts the variation of the estimates of the average s/v error in profile 14:04 for each of the four check lines surveyed at 28 August. The axis of abscissa represents survey lines, numbered from top to bottom and the units of the ordinate axis are m/s. The fact that the same s/v profile has been used for each of the four check lines makes a direct comparison between the four graphs meaningful. Given that the s/v profile was measured at the deep end of the area, one would expect all the graphs to start at zero. They do not, however, because the signature (Eeg 2008) of the Reson SeaBat 7125 changes the across track shape of the sea bed, depending on the hydrophone and on the version of the maintenance release. The odd component of this change is compensated by the calibration for roll, whereas the even part fools the surveyor into believing that his s/v profiler needs to be calibrated. Apart from this, at least two facts are worth attention in Figure 5. The first is the high correlation of each graph with the variation of the depth at the corresponding check line, as seen from Figure 3. The second is the size of the variation from survey line to survey line as the crossings by the check lines move from top to bottom.

Figure 5
Estimates of the average error in profile 14:04 for four check lines 28 August 2009. Cell size 6m

The average error in the s/v profile for the fifth check line is not depicted. Keeping within ±0.5m/s of an average value of 1.5m/s, the lack of variation is probably caused by turbulence in the water due to the weather conditions.

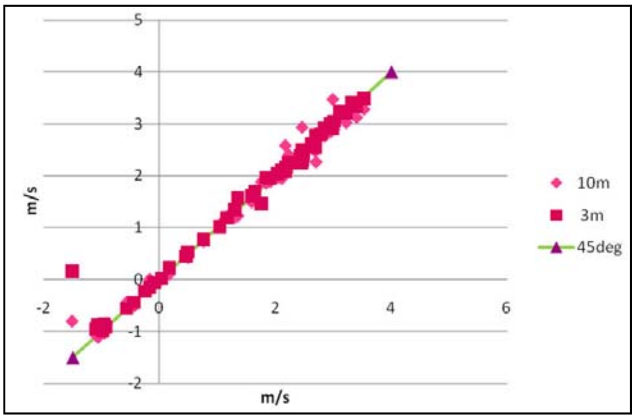

Figure 6
Plots of estimates from 6m cell size against 3m and 10m for 44 crosses of check line 15:25

In order to check up on the robustness of the estimates with respect to the chosen cell size, the Cross-Section method was recalculated for the check line surveyed 28 August at 15:25 using cell sizes of 3m and 10m. ***Figure 6*** depicts plots of the estimates of $\overline{\rho}$ from 44 homologous crossings in cell sizes 6m against 3m (red) and 6m against 10m (blue). A green line depicting positions of no influence from change in cell size serves to evaluate the variation. It appears from the figure, that the estimates are robust with respect to these variations in the cell size, the 10m cell size displaying a slightly larger variation than the 3m.

A simulation model

Above it was claimed that if the s/v at the transducer is known, then (1.1) is a valid approximation to the vertical change of a swath as a function of change in the s/v profile in the shallow Danish waters, provided that the angular sector in the swath is confined to the interval [60°, 60°] and the average relative change in the s/v profile is below 2%. As a rule of thumb, at 100m below the transducer a 1m/s average change in a profile changes the depth by 7cm, while the change at 60° is twice this amount with opposite sign. For a given s/v profile, however, it is of interest to verify that these claims hold true. The profile is extended by interpolating the discrete measurements linearly so that the ray-path segments become circular arcs. Suppose now that the profile at hand exactly represents the variation of the s/v, then we can calculate the travel times for a set of launch angles in the interval [0°,60°] from the top of the profile to an arbitrary, but fixed, depth *D*.

In order to emulate survey conditions, a s/v profile, which is close to the profile and coincides with it at transducer depth, is chosen to simulate a measured survey profile. At each launch angle θ_i, then, the survey profile and travel time is used to find the depth d_i ,i.e. in the spirit of equation (1.2) we have a set of observations equations

$$d_i(1-\tan^2\theta_i)\rho = D - d_i + \varepsilon_i$$

from which we find the estimate $\hat{\rho}$ of ρ which minimizes the sum of squared errors $\sum \varepsilon_i^2$ to be

$$\hat{\rho} = \sum d_i(1-\tan^2\theta_i)(D-d_i) \Big/ \sum d_i^2(1-\tan^2\theta_i)^2$$

The estimate results in an adjustment of the simulated survey profile, except at transducer depth where the value is fixed.

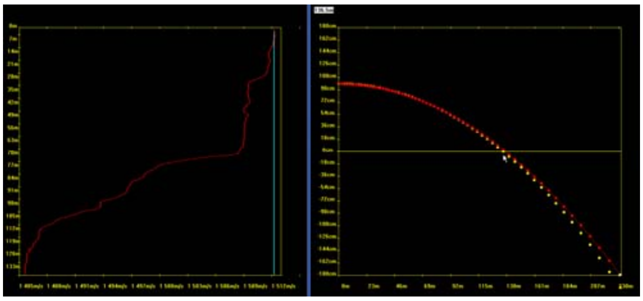

Figure 7
Left profile 14:04 (red) and the default survey profile (cyan) Right the perturbation of the sea bed (red) and the least squares approximation (yellow)

The case in point is profile 14:04 for which the Cross-Section method yielded corrections between -1.5m/s and 4m/s in Figure 4. In order to push the simulation model to its logical conclusion we shall as survey profile choose the default survey profile, which at any depth equals the value measured at transducer depth. It is tacitly understood, that if the adjusted default profile at some depth *D* approximated profile 14:04 well, then the adjustment at that depth read from Figure 4 applied to profile 14:04 is OK too. **Figure 7** left depicts the two profiles. ***Figure 7*** right depicts (in red) $d_i - D$ from the right hand side of the observations equations together with the corresponding least squares estimates (in yellow), for the set of integer angles below 60° with *D*=136.5m. ***Figure 8*** right depicts the least squares residuals $\widehat{\varepsilon_i}$, i.e. the depth differences at 136.5m caused by exchanging profile 14:04 with the adjusted default profile. This result only relates to the depth 136.5m, of course. ***Figure 8*** left illustrates the consequence of exchanging the two profiles 10m above the sea bed at 126.5m.

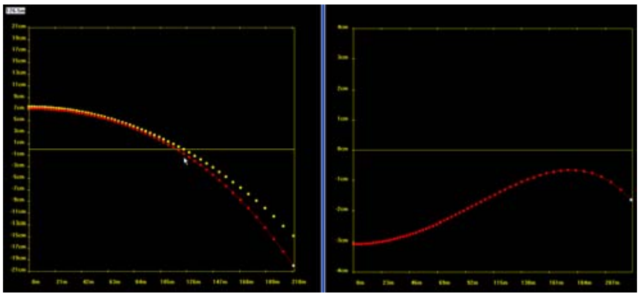

Figure 8
Change in depth caused by exchanging profile 14:04 with the adjusted default profile at 126.5m (left) and 136.5m (right)

Table 1 quantifies the differences between profile 14:04 and the adjusted default profile by depicting estimated standard deviations of the horizontal and vertical displacements based on ray-tracing for the set of integer launch angles between 0° and 60°, together with the vertical difference between the two profiles at launch angles 0°, 45° and 60°. The table depicts also the variation of this set of values for changes of ±0.2m/s at transducer depth for the default profile.

Table 1
The simulation model applied to profile 14:04 and the adjusted default profile at depth 136.5m

Online s/v	Vertical stddev.	Horiz. stddev.	Error at 0°	Error at 45°	Error at 60°	$\hat{\rho}$
+0.0m/s	0.024m	0.035m	0.03m	0.01m	0.02m	-10.5m/s
-0.2m/s	0.038m	0.036m	0.04m	0.03m	0.05m	-10.4m/s
+0.2m/s	0.017m	0.035m	0.02m	-0.01m	-0.02m	-10.6m/s

For reference, for the SVP-70 which was used to measure the s/v at the transducer depth during the survey, the factory specifies a standard deviation of 0.025m/s.

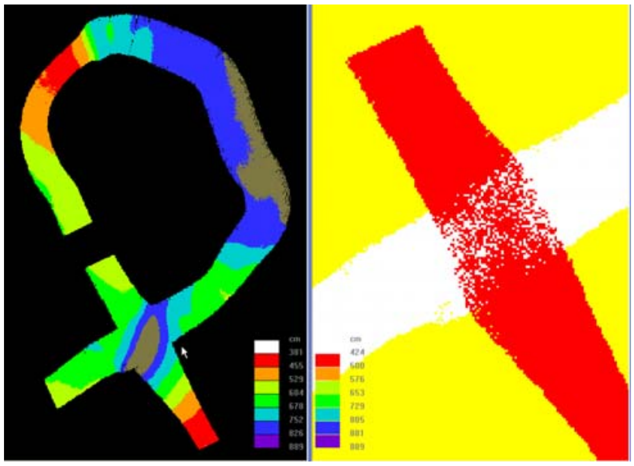

Figure 9 *Loop survey. Cell size 60cm. Reson SeaBat 8101*

The loop

Figure 6 demonstrated the robustness of the estimates with respect to cell sizes for survey 00309. The sea bed of this survey is flat relative to the sizes of the crossings of the survey lines with the check lines, a characteristic it shares with most of the sea bed in Danish waters. The question arises if the Cross-Section method requires the sea bed to be flat in order to yield usable estimates. ***Figure 9*** depicts a DTM with cell size 60cm of a loop surveyed by HDMS O-2 using a SeaBat 8101 with a SVP-C mounted at transducer depth. In order to stress the method, the crossing was positioned on top of a 1.5m deep depression in the sea bed on 6m of water. Once more the survey was RTK and the blending of the cells in the close up of the intersection to the right in the figure testifies to the integrity of the sensors.

Table 2

Parameter estimates for the loop for various cell sizes.

Cell size	$\hat{\rho}_1$	$\hat{\rho}_2$	$\hat{\delta}_{1,2}$	$\hat{\sigma}_{1,2}$
25 cm	0.18 m/s	0.11 m/s	1.6 cm	2.8 cm
30 cm	0.23 m/s	0.06 m/s	1.7 cm	2.5 cm
40 cm	0.48 m/s	0.20 m/s	1.7 cm	2.2 cm
50 cm	0.57 m/s	0.15 m/s	1.8 cm	1.9 cm
60 cm	0.73 m/s	0.33 m/s	1.7 cm	1.7 cm
70 cm	0.87 m/s	0.57 m/s	1.7 cm	1.5 cm
80 cm	1.05 m/s	0.82 m/s	1.7 cm	1.6 cm
100 cm	1.40 m/s	0.88 m/s	1.8 cm	1.6 cm
150 cm	2.83 m/s	1.94 m/s	1.8 cm	2.6 cm
200 cm	4.67 m/s	3.20 m/s	2.0 cm	3.5 cm
250 cm	6.99 m/s	5.19 m/s	2.1 cm	4.3 cm

Table 2 depicts estimates for the loop using cell sizes ranging from 25 cm to 2.5m. The last column in the table contains the square root of the a posteriori variance factor, i.e. estimates of the standard deviation $\hat{\sigma}_{1,2}$ between the two DTMs after the corrections have been applied to data.

Now, by construction the second and third column should be equal for a fixed cell size, because the crossing lines were near simultaneous. Considering that a 1m/s deviation at 7m from (1.1) corresponds to 1cm at 60° I think the reader will agree that the variation in Table 2 is acceptable.

The variation with respect to the cell sizes, however, is another matter, because the estimates rapidly become meaningless concurrently with the DTMs lacking ability to represent the sea floor. In case that there are no artefacts in data, and indeed from the blending of the cells in Figure 9 everything looks OK, it makes sense to choose the cell size 70cm which minimizes the variance between the two DTMs, although any choice between 50 cm and 1m probably will be of use.

Discussion

In hydrographic surveying, s/v in the water below the vessel is measured in profiles and a model for the variation of the s/v is adopted, in which it only depends on the depth. Any change in the s/v profile relative to the measured one will then, at a fixed depth D, lead to a perturbation $f(.)$ for which $f(x)=f(-x)$ in the co-ordinate system introduced above. In mathematical parlance $f(.)$ is an even function and may be represented to any prescribed degree of accuracy by some polynomial in even powers of x. Considering that experience shows, that multibeam measurements react to errors in the s/v profile by bending the swath gently, it is not surprising that this bending can be approximated very well by a polynomial of degree 2. The fact worth noticing, however, is that when the s/v at the transducer is known the approximating polynomial belongs to a special class (1.4) which leaves the depth at ±45° unchanged (1.1). The reason that it is so does not follow directly from (2.7), because tools like Hölder's inequality by their very nature are pessimistic and indeed, even in the shallow Danish waters one cannot expect the approximation to be good in the interval [-75°,75°] which is the standard range of many multibeam systems. Restricted to the interval [-60°, 60°] in shallow water, the matter is different. For example, the simulation model applied to 5793 s/v profiles sampled in waters deeper than 10m yields 207 cases where the change at 45° exceeds 1cm and 78 cases where it exceeds 2cm. Profile 14:04 is one such case and it is worth noticing, that even though the change at 45° is at the tail of the distribution, the residual from the approximation, depicted in Figure 6 right, is a polynomial of degree 4, just as one would expect.

Acknowledgement

I gratefully acknowledge the many fruitful suggestions to the manuscript from Thomas Eisler.

References

IHO Standards for Hydrographic Surveys (S-44) 5th Edition, Annex A – Guidelines for Quality Control, February 2008.

Eeg, J. (2004) Verification of the Z-Component in the RTK Survey of Drogden Channel. *International Hydrographic Review,* Vol. 5 No. 2, 16-25.

Eeg, J. (2008) On the Roll Calibration of a Multibeam Echo Sounder. Unpublished.

Eeg, J. (1999) Towards Adequate Multibeam Echo-sounders for Hydrography. *International Hydrgraphic Review,* Vol. LXXVI No. 1, 33-48.

Eisler, Thomas J. (2000) Ray-path Stability in Coastal Waters. *International Hydrographic Review*, Vol.1 no.2, 30-40.

Appendix

Let the surface of the transducer coincide with the origin of a co-ordinate system, where the z-axis points towards the Nadir. The travel time T from the moment the ping leaves the transducer in the direction θ_0 with the z-axis until it reaches the depth d is given by the integral

$$T = \int_0^d \frac{dz}{C\cos\theta} \tag{2.1}$$

where the velocity of sound in water,C, is supposed only to depend on the depth z and the angle θ is found from Fermat's principle as

$$\frac{\sin\theta_z}{C_z} = p \quad , \qquad z \in [0,d] \tag{2.2}$$

p being Snell's constant, the value of which for any given launch angle, θ_0 , we shall suppose is found from s/v measurements at the transducer. Suppose now, that the value of the velocity of sound in water is changed according to

$$C_z \mapsto C_z + \Delta C_z = C_z(1+\rho_z) \quad , \quad z \in \left]0,d\right]$$

while it is kept fixed at the transducer. Then, from (2.2), for the same launch angle θ_0 , the angle is changed in the water below the transducer according to

$$\frac{\sin(\theta_z+\Delta\theta_z)}{C_z(1+\rho_z)} = \frac{\sin(\theta_z)(1+\rho_z)}{C_z(1+\rho_z)} = p, \qquad z \in \left]0,d\right] \tag{2.3}$$

By (2.1) the difference in time ΔT between the two paths becomes

$$\Delta T = \int_0^d \frac{dz}{C\cos\theta} - \int_0^d \frac{dz}{C(1+\rho)\cos(\theta+\Delta\theta)}$$

or,

$$\Delta T = \int_0^d \left[1 - \frac{1}{(1+\rho)\sqrt{\dfrac{1-\sin^2(\theta+\Delta\theta)}{\cos^2\theta}}}\right]\frac{dz}{C\cos\theta}$$

Using (2.3) we find

$$\Delta T = \int_0^d \left[1 - \frac{1}{(1+\rho)\sqrt{1-\rho(2+\rho)\tan^2\theta}}\right]\frac{dz}{C\cos\theta}$$

Expanding the square root in the absolute convergent binomial series

$$\frac{1}{\sqrt{1-\rho(2+\rho)\tan^2\theta}} = 1 + \frac{\rho(2+\rho)\tan^2\theta}{2} + R(\rho(2+\rho)\tan^2\theta)$$

with remainder $R()$ we find

$$\begin{aligned}\Delta T = &\int_0^d \frac{1-\tan^2\theta}{C\cos\theta}\cdot\frac{\rho dz}{1+\rho} \\ &-\int_0^d \frac{R(\rho(2+\rho)\tan^2\theta)+\tfrac{1}{2}\rho^2\tan^2\theta}{1+\rho}\cdot\frac{dz}{C\cos\theta}\end{aligned} \tag{2.4}$$

For the remainder we have

$$R(y) = \frac{\tfrac{1}{2}(\tfrac{1}{2}+1)y^2}{2!} + \ldots + \frac{\tfrac{1}{2}(\tfrac{1}{2}+1)(\tfrac{1}{2}+2)\ldots(\tfrac{1}{2}+n)y^{n+1}}{(n+1)!} + \ldots$$

Or

$$R(y) = \frac{3y^2}{8}\left[1 + \frac{5y}{6} + \frac{5\cdot 7y^2}{6\cdot 8} + \ldots + \frac{5\cdot 7\cdots(2n+1)y^{n+1}}{6\cdot 8\cdots(2n+2)} + \ldots\right]$$

So that

$$R(y) \le \frac{3y^2}{8(1-y)} \tag{2.5}$$

Let

$$\bar{\rho} = \frac{1}{d}\int_0^d \frac{\rho dz}{1+\rho} \quad and \quad \bar{\delta} = \frac{1}{d}\int_0^d \frac{1-\tan^2\theta}{C\cos\theta}dz \tag{2.6}$$

Then we can write the first integral in (2.4) as

$$\int_0^d \frac{1-\tan^2\theta}{C\cos\theta}\cdot\frac{\rho dz}{1+\rho} = \int_0^d \frac{1-\tan^2\theta}{C\cos\theta}\bar{\rho}dz + \int_0^d \left[\frac{1-\tan^2\theta}{C\cos\theta} - \bar{\delta}\right]\left[\frac{\rho}{1+\rho} - \bar{\rho}\right]dz$$

and (2.4) becomes

$$\Delta T - \int_0^d \frac{1-\tan^2\theta}{C\cos\theta}\overline{\rho}dz = \int_0^d \left[\frac{1-\tan^2\theta}{C\cos\theta} - \overline{\delta}\right]\cdot\left[\frac{\rho}{1+\rho} - \overline{\rho}\right]dz$$
$$- \int_0^d \frac{R(\rho(2+\rho)\tan^2\theta) + \frac{1}{2}\rho^2\tan^2\theta}{1+\rho}\cdot\frac{dz}{C\cos\theta}$$

Where we can use Hölder's inequality on the integrals on the right side of the equality sign to get

$$\left|\Delta T - \int_0^d \frac{1+\tan^2\theta}{C\cos\theta}\overline{\rho}dz\right| \le \left\|\frac{1-\tan^2\theta}{C\cos\theta} - \overline{\delta}\right\|_2 \left\|\frac{\rho}{1+\rho} - \overline{\rho}\right\|_2$$
$$+ \left\|\frac{R(\rho(2+\rho)\tan^2\theta) + \frac{1}{2}\rho^2\tan^2\theta}{1+\rho}\right\|_\infty \left\|\frac{1}{C\cos\theta}\right\|_1$$

Or, using (2.1) and (2.5)

$$\left|\Delta T - \int_0^d \frac{1-\tan^2\theta}{C\cos\theta}\overline{\rho}dz\right| \le \left\|\frac{1-\tan^2\theta}{C\cos\theta} - \overline{\delta}\right\|_2 \left\|\frac{\rho}{1+\rho} - \overline{\rho}\right\|_2 + \sup\left[\frac{\frac{3(\rho(2+\rho)\tan^2\theta)^2}{8(1-\rho(2+\rho)\tan^2\theta)} + \frac{1}{2}\rho^2\tan^2\theta}{1+\rho}\right]T \tag{2.7}$$

Now, for a given depth d and s/v profile we can for any $\varepsilon > 0$ find values $\rho_0 > 0$ and $\theta_0 > 0$ so that

$$\left|\Delta T - \int_0^d \frac{1-\tan^2\theta}{C\cos\theta}\overline{\rho}dz\right| < \varepsilon \quad \forall|\rho| < \rho_0 \wedge \forall|\theta| < \theta_0 \tag{2.8}$$

In order to be of interest for multibeam surveying, however, it is necessary that (2.8) for sufficiently small ε holds for θ_0 .> $\pi/4$, so that the minimum of the integral implies that ΔT, regarded as a function of θ, attains a minimum at $\theta \simeq \pm\pi/4$ too. In the Danish Maritime Safety Administration it is natural to consider (2.8) for values of θ inside $[-\pi/3,\pi/3]$ because observations in a swath outside this angular sector are flagged out automatically during post-processing. For launch angles inside this sector, inspection of more than 13000 s/v profiles sampled during the period 2000 to 2009 shows, that (2.1) is well defined at the depth of the bottom of the profile. Moreover, measuring the variation of the s/v in the profile relative to the s/v at the transducer,

$$C_z = C_0(1 + \mathrm{P})$$

$|\mathrm{P}|$ was found to be less than 1% for five out of six profiles, whereas it was larger than 2% for 2% of the profiles. In terms of angular variation of the ping through the water column (2.3) yields, that for a launch angle of 60° the ray path varies between ±1° and ±2° respectively. These deviations decrease with decreasing launch angles, being diminished by almost one half at a launch angle of 45°, so we can write

$$\Delta T \simeq \int_0^d \frac{1-\tan^2\theta}{C\cos\theta}\overline{\rho}dz \simeq \frac{d(1-\tan^2\theta_0)\overline{\rho}}{C_d\cos\theta_d} \tag{2.9}$$

Or, using the differential form of (2.1)

$$\Delta z \simeq d(1-\tan^2\theta_0)\overline{\rho}$$

Biography of the author

Jørgen Eeg is head of validation of hydrographic data at the Danish Maritime Safety Administration. He gradated as a geodesist from the University of Copenhagen in 1972 and worked with approximation of the potential field of the earth by collocation, integrated geodesy and continuous modelling of plane networks until 1987. At that time the emerging graphic capabilities of workstations and the need to automate work with large data sets led him, following a brief spell of digital picture processing and digital cartography, into the field of hydrography, where he has worked since 1990.
e-mail: eeg@frv.dk

Article

A QUALITY ESTIMATOR OF ACOUSTIC SOUNDING DETECTION

By Xavier Lurton, Yoann Ladroit and Jean-Marie Augustin (France)
IFREMER

Abstract

Swath sonar bathymetry accuracy depends on the intrinsic performance of acoustic signal processing. We propose here a quality factor, quantifying the accuracy associated with every sounding computation. This descriptor is derived from simple models either for amplitude (variance of the centre-of-gravity instant of a fluctuating bell-shaped envelope) or for interferometric phase (local variance for a number of processed samples). The purpose is to attach to each individual sounding an objective quality level that is sonar independent, and directly applicable in bathymetry processing, either in data editing, or as an input parameter to statistical post-processing. This concept is illustrated by examples from experimental data.

Résumé

La précision des sonars bathymétriques dépend des performances intrinsèques du traitement des signaux acoustiques. Nous proposons ici un facteur de qualité, quantifiant la précision associée à chaque calcul de sonde. Ce descripteur est obtenu à partir de modèles simples soit pour l'amplitude (variance du centre de gravité d'une enveloppe fluctuante) soit pour la phase Interférométrique (variance locale pour un nombre donné d'échantillons). L'objectif est d'affecter à chaque sonde individuelle un niveau objectif de qualité valide quel que soit le sonar, et applicable directement dans le traitement bathymétrique, soit pour l'édition des données, soit comme paramètre d'entrée d'un post-traitement statistique. Ce concept est illustré par des exemples de données expérimentales.

Resumen

La exactitud de la batimetría obtenida por sonar de sector depende del rendimiento intrínseco del procesado de señales acústicas. Proponemos aquí un factor de calidad, cuantificando la exactitud asociada al cálculo de cada sondeo. Este descriptor se deriva de modelos sencillos para la amplitud (variación del instante del centro de gravedad de una envoltura fluctuante campaniforme) o para una fase interferométrica (variación local para un número de muestras procesadas). El objetivo es atribuir a cada sondeo individual un nivel de calidad objetivo que sea independiente del sonar y directamente aplicable en el procesado de la batimetría, al editar los datos o bien como un parámetro de entrada para el posprocesado estadístico. Este concepto está ilustrado mediante ejemplos de datos experimentales

1 Ifremer, NSE/AS, BP 70, 29280 Plouzané, France
2 Telecom-Bretagne, Dpt ITI, CS 83818 - 29238 Brest Cedex 3, France
3 DGA/D4S/MRIS, 92220 Bagneux (France)

1. Introduction

Multibeam echosounders (MBES) and interferometric sidescan sonars (ISSS, based on phase difference measurement)) provide a large number of sounding values per ping, obtained from the detection, inside each beam (MBES) or at each time sample (ISSS), of the seafloor impact location from either amplitude or phase processing (Lurton, 2010). The accuracy of this determination depends on many factors associated with either the environment of the sonar and its ancillary sensors such as sound speed or motion (Hare, Godin and Mayer, 1995; Hare, 1995) or to the intrinsic quality of the received acoustic signal and its processing (Lurton, 2003). Although crucial, this latter issue is the less well known, and is often treated as confidential by manufacturers, although some manufacturers have attempted to provide both sonar uncertainty models and real-time quality factors..

It is proposed here that the bathymetric detection from acoustic signals can be associated with a quality factor, describing the measurement performance associated with each sounding computation. Such a concept is expected by users of seafloor-mapping sonars, who need it for data quality estimation during field survey operations, for bathymetry data editing, and for post-processing (particularly the creation of digital terrain models). In this approach, the measurement quality should be directly available under an objective quantified form with a universal character (meaning that the quality descriptor should be the same – at least that its values are directly comparable-, whatever the sonar type, model and brand). Several attempts in this direction have already been made by sonar manufacturers (Reson 2007, Kongsberg 2008). Unfortunately, none has been really conclusive, for two main reasons:

- Usually the descriptor addresses the signal rather than the sounding itself, which is not what the user really needs; even an excellent estimation of the signal -to-noise ratio is only a step towards the expected sounding accuracy, involving a series of modelling steps (Lurton 2003).

- The signal- or sounding-quality estimation often includes some heuristic parts linked to one particular model of sonar, hence providing results valid only for a single configuration.

Hence the need for a universally accepted descriptor has not been fulfilled by these attempts.

The Quality Factor (*QF*) proposed in this paper is simply defined as the logarithm value of the relative depth error estimated directly from the signal used for detection. It is based on elementary models either for amplitude (the variance, in the time domain, of the centre-of-gravity instant of a bell-shaped envelope with fluctuating amplitude) or for interferometric phase (obtained from the local phase fluctuation variance, accounting for the number of processed samples). For one sounding, the uncertainty model is computed using the local characteristics of the actual signal and detection method used. The end goal of this approach is to assign to any sounding an intrinsic quality level valid whatever the sonar considered, and usable directly in the bathymetry processing, either for data flagging and selection, or as an input parameter to post-processing software such as CUBE (Calder 2003).

Thanks to the possibilities of recording intermediate data (signals at the beamformer output) in modern swath bathymetry sonars, the Quality Factor could be computed for a number of practical configurations. Comparisons have been conducted between the proposed *QF* and the estimated bathymetry accuracy, estimated from the statistical sounding value variance computed from an ideal terrain model. This process makes it possible to prove good agreement between the *QF* computed value and the objective uncertainty estimated according to the classical method used as an acceptance test for swath bathymetry sonars.

2. Sounding detection methods

For a huge majority of bathymetry sonars, each sounding value is actually computed by a basic operation (see Lurton 2003; for convenience, most notations are the same in this reference and in the present paper) applied to series of signal samples at the receiving channel output:

- Centre of gravity of the amplitude envelope, for the maximum amplitude instant method (MAI) in MBES;

- Zero-phase difference instant estimation (ZDI), for phase processing in MBES;

- Phase difference direction (PDD) estimation, for ISSS.

In all cases, a sounding computation is obtained from the estimation of a couple (range R, angle θ), or rather (time t, angle θ); see ***Fig.1*** for illustration and notation definition. These measured quantities are then converted into the space coordinates of the impact point geometrically referenced to the sonar arrays, accounting for refraction of the propagation paths; the georeferenced coordinates of the sounding are finally obtained by accounting for the sonar navigation and attitude. The sounding accuracy is hence a combination of the uncertainties caused by acoustical signal detection, refraction by sound speed variations, uncertainties in navigation and motion measurements, and installation geometrical parameters; see a detailed analysis in (Hare, Godin and Mayer 1995) and (Hare 1995). Only the phenomena linked to acoustical signal processing are considered here.

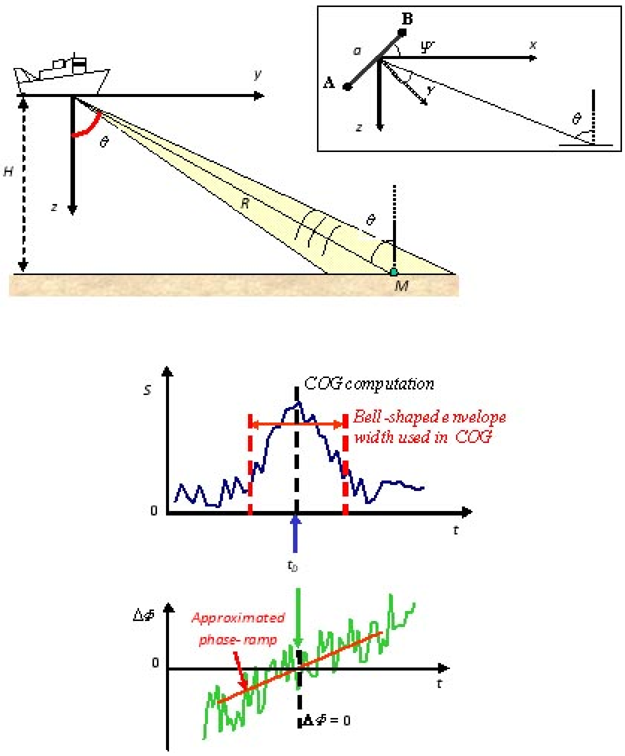

Figure 1. Multibeam sounding geometry (*top*) and notation definition, with a detailed view of the phase-difference measurement case. Arrival time detection by amplitude processing (*center*) (computation of the center of gravity of the bell-shaped envelope) and by interferometric phase (*bottom*) (detection of the zero-phase crossing instant of the phase ramp).

2.1. Amplitude detection

In beams incident at steep angles onto the seafloor, time detection is obtained from the amplitude envelope of the received signal. The most commonly applied processing consists in computing the centre of gravity of the time signal envelope (Fig.1). The accuracy is hence given by the time standard deviation of the COG of a bell-shaped signal perturbed by noise.

In the simplest case where the received time signal is a square window of duration *T*, assuming a Rayleigh-distributed amplitude, the COG instant variance (Ladroit *et al.* 2010) can be expressed as:

$$\delta t_D^2 = \frac{4-\pi}{\pi}\frac{N(N+2)T^2}{12(N+1)} \quad (1)$$

where *N* is the number of statistically-independent samples used in the COG computation.

In the more realistic case of a bell-shaped received signal, it is possible to change Eq.(1) into the more general shape :

$$\delta t_D^2 = B^2\frac{4-\pi}{\pi}\frac{N(N+2)T^2}{12(N+1)} \approx 0.0228 B^2 N T^2 \quad (2)$$

where *B* is a constant depending on the bell shape and on the width considered for the COG computation (Ladroit *et al.* 2010); this width can be defined e.g. by computing the second order moment of the envelope (see 3.2.1). The approximate form in Eq.(2) is valid for high values of *N* (an accuracy of 5% over δt_D is obtained beyond *N*=8). Note that *T* is the transmitted pulse duration for a CW signal; for a chirp, *T* should be replaced by 1/*W*, where *W* is the modulated bandwidth.

2.2. Phase detection

2.2.1. Detection of the zero-phase instant

In oblique- and grazing-incidence beams of MBES, detection generally consists in searching for the instant of null phase difference (Fig.1 and Fig.2) between the signals at the output of two sub-arrays forming beams in the nominal steering direction (Lurton 2003). This detection is blurred by the fact that the phase difference *vs* time is usually not a smooth line, but is strongly perturbed by noise. The dependence of phase variance on the signal to noise ratio (SNR) is given by :

$$\delta\Delta\Phi^2 \approx \frac{D-\gamma+\ln d}{d} \quad (3)$$

where *d* is the power SNR at the input of the phase-difference processing, $D \approx 3.1484$ and $\gamma \approx 0.5772$; this expression is valid for a Rayleigh-fluctuating echo with a sufficiently high SNR.

The fluctuation level of the individual phase-difference values is normally quite high (for instance, a 10 dB SNR should provide a 40° standard deviation of the phase difference). It is usually improved by averaging a number *N* of complex signal samples prior to the phase value computation. Then the phase difference variance after averaging becomes:

$$\delta\Delta\Phi_N^2 = \frac{1}{(N-1)d} + \frac{N}{2(N-1)(N-2)d^2} \approx \frac{1}{Nd} \quad (4)$$

considering that the *N* samples are statistically independent; the approximate form in 1/*Nd* comes for sufficiently high values of SNR *d* and sample number *N*. The derivations of formulas (3) and (4) are detailed in (Lurton and Augustin 2010).

The zero-phase difference instant is obtained by matching the fluctuating phase ramp with a straight line, or better with a second-order polynomial; this fitted ideal shape is then used for determining the zero (or possibly other phase angle) crossing within each beam. Statistically, this is equivalent to decreasing the fluctuation rate according to the number of samples used in this processing (Fig.2), equivalently to the averaging process of a random variable. Practically, fitting the phase ramp over N_A samples decreases the effective measurement variance by a factor $1/N_A$.

$$\delta\Delta\Phi_{N_A}^2 \approx \frac{\delta\Delta\Phi_N^2}{N_A} \tag{5}$$

Hence the higher the sample number N_A, the better the detection accuracy - with the disadvantage that the resolution is then degraded, raising the risk that small-size features may not be detected (Lurton and Augustin 2008).

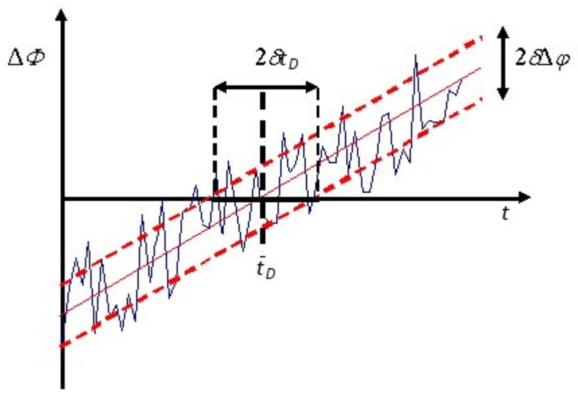

Figure 2. Arrival time uncertainty associated with phase-difference fluctuations. The time standard deviation is given by the projection of the phase-difference uncertainty onto the time axis.

2.2.2. Angle measurement from the phase difference

In an ISSS, the measurement uncertainty is to be considered as an angle error measured at a given instant. The relation between the measured phase difference and the incoming signal angle is given by the fundamental relation of interferometry :

$$\Delta\Phi = \frac{2\pi}{\lambda} a \sin\gamma \tag{6}$$

where a is the interferometer spacing, λ is the acoustical wavelength, and angle γ is referenced to the baseline axis (see Fig.1 for illustration and notation definition).

The angle error $\delta\gamma$ (equal to $\delta\theta$) corresponding to an uncertainty $\delta\Delta\Phi$ in the phase-difference value is hence given by:

$$\delta\gamma = \frac{\lambda}{2\pi a \cos\gamma} \delta\Delta\Phi \tag{7}$$

This last result illustrates the well-known observation that the phase-derived arrival angle estimation is better for large baselines, and directions close to the interferometer axis.

It is clear from the above that the angle accuracy will be improved by a decrease of the measured phase difference noise (given by Eq.(3) for elementary samples), which can readily be obtained by averaging over a number of consecutive samples, as given by Eq.(4). However in current ISSS, it is often chosen to limit (or possibly to omit) this averaging operation, and to provide raw estimates from individual samples, whose filtering is left to post-processing operations.

2.3. Sounding accuracy

The resulting sounding accuracy can be defined, in the general case, by the following relation (Lurton 2003):

$$\frac{\delta H}{H} = \frac{\delta t}{t} + \tan\theta . \delta\theta \tag{8}$$

Practically, time and angle are not estimated jointly: only one is, the other being fixed. In MBES, the measured quantity is the time of arrival, at a fixed angle (given by the beam steering angle), and Eq.(8) simplifies into :

$$\frac{\delta H}{H} = \frac{\delta t}{t} \tag{9}$$

For an ISSS, an angle measurement is performed at fixed values of time from the phase difference estimation, and the corresponding depth error writes:

$$\frac{\delta H}{H} = \tan\theta . \delta\theta \tag{10}$$

In both cases a residual component of the other parameter may be found (angle for MBES, time for ISSS) but it can usually be neglected.

Although the depth error is normally the main cause of concern in bathymetry data quality, the sounding location error in the horizontal transverse direction y is also to be considered:

$$\frac{\delta y}{y} = \frac{\delta t}{t} + \frac{\delta\theta}{\tan\theta} \tag{11}$$

However this aspect is not considered in the following. Similar developments to the depth error analysis proposed here can be readily derived in this respect.

3. The Quality Factor

3.1. Definition

For each one of the three bathymetry methods presented above (MAI, ZDI and PDD), an estimation of the relative depth error can be obtained directly from the corresponding modelling, parameterised by the local characteristics of the signal.

The purpose of the *QF* concept proposed here is hence to provide an *a priori* estimate of the sounding accuracy, based on the actual characteristics of the processed signal obtained from elementary observations and computations. **3**

The fundamental definition of the Quality Factor (noted q_F and *QF*) is given by:

$$q_F = \frac{H}{\delta H} \quad (12)$$

or, in a more convenient way, in logarithmic values:

$$QF = \log(q_F) = \log\left(\frac{H}{\delta H}\right) \quad (13)$$

With this definition, the *QF* value is greater for high-quality measurements, which is coherent with the concept of a quality descriptor. It takes typical values of 2 and 3 for relative depth errors of respectively 1% and 0.1%.

It can be inferred from Section 2 above that the practical computation of *QF* is dependent on the type of sonar considered; the various cases are developed below.

3.2. Multibeam amplitude processing

For amplitude-detected soundings from an MBES, the *QF* expression comes from the model presented in section 2.1, namely Eq.(2):

$$q_F = \frac{H}{\delta H} = \frac{t_D}{\delta t_D} \approx \frac{t_D}{0.15\, BT\sqrt{N}} \quad (14)$$

where t_D is the estimated detection instant, N is the number of independent time samples, T is the transmitted pulse duration, and B is the factor depending on the envelope shape.

3.2.1. Effective signal width

As evoked above, several definitions can be used for the processed width of the bell-shaped echo. A fall-off rate (typically –10 dB) is often considered. In order to improve the processing robustness, we preferred to consider a width N defined as twice the second-order moment of the normalized form $a(t)$ of the received time signal $s(t)$.

$$N = N_S / N_T$$
$$= 2 f_s \sqrt{\int_0^{+\infty} a(t) t^2 dt - \left(\int_0^{+\infty} a(t) t\, dt\right)^2} \; / N_T \quad (15)$$

with $$a(t) = s(t) / \int_0^{+\infty} s(t) \quad (16)$$

where the integrals are practically computed over a limited time window on the received echo. The number N of independent samples is expressed as a function of the number N_S of signal samples, and the number N_T of time samples inside the duration T. It was found that this approach is more effective than using an envelope fall-off rate, since it is less sensitive to the signal instantaneous fluctuations caused by multiplicative (Rayleigh-like) noise.

Using this width definition for simulations, we obtain the values of the B factor for several envelope types, given in Table I. Note that B is no longer unity in the case of the square window, since the definition of N given by Eq.(15) changes this value

Envelope Shape	***B* factor**
Square window	$\sqrt{\sqrt{12}/2} \approx 1.32$
Sinc	1.04
Sinc²	0.96
Cos	1.05
Cos²	0.99

Table I.
Proportionality factor B giving the effective width of bell-shaped envelopes of various types, when using the width definition from Eq.(16).

3.2.2. Validity limit of the QF definition in amplitude

The *QF* definition provided here is valid only if the original signal fulfils sufficiently well the requirement of a “bell-shaped” envelope.

If this is not the case, the *QF* value, computed over too short a time interval without guarantee of the selection relevance, will be overestimated. Checking the bell-shape character is readily done by computing the normalized integration of the squared signal as a function of time over the analysis interval duration T_A:

$$Y(t) = \int_0^t s^2(t)dt \,/ \int_0^{T_A} s^2(t)dt \qquad (17)$$

or $t \in [0,T_A]$. As a rule of thumb, the bell-shape criterion is admitted to be fulfilled if the difference $Y(0.7T_A)$-$Y(0.3T_A)$ is greater than 0.8.

This issue is particularly important if *QF* is used as an input for a post-processing algorithm such as CUBE (Calder 2003), where sounding values are weighted by their uncertainty: an erroneous high *QF* would cause the propagation of the value of this sounding in its adjacent nodes though its relevance is not as good as it seems. Also when using *QF* values for the choice between amplitude- or phase-detected sounding results, an inappropriate estimate of the amplitude *QF* may lead to a pointless elimination of phase-detected values : this is prone to happen at grazing angles where the bell shape is less pronounced while the phase difference processing is normally the best option.

3.3. Multibeam phase-difference processing

Phase fluctuations cause inaccuracy in the time detection applied in the ZDI method. Fig.2 illustrates the simple observation that the time detection δt_Φ uncertainty is given by the projection of the phase fluctuation onto the time axis, hence depending on the slope of the phase-ramp variation with time, it has to be increased by the uncertainty δt_T linked to the pulse duration T (Lurton & Augustin 2010). Hence the quality factor is defined as $q_F = t_D/\delta t_D$, where the detection time standard deviation is finally obtained as:

$$\delta t_D = \sqrt{\delta t_\Phi^2 + \delta t_T^2} \qquad (18)$$

$$\delta t_\Phi = \frac{\delta\Delta\Phi}{A\sqrt{N_A}}$$

$$\delta t_T = \frac{T}{\sqrt{12}}$$

where $\delta\Delta\Phi$ is the phase standard deviation measured over the effective part of the phase ramp used for curve fitting (featuring N_A statistically independent points); A is the phase-ramp slope; the$1/\sqrt{12}$ factor expresses the standard deviation of a uniformly distributed variable over the time duration T. Practically the phase-ramp is first to be matched with the approximated ideal curve, which provides the slope value A; the standard deviation $\delta\Delta\Phi$ is computed from the variations of the actual phase values around the ideal fitted ramp.

The phase-*QF* definition proposed for MBES is relevant provided that the null phase-difference detection is applicable over a long enough phase-ramp segment. This can be determined by analysing the number of time samples involved in this computation; typically a minimal number of 5 samples over the analysis interval is required. This defines the phase-detection applicability limit for beams at steep incidences.

3.4. Sidescan sonar interferometry

In ISSS processing, phase-difference fluctuations cause angle estimation uncertainty, which can be in turn expressed as a depth error, hence the quality factor comes as:

$$q_{F\Phi} = \frac{H}{\delta H} = \frac{1}{\tan\theta\ \delta\gamma} \qquad (19)$$

The angle measurement uncertainty $\delta\gamma$ can be expressed as the quadratic summation of two components $\delta\gamma_\Phi$ and $\delta\gamma_T$ linked respectively to the interferometric phase estimation noise and to the transmitted pulse duration:

$$\delta\gamma = \sqrt{\delta\gamma_\Phi^2 + \delta\gamma_T^2} \qquad (20)$$

$$\delta\gamma_\Phi = \frac{\lambda}{2\pi a\cos\gamma}\delta\Delta\Phi$$

$$\delta\gamma_T \approx \frac{cT}{2H\sqrt{12}}\frac{\cos^2\theta}{\sin\theta}$$

The phase component $\delta\gamma_\Phi$ is the one presented in Eq.(7). The pulse duration component $\delta\gamma_T$ given here is a first-order approximation, and can be improved by a more detailed derivation for small values of θ ; the $1\sqrt{12}$ factor expresses the standard deviation of a uniformly distributed variable over the angle sector spanned by the time duration T.

Practically the phase-difference standard deviation $\delta\Delta\Phi$ has to be estimated over a time interval surrounding the detection instant; this can be done conveniently by matching locally a linear phase-ramp segment on the actual data, similarly to what is done in ZDI processing (see Section 3.3).

Note that the differential phase may have been preliminarily processed (or not) by averaging over a number of time samples, depending on the details of the sonar receiver considered. Note finally that the *QF* definition provided here holds for the basic configuration of a simple interferometric measurement (with two receivers); it should be extended, in future works, to the case of more complex ISSS systems processing more than two receivers for an optimal combination of multiple angle estimations.

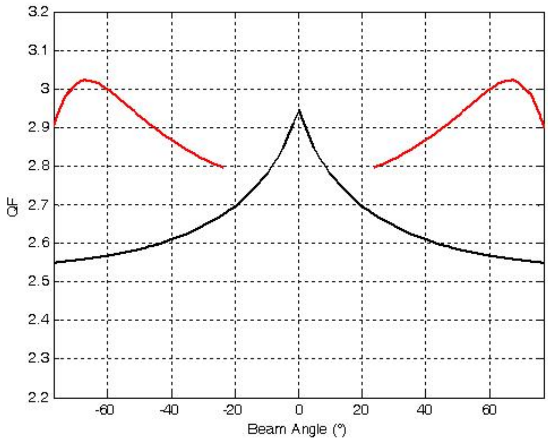

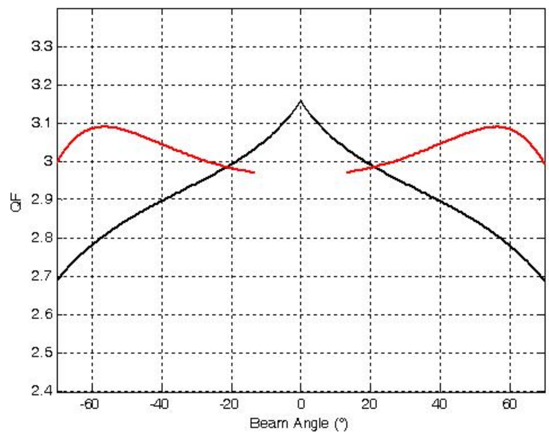

Figure 3. Example of *QF* computation over two simulated configurations. (*Top*) Shallow-water (30 m) high -frequency (100 kHz) case. (*Bottom*) Deep-water (2000 m) mid-frequency (24 kHz) case. These two configurations are close to the ones corresponding to the experimental results given in Fig.4. (*red is for phase processing, black is for amplitude*).

3.5. Simulation and first conclusions

The above models are used for simulating the computation of *QF* values as a function of the incident angle for two MBES configurations. Note that the two cases are very close to the configurations whose experimental results will be presented in Section 4.1.

The shallow-water case is a water depth of 25 m, a MBES at 100 kHz with 301 beams of 1.8°x 1.8° (beamwidth at –3 dB) over 152°, and a cylindrical array (neglecting in first approximation the beam aperture variation with steering angle).

The deep-water case is a 2000-m depth, a MBES at 24 kHz with 400 beams of 0.5° x 0.5° each (beamwidth at –3 dB) over 140°, and a flat horizontal array (hence causing an increase of the beam aperture with steering angle).

The *QF* values computed from these simulations are displayed in Fig.3. They make it possible to draw a number of first conclusions:

- Typical *QF* values are expected to range between 2.3 and 3.3 (i.e. relative depth errors of 0.5% to 0.05%);

- The amplitude *QF* is at its best at the normal from the seafloor; it then decreases as the incidence angles get more tilted from normal incidence;

- The amplitude *QF* either decreases continuously with incidence angle (for flat arrays with an increasing aperture of steered beams) or tends to a lower limit (for cylindrical arrays providing constant-aperture beams).

- The phase *QF* cannot be computed at normal incidences, where the interferometry processing is not applicable. It increases with the incidence angle, up to an optimal point, and then decreases at the swath extremities.

- The phase *QF* values, at their optimum, are as high or higher than the maximum value of the amplitude *QF*.

An intermediate regime with medium *QF* values is observed at the junction between the two regime (amplitude and phase)

All these preliminary conclusions regarding sounding quality are indeed in close compliance with practical field experiences of surveyors involved in MBES operation and data processing.

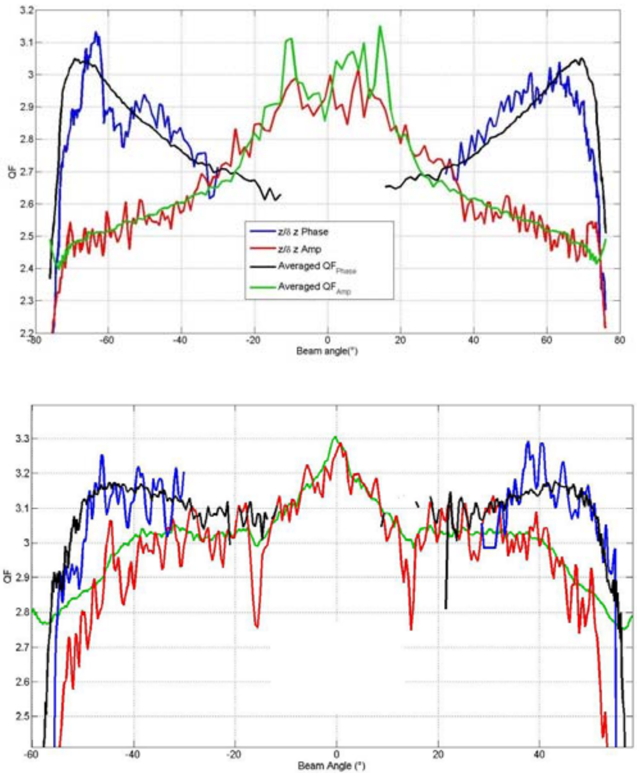

Figure 4. Comparison of the QF prediction and the actual sounding uncertainty, for a high-frequency shallow-water case (top) and a low-frequency deep-water case (bottom). The Quality Factor average predictions are presented for amplitude (green) and phase (black); the sounding uncertainty levels computed for amplitude (red) and phase (blue).

4. Validation over real data

4.1. Methodology

To compare the *QF* predictions with results obtained from actual bathymetry systems, we took advantage of the capacity of recent sonars to record data at the stage of raw signals (i.e. before the detection operations). This is made possible either as a dedicated optional module provided with the sonar, or by courtesy of the manufacturer providing experimental data.

On one side, the detected soundings delivered by the sonar are processed following the classical method used for bathymetry accuracy estimation. If a reference digital terrain model (DTM) is not available, then the soundings collected over a given area are used to generate it, by considering, as far as possible, multiple runs over the area and preferentially selecting the best-quality soundings (coming from MBES beams with moderate tilt). The obtained DTM is smoothed at a relevant scale, and the actual soundings are statistically compared to it, e.g., as a function of beam angle. This approach (that is the one classically used for checking the compliance of swath echosounders with accuracy requirements, e.g., during sea acceptance tests after installation) provides a reliable estimate of the actual sounding uncertainty. When possible, the two candidates for one sounding (in phase and amplitude) are considered.

In parallel with this, the raw signals are used for computing the *QF* values according to the formulas detailed in the above sections. Finally the results from the two methods are compared – the purpose being to check that the *QF* predictions are in good agreement with the sounding statistical uncertainties obtained from the bottom detection module.

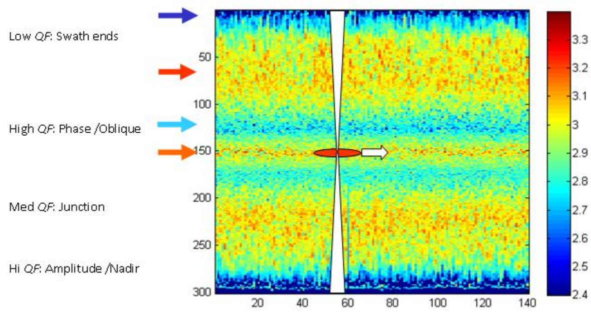

Figure 5. *Map of the resulting quality factor (high-frequency shallow-water case presented in Fig.4) represented as a function of ping number (abscissa) and beam number (ordinate). This illustrates the stability of the various regimes observed in the (top) plot: good quality factor (2.8 to 2.9) around nadir, excellent values at oblique intermediate angles (3.0 to 3.1); medium values (2.7) at the junction between the two regimes (around 30°) and poor quality (2.6 and below) on the swath extremities.*

4.2. Multibeam echosounder

A first example of comparison is given in *Fig.4* (*top*). This was obtained in a shallow-water configuration (depth about 30 m) with a flat horizontal seafloor, which is a favourable case for estimating the sounding accuracy. The echosounder is a Reson Seabat 7111 installed onboard *RV Pourquoi pas?*. Its main characteristics are: 301 beams of width 1.8° × 1.8°; total aperture 152°; frequency 100 kHz; equidistant soundings.

The sounding uncertainties are plotted both for the amplitude and phase detection. They are compared to the result of the *QF* computation; the agreement obtained is very satisfactory.

A second example of comparison is given in ***Fig.4*** (*bottom*). This was obtained in 2200 meters of water on a flat seafloor, using a Reson Seabat 7150 at 12 kHz. Its main characteristics are: 880 beams of width 0.5°x 0.5°, total effective aperture 135°, equidistant soundings.

Here again the agreement is very good between the estimated fluctuations of the measured bathymetry and the predictions provided by the *QF* computation.

Fig.5 illustrates the variations of *QF* plotted in the horizontal plane. It makes clear the stability of the various regimes: high values of *QF* close to normal incidence and at intermediate oblique angles (where interferometry works at its best); low values at the swath ends (corresponding to the decrease in SNR); and a local minimum at the junction between the amplitude and phase detection modes.

Fig.6 presents an example of practical application of *QF* computation to the processing of data from a scene featuring a wreck over a flat shallow seafloor. It includes the bathymetry data obtained from the amplitude and the phase processing; the *QF* values computed for both detection modes; and finally the resulting bathymetry, obtained by retaining the sounding candidates presenting the highest *QF* values, displayed together with the resulting *QF* map. This example clearly illustrates the interest of the *QF* concept in the sounding detection process.

4.3. Interferometric sidescan sonar

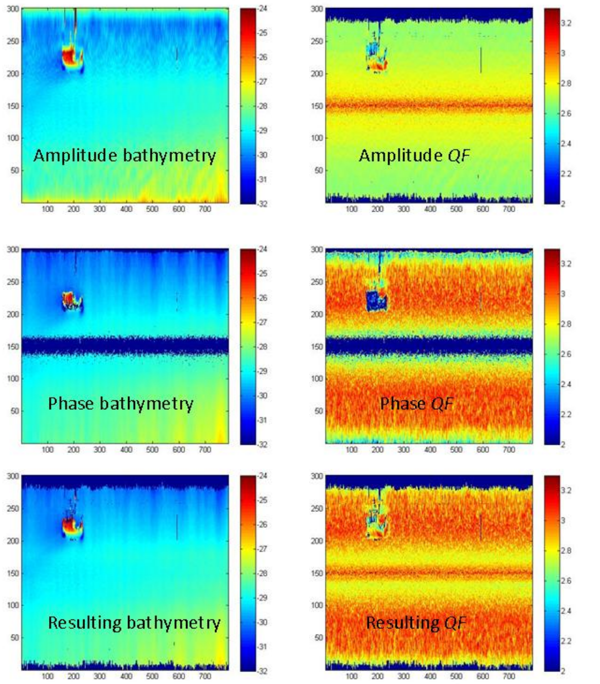

Figure 6. *Example of application of QF computation for the selection of soundings when both phase- and amplitude-detected candidates are in competition. The configuration is a high-frequency shallow-water case with a wreck present. The amplitude results (bathymetry and QF) are given in the top row ; the phase-difference detection results (bathymetry and QF) are in the central row; the lower row presents the resulting bathymetry and the corresponding quality factor.*

In this case the data made available by the manufacturer were the complex signals recorded from the receiving baselines. The sonar is a Klein series 5000, frequency 455 kHz, baseline spacing 4 wavelengths, pulse duration 0.2 ms; the signals were recorded over a flat sediment seafloor, at a sonar altitude of 9 m, with a sampling rate about 22 kHz.

The raw data were first used for computing the sounding values, using a classical process: the phase difference is computed between the baseline signals and unwrapped, then transformed into a signal arrival angle and finally the bathymetry values. The latter are filtered to obtain a smoothed terrain profile; a simple average over a square window was applied in this case. Finally, the local variance of the sounding values are computed from this smoothed bathymetry values.

The *QF* values are computed in parallel. Starting from the phase-difference values, a series of 30 samples is considered as a phase ramp (similarly to what is done in MBES processing) and fitted with a straight line; the phase variance around the ideal fitted phase ramp is then computed, and transformed into a depth uncertainty, which is completed by the term linked to the pulse duration. The resultant depth uncertainty is finally transformed into the *QF* value.

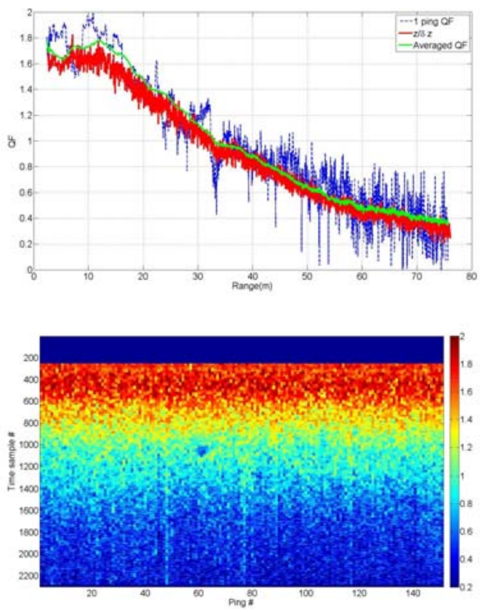

Figure 7. *Example of QF computation applied to an interferometric sidescan sonar (Klein 5000, frequency 455 kHz, baseline spacing 4 wavelengths, pulse duration 0.2 ms; signals recorded over a flat sediment seafloor, sonar altitude 9 m, sampling rate 22.5 kHz) .The upper plot presents the comparison between the estimated uncertainty in depth (red, log(z/dz)) and the QF prediction either averaged (green) or for one particular ping (blue). The second plot (bottom) depicts the computed QF plotted as a function of ping number (abscissa) and sample number in reception (ordinate).*

The comparison of these two processing results is given in ***Fig.7.*** It shows a very satisfactory agreement, in the sense that the *QF* values nicely describe the bathymetry fluctuations. This observation is not very surprising in itself considering that the bathymetry and the *QF* computations use the same formulas and input signals.

Also it is to be noticed that the *QF* values presented here (ranging from 0.3 to 1.8) are far poorer than the ones obtained with a MBES, and are characteristic of very inaccurate depth measurements. This should be tempered by the remark that absolutely no averaging has been applied in the processing; the phase-difference time samples have all been processed individually, which should normally not be the case in current situations, where some form of smoothing should occur, either over the individual soundings, or (better) over the input complex signal.

5. Conclusion: capabilities and limitations of the quality factor

The concept of a Quality Factor for individual soundings provided by swath bathymetry sounders has been proposed here for the most common configurations of modern sounding systems. Under this form, it shows a very good agreement between its estimates and the statistical results obtained from a classical analysis of the sounding uncertainty. The generality of the processing principles analysed here make it very versatile, independent of the sonar type, while of course depending on the details of the processing applied. In this respect, it is clear that the best option for its estimation is that manufacturers implement it in the bottom detection module, in order to provide it along with the sounding values as part of the output datagrams.

QF constitutes then a valuable and objective estimator of the local sounding quality. A major feature is that it gives direct access to the beam-by-beam bathymetric uncertainty (which for instance an estimation of the local SNR cannot provide directly). Based jointly on a model of the detection operations and on the received signal characteristics, it is an estimator of both the bottom-detection processing performance and the local signal quality.

One should keep in mind that *QF* only addresses the “acoustical component” of uncertainties in the sounding measurement process. The “global” bathymetry accuracy has to be completed by the components linked to ancillary sensors, vessel dynamics and environmental variables.

Moreover, *QF* is restricted to the simple configurations presented above, while the acoustical reality can be more complex. Several well-known issues in sonar bathymetry cannot be addressed, namely:

- ambiguities in phase-difference determination; this is one of the main problems met by ISSS. *QF* only estimates the quality of a correctly-unwrapped phase signal;
- the specular return influence close to normal incidence; a bottom detection biased by a strong specular signal may correspond to a high value of *QF*, which is hence inefficient for identifying such a problem;

similarly, external interferences from e.g. transmission from other sonar systems may be given excellent *QF* values (since they feature a very high SNR and a short duration); here again, *QF* is of no help for eliminating these unwanted signals.

The *QF* algorithm can be easily implemented in the standard bottom-detection software modules featured in the various bathymetry sonars; its computation time is negligible compared to the rest of the sounding detection operations. Its results are applicable to:

- the bottom detection algorithm, since it provides an objective criterion of choice between amplitude- and phase-determined candidate values for one given sounding (or, optionally, a weight that could be applied in an amplitude-phase blended detection solution);
- bathymetry data editing; once available in the datagrams, the *QF* values provide to the hydrographer a reliable tool for estimating the credibility of soundings, and help him in data cleaning (this suggests evolutions in post-processing software tools and in the training of hydrographers);
- quality control of bathymetry data; the locally-computed *QF* may be of interest for addressing objectively the trade-off between accuracy and resolution; bathymetry post-processing, in the case of high-density data; in such configurations, the statistical processing (Calder 2003) makes use of quality criteria for the measurement results, and *QF* can prove to be a very efficient input parameter for such an approach. In particular, this should enable multiple data sets from various sensors to be integrated (including e.g. both MBES and ISSS) in a single CUBE processing run.

Besides the ongoing works dedicated to refinements of the modelling and validation upon more experimental data, the next step in the *QF* development will be its transfer to sonar manufacturers for implementation in current bathymetry systems.

Hopefully this concept, once made operational, will prove to be a useful tool in bathymetry data acquisition and processing, especially given today's general trend toward the sounding density increase linked to progress in sonar technology, and the subsequent need for more automated methods of bathymetry data processing.

Acknowledgements

The authors are grateful to C.Sintes (Telecom-Bretagne) for providing the Klein 5000 data presented in Figure 7. The PhD of Y.Ladroit is funded by DGA (*Direction Générale de l'Armement*) and supervised by SHOM (*Service Hydrographique et Océanographique de la Marine*).

References

Calder B. (2003) Automatic Statistical Processing of Multibeam Echosounder Data. *International Hydrographic Review*, Vol.4, No.1, pp53-68

Hare, R. (1995) Depth and position error budgets for multibeam echosounding, *International Hydrographic Review*, Vol.72, No.2, pp.37-69

Hare, R., Godin, A., & Mayer, L. (1995) Accuracy estimation of Canadian swath (multibeam) and sweep (multi-transducer) sounding systems. *Canadian Hydrographic Service Internal Report*

Kongsberg (2008) *Instruction Manual - EM series Multibeam Echosounders Datagram Formats*, pp 44 & 52

Ladroit Y., Lurton X., Augustin J.M & Garello R. (2010) Accuracy modelling of bathymetry measurement by amplitude processing for multibeam echosounders. *Canadian Hydrographic Conference*, Québec, Canada

Lurton X. (2010) *An Introduction To Underwater Acoustics – Principles and Applications*, 2nd ed., Springer-Verlag, Berlin

Lurton X. (2003) Theoretical Modelling of Acoustical Measurement Accuracy for Swath Bathymetric Sonars. *International Hydrographic Review*, vol.4, N°2, pp 17-30

Lurton X. & Augustin J.M. (2008) Interferometry for Bathymetry Sonars: Accuracy, Resolution and Quality Factor, *Shallow Survey'08*. University of New Hampshire, Portsmouth N.H.

Lurton X. & Augustin J.M. (2010) A Measurement Quality Factor for Swath Bathymetry Sounders. *IEEE Journal of Oceanic Engineering*, accepted for publication

Reson (2007) *SeaBat 7125 High-Resolution Multibeam Echosounder System Operator Manual*, pp 85-86

Biographies of the authors

Xavier Lurton received the PhD degree in Applied Acoustics from the University of Le Mans (France) in 1979. He was first for eight years with Thomson-Sintra ASM, mainly specializing in sound propagation modeling for naval applications. In 1989 he joined Ifremer in Brest as an R&D engineer for underwater acoustical applications to oceanography. He is now head of the Underwater Acoustics service of Ifremer, and in charge of technological research programs on advanced methods for seabed-mapping sonars, his current interests being both in seabed backscattering physics, sonar signal processing and engineering of sonar systems, especially multibeam echosounders. He has also been teaching underwater acoustics in French technical universities for many years.

Yoann Ladroit received the Engineering Diploma in Telecommunications from Telecom-Bretagne (Brest, France) in 2009, with a specialization in signal processing; he also spent one training year with CEA (the French government agency for nuclear energy). After a stay at the University of New Hampshire and a polar cruise aboard *R/V USGC Healy*, he started his PhD works in October 2009, about bathymetry sounding qualification and new bottom detection methods for multibeam echosounders.

Jean-Marie Augustin received an Engineering Diploma in Electronics and a Master in Signal Processing from the Université de Rennes (France) in 1982. He joined Ifremer in 1984, as a R&D engineer in data processing, and has been working since then in the field of software development for oceanography applications, specializing mainly in sonar applications to geosciences. He is now a senior engineer at the Underwater Acoustics service of Ifremer; his main activity is software development for signal and data processing of seafloor-mapping sonars, in domains of bathymetry computation, backscatter reflectivity analysis and image processing. His personal R&D works are in the fields of image segmentation and filtering, sonar data processing, and advanced programming methods.

Article

PRESENTING AN AUTOMATED CALIBRATION PROCEDURE FOR AN AIRBORNE LIDAR SYTEM AND ITS POTENTIAL APPLICATION TO ACOUSTIC HYDROGRAPHY.[1,2]

By Lt Michael O. GONSALVES (USA)
NOAA National Geodetic Survey, Remote Sensing Division – JALBTCX
Department of Marine Science, University of Southern Mississippi

Abstract

Whether using an airborne lidar or a ship-based acoustic system, all hydrographers must contend with geometric system calibrations. A poorly aligned system leads to erroneously reported depths, diminished system resolution and internally inconsistent datasets. Most of today's calibration procedures are cumbersome and subjective enterprises that possess little statistical merit. This paper presents a least squares adjustment algorithm designed to calibrate a (presently under-development) lidar. This method is automated, objective, repeatable, and reports a confidence on the calibration values. Using simulated lidar datasets, the algorithm is explained and demonstrated. A brief modification is also proposed to expand the use to multibeam echosounders.

Résumé

Que ce soit à l'aide d'un lidar aéroporté ou d'un système acoustique embarqué, tous les hydrographes doivent faire face à des étalonnages de systèmes géométriques. Un système mal aligné conduit à des erreurs dans les profondeurs indiquées, à une diminution de la résolution du système et à des ensembles de données inconsistants en interne. La plupart des procédures d'étalonnage actuelles sont compliquées et sujettes à des tâches qui n'ont qu'un faible mérite statistique. Cet article présente un algorithme d'ajustement à l'aide de la méthode des moindres carrés conçu pour étalonner un système lidar (actuellement en développement). Cette méthode est automatique, objective, répétable et rend compte d'une confiance dans les valeurs d'étalonnage. A l'aide d'ensembles de données lidar simulées, l'algorithme est expliqué et démontré. Une brève modification est également proposée afin d'étendre leur utilisation aux échosondeurs multifaisceaux.

Resumen

Independientemente de si se usa un lidar aerotransportado o un sistema acústico embarcado, todos los hidrógrafos deben enfrentarse a las calibraciones de sistemas geométricos. Un sistema escasamente alineado conduce a errores en las profundidades indicadas, a disminución de la resolución del sistema y a colecciones de datos internamente inconsistentes. La mayoría de los procedimientos de calibración actuales son complicados y sujetos a tareas que poseen poco mérito estadístico. Este artículo presenta un algoritmo de ajuste mediante un método de mínimos cuadrados designado para calibrar un lidar (en vías de desarrollo actualmente). Este método es automatizado, objetivo, repetible, e indica una confianza en los valores de calibración. El algoritmo se explica y se demuestra utilizando colecciones de datos del lidar simulado. Se propone también una breve modificación para ampliar el uso a los sondadores acústicos multihaz.

---

1. Portions of this work were completed as part of the graduate program requirements of the University of Southern Mississippi.
2. This work is a revised version of a paper presented at the 2010 Canadian Hydrographic Conference.
3. Electronic mail: michael.gonsalves@noaa.gov

I. INTRODUCTION

Practitioners of acoustic multibeam hydrography are well-versed in the process of field calibration, referred to as the "patch test". The standard patch test seeks to resolve, through a series of coupled survey lines, the angular misalignments (pitch, roll, heading) between the Inertial Navigation System (INS) and the sonar. These lines, acquired over a particular grade of seafloor, are designed to isolate and identify a single parameter at a time. Final determination of these misalignments can be a subjective affair and is dependent upon the sound velocity (SV) and tidal characteristics being well known. In contrast, the geometric calibration of an airborne bathymetric laser, or lidar, can be performed on land, thus eliminating SV and tidal concerns. Further, rather than search the seafloor for suitable acoustic calibration targets, a lidar calibration can use cultural features like roads and gabled roofs.

The Coastal Zone Mapping and Imaging Lidar (CZMIL), a system presently under development by Optech International for the U.S. Army Corps of Engineers, will employ a prototype circular scanner using a refracting prism. This new design has the potential for geometric misalignments not previously confronted in a contemporary system and has forced its developers to rethink their calibration strategy. To this end, an automated least-squares adjustment (LSA) routine has been developed that allows all flight lines to be conducted over a single flat featureless surface (e.g. an airport runway or the sea surface).

In this paper, a brief background is presented on the current practices of multibeam echosounders (MBES) and lidar calibration, emphasizing some of the unique advantages airborne lidar has to offer. The LSA method of calibration is then discussed using synthesized datasets that simulate the CZMIL scan pattern.

Preliminary results will show that the technique is so robust the calibration routine can be expanded to simultaneously adjust up to 13 calibration parameters (some unique to CZMIL, and some that would be of interest to those who work with acoustic sounders). Finally, a discussion of the feasibility of modifying the algorithms for the development of an automated multibeam calibration utility is presented.

II. COMPARING TRADITIONAL CALIBRATION TECHNIQUES

A. Multibeam Echosounders

The National Oceanic and Atmospheric Administration (NOAA) offers several good descriptions for multibeam calibration (NOAA 2010a, NOAA 2010b). The goal of this calibration, or patch test, is to determine the angular alignment between the INS reference frame and the sonar reference frame (the pitch, roll and yaw bias), in addition to any time latency between the systems. For the purposes of this paper, it is assumed the systems being discussed will use some form of precise timing protocol (PTP) like those discussed in Calder and McLeod (2007). As such, time latency will not be further considered as a calibration parameter.

Calibration lines are typically acquired in pairs in such a way that the bias of a single parameter is isolated from the others. Depending on the parameter being investigated, these survey lines can be focused on a prominent feature on the seafloor (e.g. a rock) or on a featureless bottom. *FIG. 1* shows a simple line plan to be used by NOAA on a featureless bottom. Generally speaking, the pitch lines are run in opposing directions up-and-down a sloping bottom; the roll lines are run in opposite directions over any bottom profile; and the yaw lines are run in opposite directions such that their outer beams overlap (where a sloping bottom is required for yaw determination).

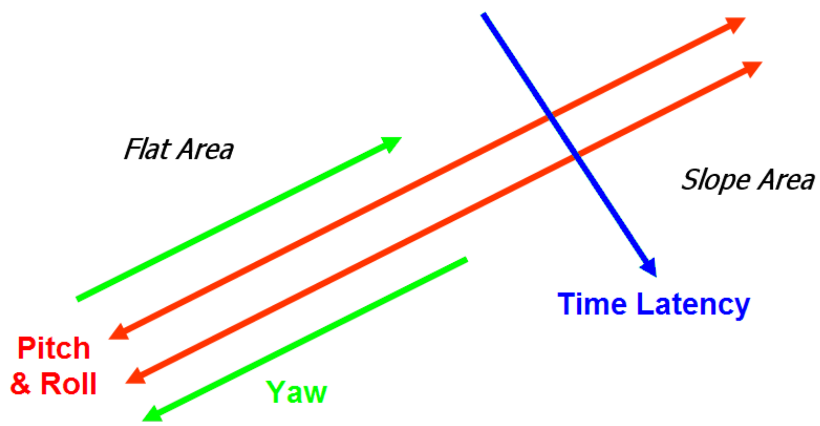

***FIG. 1**. A typical line plan for the calibration of a MBES (note the second set of pitch/roll lines is included for redundancy). Modified from NOAA (2010a).*

Once the survey lines are acquired, carefully chosen subsets of the soundings are examined to systematically determine each calibration value. For example, ***FIG. 2*** shows a subset of two swaths as viewed in the across-track direction, which are used to determine the system's roll bias. The roll values for each line are manually incremented until the two adjacent swaths appear to overlap. While this can be a subjective affair, some software packages do offer the ability to semi-automate this process.

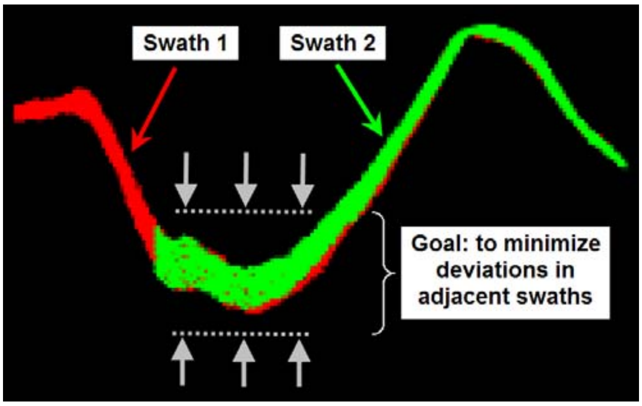

FIG. 2. *Two swaths of overlapping data are used to determine the MBES system roll bias. By steadily incrementing the misalignment, the two swaths are "rotated" until the swaths agree.*

If available, a prominent feature on the seafloor can be used as a calibration target. As depicted in ***FIG. 3***, a vessel travels over a rock going in opposite directions. The presence of a positive (forward-looking) pitch bias will result in the detection of the feature in advance of the vessel passing over the object, thus misrepresenting the objects location. By surveying in both directions, the two misrepresentations of the object can be brought into unison by adjusting the pitch bias. The scene depicted in ***FIG. 3*** can be used to adjust for a yaw bias if the rock is depicted in the swath's outer beams.

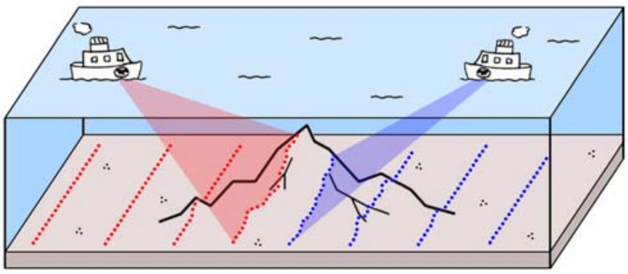

FIG. 3. *Prominent features on the seafloor are used to determine both pitch and yaw biases, as well as navigation time latency. As shown above, the two swaths are compared to determine the pitch bias. Note: due to the limited sonar ping rates, the swaths being compared are not exactly coincident; leading to an uncertainty in the calibration values.*

The drawback to using a target in the calibration procedure is that only a few "pings" of data are actually used during the adjustment. Additionally, these thin swaths may not necessarily even be at the peak (least-depth) of the feature, which is what the operator is using as a reference point in the adjustment. As a result, the confidence in the determined calibration values is diminished.

B. Lidar

The biggest difference between the calibration of a bathymetric lidar versus a multibeam is that the lidar isn't restricted to performing its calibration routine over the water. By performing the alignment on land, all uncertainties associated with sea swell, beam attenuation, and tidal effects are removed. While hydrographers must invest time in searching for appropriate study areas (flat bottom or prominent features), terrestrial targets are abundant in the form of roadways and buildings. Absolute positioning is an important aspect of survey accuracy control. It is a complicated enterprise to establish the absolute position of a feature on the seafloor; whereas, ground truthing on land can be accomplished by occupying desired calibration targets with static GPS base stations.

Most lidar calibrations are performed by acquiring data over cultural targets, like buildings (***FIG. 4***). The method of adjustment is similar to that of a multibeam calibration target in that cross-sections of the lidar swaths are examined, and the calibration values are steadily adjusted until data between overlapping strips match. Because it is difficult to establish conjugate points from one lidar swath to another, some adjustment procedures instead extract linear and planar features from the individual swaths (Habib et al 2008, Vosselman and Djikman 2001, Schenk 2001). Rather than adjust the points from one swath to another, these planar features are used instead (***FIG. 5***).

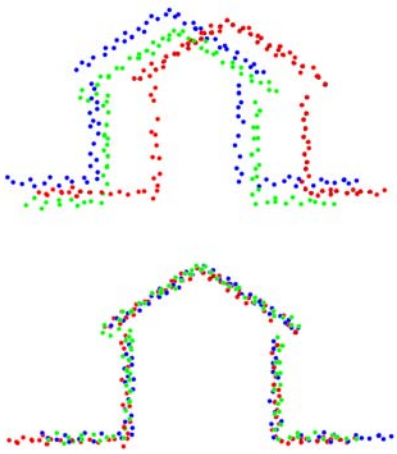

FIG. 4. (*top*) *A lidar point cloud (colored by acquisition) line as acquired over a gabled roof. The disagreement among lines reveals a poor alignment of the sensor. (bottom) By adjusting the calibration values, the building is brought into focus.*

The method of least-squares is increasingly used in lidar calibrations; the sections that follow give a brief overview of a new adjustment model. Rather than trying to best-fit neighboring strips or adjusting extracted roof tops to each other, the proposed model will fit the entire dataset to a single planar surface. This surface could be a cultural feature (like an airport tarmac) or the surface of a lake or ocean

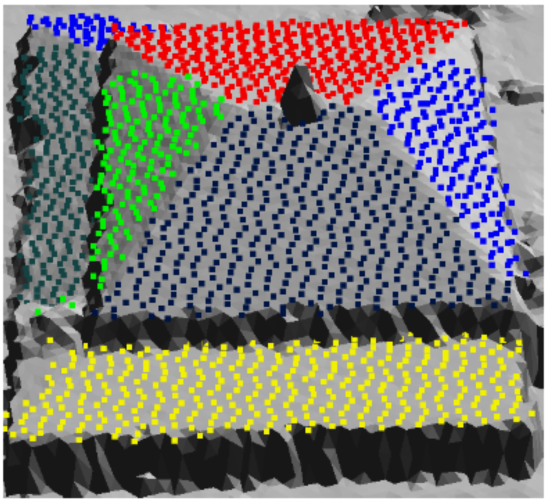

FIG. 5. A lidar point cloud acquired over a building. A planar extraction algorithm was performed to identify each of the surfaces of the building's roof. Reproduced from Freiss (2006).

III. A LEAST SQUARES APPROACH

A. A historical perspective

The application of an iterative least squares adjustment procedure is not unprecedented in the oceanographic world. In a pre-GPS constellation world, establishing a long baseline (LBL) acoustic positioning network was considered the most accurate technique for deep ocean positioning of a vessel and the only method for positioning equipment at or near the sea floor (McKeown 1975). The technique involves determining the position of a rover station (ship, submersible, etc.) through a series of acoustically-determined range observations from three or more deployed transponders of known (relative or absolute) position (FIG. 6).

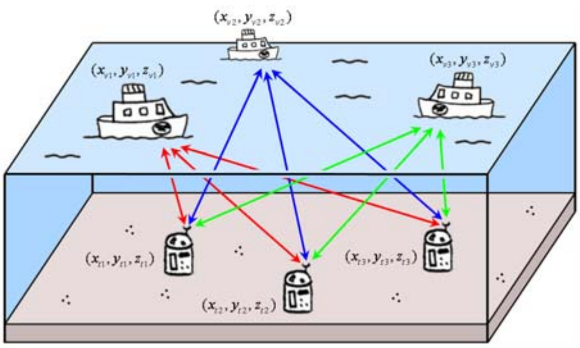

FIG. 6. A long baseline acoustic network: a collection of transponders of known positions (x_t,y_t,z_t) used to position a vessel in the water column or at the surface. (x_y,y_y,z_y)

When the transponders are first deployed, their positions relative to each other must be determined. To that end, several calibration lines are performed by a surface vessel: cloverleaves over each transponder to determine their least depth, and transect lines to determine baseline lengths for each transponder pair. These datasets establish a relative network and, with surface vessel position data collected in conjunction with the transponder ranges, establish "absolute" fixes of the network nodes. The principle drawbacks to this method are that it requires excessive ship time and tends to produce biased depth measurements.

A more efficient method proposed by Lowenstein (1965), invokes a least-squares adjustment. Under this method, the calibration lines are omitted and the vessel immediately begins its intended operations. During operations, the vessel logs the ranges to all the transponders. Once a nominal number of measurements are taken, the LSA adjusts the positions of the transponders until a best fit of all the measured slant ranges is determined.

Hydrographers may be familiar with a similar adjustment model in performing a static vessel survey. Here redundant angle and range measurements are taken among system components (GPS antennas, sonar head, vessel reference point, etc.) using a total station. These measurements are entered into an adjustment model which then estimate the relative positions of the components.

A least-squares adjustment procedure offers several advantages besides automation. Not only will systematic errors be identified, but analysis of the covariance matrix will provide estimates of the random uncertainty of each input parameter. Examination of the residuals can be used to detect blunders in the measurements. Lastly, and of critical importance in estimating the sounding confidences, an LSA provides uncertainties for the calibration values which can be used to compute estimated errors of the final depth measurements.

B. The adjustment model

To describe the least-squares adjustment model, first consider a generic function:

$$f(\vec{\ell},\vec{x}) = 0 \tag{1}$$

which has a first-order approximation:

$$f(\vec{\ell},\vec{x}) \approx \underbrace{f(\vec{\ell}_0,\vec{x}_0)}_{\vec{g}} + \underbrace{(\vec{\ell}-\vec{\ell}_0)}_{\vec{r}} \underbrace{\frac{\partial f}{\partial \ell}\bigg|_{\vec{\ell}=\vec{\ell}_0,\vec{x}=\vec{x}_0}}_{\mathbf{D}} + \underbrace{(\vec{x}-\vec{x}_0)}_{\vec{\delta}} \underbrace{\frac{\partial f}{\partial x}\bigg|_{\vec{\ell}=\vec{\ell}_0,\vec{x}=\vec{x}_0}}_{\mathbf{A}} \approx 0 \tag{2}$$

where:

f = the observation equation

$\vec{\ell}$ = observables' true values (laser range, vehicle position, etc.)

$\vec{\ell}_0$ = observables' measured values

$\vec{x}$ = adjusting parameters' true values (pitch bias, roll bias, etc.)

$\vec{x}_0$ = adjusting parameters' initial guesses

$\vec{r}$ = corrections to $\vec{\ell}_0$ (residuals)

$\vec{\delta}$ = corrections to $\vec{x}_0$ (adjustments).

Equation (2) can be rewritten as:

$$f(\vec{\ell},\vec{x}) \approx \vec{g} + \mathbf{D}\vec{r} + \mathbf{A}\vec{\delta} \approx 0 \qquad (3)$$

which, when applying the least squares model and solving for $\vec{\delta}$ yields:

$$\vec{\delta} = \left(\mathbf{C}_{x_0}^{-1} + \mathbf{A}^{\mathrm{T}}\left(\mathbf{D}\mathbf{C}_{\ell}\mathbf{D}^{\mathrm{T}}\right)^{-1}\mathbf{A}\right)^{-1}\mathbf{A}^{\mathrm{T}}\left(\mathbf{D}\mathbf{C}_{\ell}\mathbf{D}^{\mathrm{T}}\right)\vec{g} \qquad (4)$$

where:

$\mathbf{C}_{x_0}^{-1}$ = a priori estimate of uncertainties in $\vec{x}_0$

$\mathbf{C}_{\ell}$ = a priori estimate of uncertainties in $\vec{\ell}$.

To perform the geometric calibration, the lidar data will be acquired over a flat surface. The above least-squares adjustment will then be performed which will adjust the lidar calibration values to best fit the point cloud to that planar surface. A similar model was suggested by Freiss (2006), in which Equation takes the form:

$$f(\vec{\ell},\vec{x}) = \vec{n}\cdot\left(x_{OBS} - x_P\right) \qquad (5)$$

where:

$\vec{n}$ = vector normal to planar surface

x_{OBS} = 3D coordinates of laser point from laser location equation

x_P = 3D coordinates of fixed point on planar surface

In studying equation (5), one should note the dot product of two vectors is zero if the vectors are orthogonal (perpendicular). Given $\vec{n}$ is already normal to the plane (***FIG. 7***), that implies the vector $(x_{OBS} - x_P)$, and thus the point x_{OBS}, must be on the plane. Accordingly, equation fits the laser points x_{OBS} to a planar surface.

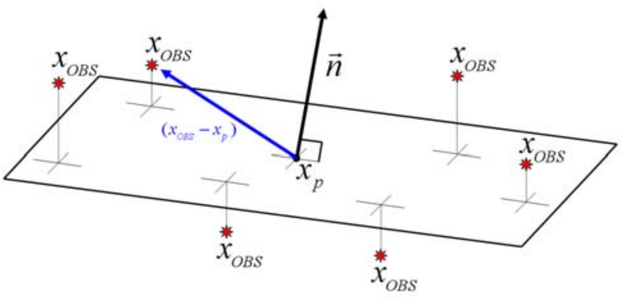

FIG. 7*. In fitting the point cloud to a planar surface, the dot product of the planar normal vector, $\vec{n}$, is taken with respect to the offset vector of each laser point, $\vec{x}_{OBS}$, and a fixed point on the plane, $\vec{x}_p$.*

C. A simplified calibration procedure (pitch, roll and yaw)

On initial inspection, one might think it is impossible to extract pitch, roll and yaw boresight misalignments from a featureless planar surface. What follows is an abbreviated geometric argument showing such a technique is possible. First, consider a circular-scanning lidar with no geometric misalignments that is flown over a horizontal planar surface (FIG. 8 – left). In a well-aligned system, the measured point cloud will perfectly describe the planar surface, and assuming a level flight, every laser pulse will report the same range between the laser and the laser footprint (within the measurement noise level).

Now consider if, unknown to the operator and processing algorithms, the laser is pitched 10° towards the nose of the aircraft (FIG. 8 – right). Under such a configuration, the forward-looking beams will travel a greater distance, while the aft-looking beams will travel a relatively shorter distance. The operator, still believing the lidar to be properly oriented, will interpret the longer-length forward beams, coupled with the shorter aft beams to mean the system is acquiring data down the backside of a hill. The key is that the biased point cloud will no longer describe a planar surface, but a helix with a vertical deflection that is proportional to the bias in the pitch boresight angle. This deflection from a planar surface is what will be resolved with the least-square adjustment.

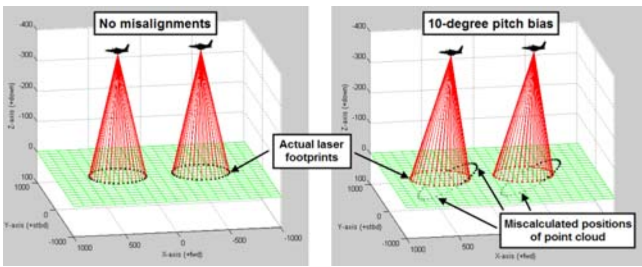

FIG. 8*. (left) Two revolutions of the laser scanner with no boresight misalignments – notice both circular traces are co-planar. (right) With a 10° forward (i.e. towards the nose) pitch boresight bias, two revolutions are again depicted with the actual laser footprints shown in red and the miscalculated point cloud shown in black – notice the biased points are no longer co-planar.*

Already, the circular-scanner design shows its advantages over a lateral swath design with regard to a geometric calibration routine; in the former case, a single level flight line will reveal the pitch boresight angle. Not all calibration parameters will immediately reveal themselves with such a flight itinerary. For example, introducing a roll boresight misalignment would cause the point cloud on the ground to also roll en masse (***FIG. 9***). Though the biased points from a single flight line would be *tilted*, they would still be co-planar, and thus immune to an LSA which seeks to adjust the point cloud to a planar surface. However, much like the acoustic patch test, if a second line of data is acquired with an opposing heading from the first, the resulting biased point cloud will not be co-planar with the first biased point cloud (***FIG. 9***). Thus the LSA can be applied jointly to these two datasets, adjusting the roll boresight calibration angle until the data is aligned with a single planar surface.

The previous discussion of roll encapsulates the flight line strategy associated with this adjustment procedure. The vessel must be maneuvered in such a way that any misalignments manifest themselves as a deviation from the otherwise flat planar surface.

If a vessel were to fly level over a horizontal ground (as in ***FIG. 8*** – left), then any yaw boresight misalignment would cause the point cloud to experience a radial shift across the ground; but would still be co-planar. To determine the yaw angle, the vessel must have a change in attitude. As depicted in ***FIG. 10***, if a vessel is pitching nose up, with no boresight misalignments, then the greatest measured laser range will be produced from the forward-most beam. Were this same vessel to have a yaw boresight misalignment, then the range from the forward-most beam would be erroneously assigned to an azimuth rotated by the yaw angle from the forward direction. The end result is a biased cloud that is sometimes below and sometimes above the actual ground plane, which permits solving for the yaw bias by adjusting to the planar surface model.

As an example of the algorithms' effectiveness, two 20-second flight lines were simulated flying in opposing directions (heading 0° and 180°) with vessel pitches of ±10° respectively (***FIG. 11***). The simulation added roll, pitch and yaw boresight misalignments of 10°, 15° and 20°. The calibration procedure converged to the correct misalignments with uncertainties (1-sigma) of 0.0022° in roll, 0.0023° in pitch and 0.0118° in yaw. The reported uncertainties are those output by the LSA algorithm. In all cases, the algorithm's calculated calibration values agreed (to within the predicted tolerances) of the "real" calibration values used in the simulation.

Regarding the simulation, noise was added to all the observations based on the manufacturer's specifications of the hardware. The planar surface was assumed to be flat, however even a rough surface can produce satisfactory results (Gonsalves 2010a). The reader should not be distracted by the large magnitude of the misalignments used in the simulation (10°, 15° and 20°); the algorithm performs equally well on a system with misalignments of only a few tenths of a degree.

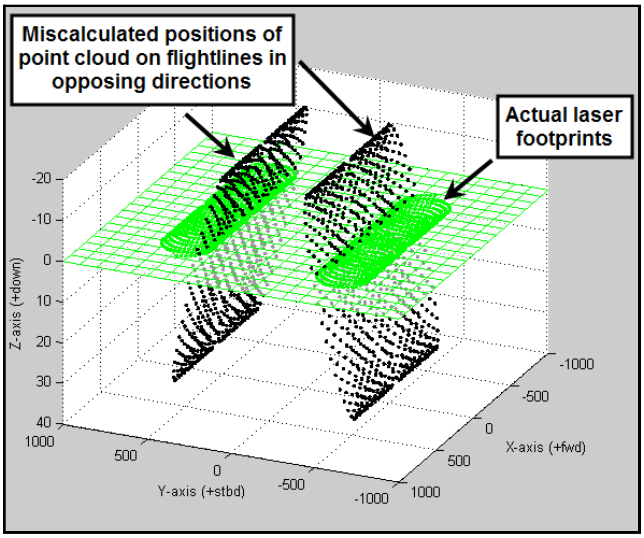

FIG. 9. *Two survey lines acquired with an unknown roll bias and opposing headings. The actual point cloud is shown in green; the miscalculated point cloud is shown in black. Notice the biased points for any given flight line are respectively co-planar, but are not co-planar with each other*

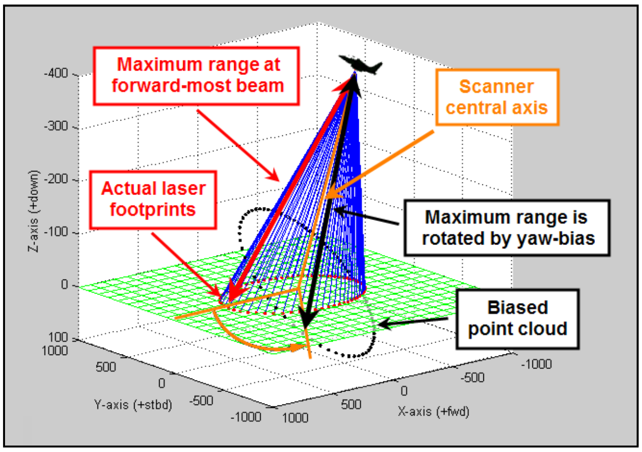

FIG. 10. *A vessel pitching nose-up will measure the longest slant range in its forward-most beam (indicated by red arrow). If this same vessel, however, has a yaw misalignment (i.e. a rotation about the scanner's central axis – in orange), then the range previously associated with the forward-most beam will be rotated by the yaw angle bias (indicated by black arrow).*

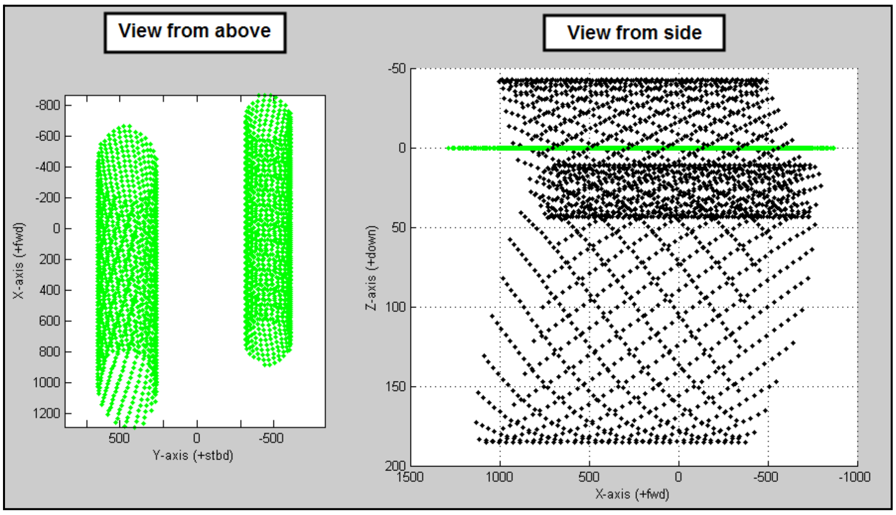

FIG. 11. *(left) Top view of two simulated flight lines used in a roll-pitch-yaw boresight calibration. (right) The incoherent point cloud pre-calibration (black) shown with the post-calibrated data (green) which has been fit to a planar surface.*

No. of flight lines used (Acquisition scheme - Laser pulse rate)	No. of laser strikes used	No. of parameters adjusted	Confidence in both the calibration parameters and maximum point cloud propagated uncertainty (horizontal and vertical)				
			1σ-roll	1σ-pitch	1σ-yaw	Horiz. TPU	Vert. TPU
Two lines (opposing direction - 50Hz)	~1,900	3 (roll/pitch/yaw)	0.0022°	0.0023°	0.0118°	0.074m	0.017m
One line (slow change in roll and heading - 50Hz)	~1,900	3 (roll/pitch/yaw)	0.0155°	0.0061°	0.0370°	0.251m	0.051m
One line (slow change in roll and heading - 10000Hz)	~188,000	3 (roll/pitch/yaw)	0.0005°	0.0002°	0.0011°	0.008m	0.002m
Four lines (2 rolling/yawing, 2 pitching/heaving - 10000Hz)	~751,000	11 (boresight, IMU offset, etc.)	0.0014°	0.0014°	0.2415°	0.012m	0.002m

Table 1.
Performance of calibration algorithm for various sized datasets and flight configurations

D. A more robust calibration

In the previous discussion, a means of determining the roll boresight misalignment was proposed by conducting two flights in opposing directions. Such a technique is in keeping with the traditions of the acoustic patch test in which a pair of coupled survey lines are designed to isolate a single parameter at a time. Interestingly, two separate flight lines are not required to determine the roll angle. What is required is merely a flight line where the heading changes. A single flight line in which the pilot makes a slow turn to the left or right provides enough linearly independent information to extract both the pitch and roll calibration values. Similarly, by also rolling the vessel, all three boresight angles can be determined from a single flight line (FIG. 12). For the purposes of the simulation, the vessel will roll 5° to the right, then 5° to the left, then return to a level attitude (a similar 5° oscillation will be imposed on the vessel heading).

The results of the calibration from the single dynamic flight line discussed above are shown in Table 1 – 2nd entry. Notice with the same number of data points the confidence (reported by a smaller standard deviation) is greater for the flight lines conducted in opposing directions. This is because flight lines in opposite directions present a stronger geometric alignment in which the biases due to roll are most pronounced. Ultimately the field personnel will decide whether to trade the greater confidence provided in multiple flight lines with the cost and time savings of a single wiggly line. It should be noted, however, that only 1/200th of the available data were used in the previous calibrations. If the full 10,000Hz dataset is included in the adjustment, then a 20-second flight line can successfully determine the three boresight angles to within a thousandth of a degree (Table 1 – 3rd entry).

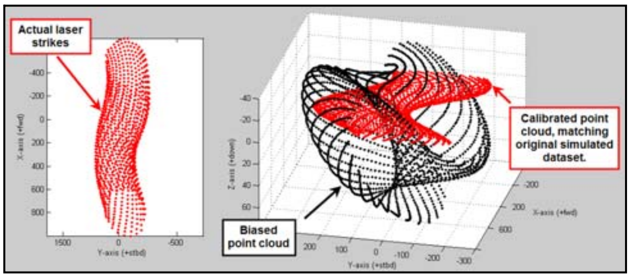

FIG. 12. *(left) Top view of a simulated flight line where the vessel exhibits a slow roll and change in heading. (right) Before calibration the point cloud is incoherent (black), but after application of the LSA, the calibration values are determined and the point cloud is restored.*

More important than the calibration values themselves is how the calibration uncertainties carry forward to the ultimate location of the soundings (as derived using the general law of the propagation of variances). For the 10,000Hz trial, the uncertainties in the calibration parameters will only contribute 0.008m (1σ) to the soundings horizontal uncertainty and 0.002m (1σ) to the vertical uncertainty (Table 1 – 3rd entry). When compared to the uncertainties of either ellipsoidal positioning or tides, the uncertainty of the calibration values are negligible.

As mentioned earlier, CZMIL is a prototype lidar with a novel scanner design. The impetus for pursuing a new method of calibration is in anticipation of having to calibrate a system which may exhibit geometric misalignments not previously seen. Going beyond just the roll/pitch/yaw boresight calibration, a total of 15 parameters are being investigated for calibration (***FIG. 13***). Using conventional "patch test" wisdom, in which a pair of survey lines are used to decouple each parameter, then one could conservatively anticipate having to run 16 survey lines to estimate all the parameters. The ability to solve for several calibration parameters at once (as demonstrated in ***FIG. 12***) showcase the flexibility afforded by the LSA approach.

While most of the parameters shown in ***FIG. 13*** are beyond the scope of this paper, one has received some attention in the hydrographic literature: aligning the vessel reference frame (VRF) with the INS reference frame (IRF). Any misalignments along this vertical axis will lead to cross-talk between the INS-sensed pitch and roll (Hilster 2008). For example, consider a vessel with a laser mounted one meter forward (measured with respect to the VRF) of the INS (***FIG. 14 - #1***). If this vessel were to strictly pitch, then the laser head would pivot up and aft (***FIG. 14 - #2***). However, should the INS be misaligned, while the vessel is pitching, the INS senses that it is mostly pitching along with a slight roll (***FIG. 14 - #3***).

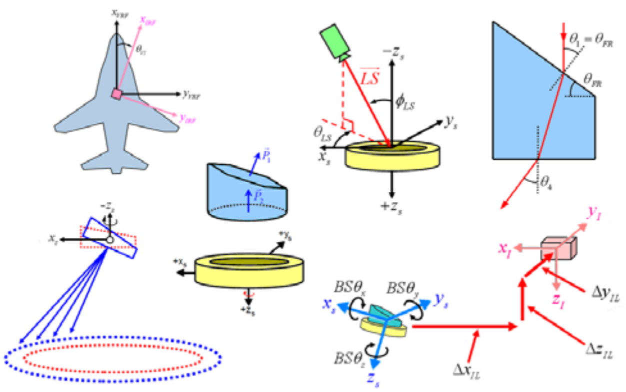

FIG. 13. *Some of the calibration parameters being adjusted for CZMIL include vessel-to-INS heading bias (upper left), scanner-to-prism alignment (lower left), prism slope (upper right) and INS-to-laser offsets (lower right).*

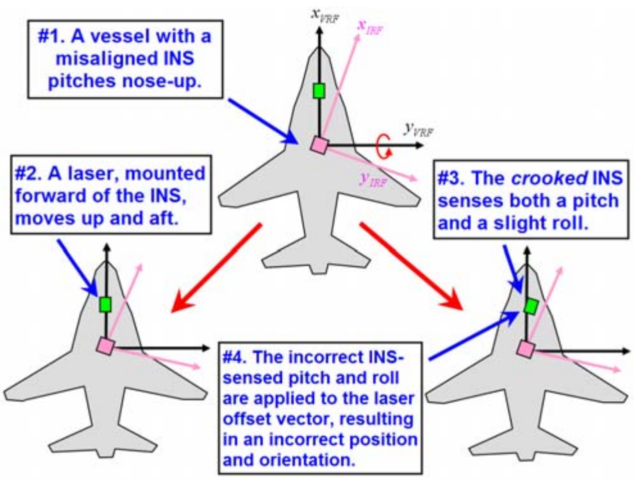

FIG. 14. *The effects of cross-talk in a poorly-mounted INS. Incorrect rotations are applied to the lever arms resulting in both translational shifts and angular biases.*

This sensed data is recorded and later applied when the vessel's trajectory is computed. By applying these incorrect rotations to the laser head it a) is computed to be in the wrong spot and b) will have an incorrectly computed orientation (FIG. 14 - #4). These induced errors are relatively minor and until recently, with system noise and poor GPS resolution, have been considered inconsequential (Hughes Clark 2003). With improved positioning techniques (real-time kinematics), which can achieve positional accuracies on the order of centimeters, these errors are rising above the noise. Finding a means of addressing this misalignment is important because, in the acoustic world, the conventional patch test methodologies do not provide any means of aligning a vessel reference frame to that of the INS (Hilster 2008, Hughes Clark 2003).

Returning to Table 1, one final calibration trial was simulated, this time attempting to calibrate eleven parameters at once (including the three boresight angles discussed previously). The greater number of parameters requires a more ambitious flight plan. In this case, four lines are flown: two crossing lines (one experiencing a slight change in roll attitude and heading and the second line experiencing a change in pitch and heave) and a second set of similar lines acquired at a different altitude. The calibration software succeeded in determining all eleven of the simulated misalignments. As an aside: among those calibration parameters was the INS-to-laser offset vector. Determining this vector through an LSA is equivalent to performing a static survey on a ship's sonar without ever hoisting the vessel from the water.

The observant reader will notice the larger reported uncertainty for the yaw boresight angle in the final calibration trial (0.2415° – 1σ). This increase in uncertainty can be attributed to the large correlation with the parameter modeling the VRF-IRF misalignment shown in ***FIG. 14***. When both the variances and the covariance of these two terms are taken into account, the contribution to the point cloud uncertainty from all the calibration parameters is again negligible (0.012m horizontal and 0.002m vertical - 1σ). For a complete discussion of the calibration uncertainties and the affects of covariance on the sounding accuracy, the reader is directed towards Gonsalves (2010b).

IV. FUTURE WORK

A. A multibeam calibration proof-of-concept

Even with an idealized piece of sea floor available (completely flat and featureless), there may still be some concerns whether a calibration routine, as discussed in this paper, is possible. That is, the lidar considered has beams looking both forward and backward, as well as port and starboard. The question is whether a multibeam echosounder, with its nadir-directed fan of beams is geometrically interesting enough to be calibrated in such a manner. The short answer is: yes, the geometry is present to develop a calibration routine similar to that outlined above.

To test the feasibility of a multibeam calibration routine, first a simplified sonar simulator is created, (***FIG. 15***). This simulation permits the input of any alignment between the INS reference frame and that of the sonar. For the purposes of this proof-of-concept, the water column is assumed to be of uniform density in which the sonar pulses do not refract. It is important to note that no form of beam stabilization (e.g. roll compensation) was incorporated, as the dynamics of a rotating swath are what feed the calibration.

Respective misalignments of 5°, 10° and 15° were introduced into the roll, pitch and heading mounting angles of the sonar with respect to the INS.

The virtual vessel was then cast off for one minute in a sea state that induced a ±5° roll every 10 seconds and a ±10° pitch every 20 seconds (data collected at 1 Hertz). The results of the calibration are shown in ***FIG. 16***. Not only was the least squares algorithm capable of correctly determining the system misalignments, but it did so with a confidence of greater than one decimal place for all misalignments (standard deviations of 0.02°, 0.04° and 0.05° for roll, pitch and yaw – results as reported by the LSA and though agreement between the predicted and "actual" misalignments). Similar to the lidar calibrator, preliminary simulations suggest the calibration works equally well whether the misalignments are large (as shown above) or only a few tenths of a degree.

While these results are by no means definitive, they are compelling. Plans are presently in development to acquire and calibrate actual sonar datasets. It will be interesting to see whether the calibration algorithms are robust enough to handle the additional complications of sound speed ray tracing, tides, vessel dynamic draft, and the intrinsic system noise.

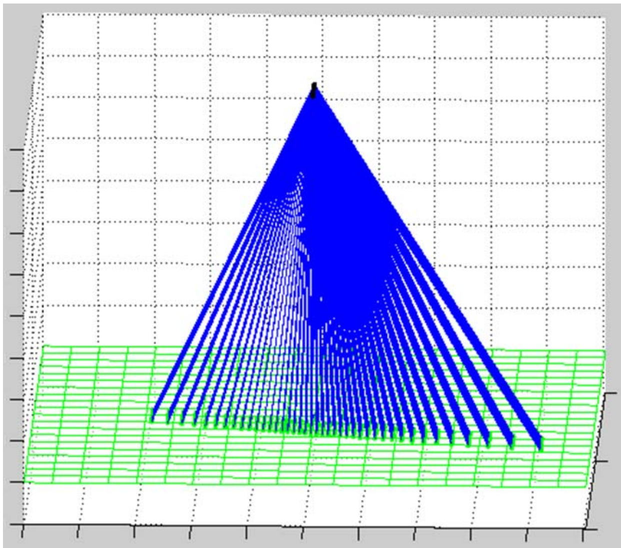

FIG. 15. *A simulated sonar scan pattern from a dynamic vessel.*

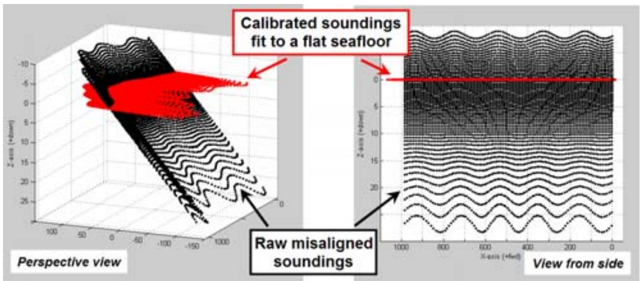

FIG. 16. *A simulated sonar dataset shown both before (black) and after (red) application of the least squares calibration routine.*

B. Closing remarks

It should be emphasized that thus far the methodology presented in this paper has only been performed in a simulated environment. Once CZMIL is delivered, the algorithms can be tested in an operational setting. With the brunt of the work already done, the lidar simulator and calibrator can be easily adapted for other lidar (or sonar) scanner designs.

Because the proposed LSA technique only requires a sea surface return (which is always present in the case of a bathymetric lidar) and a dynamic vessel attitude (which is provided by the atmosphere and the natural motion of the aircraft), production lines may contain all the information necessary for a calibration. This would imply an end to dedicated calibration lines, resulting in more time “on-project”. Further, a calibration routine could always be running in the background during survey, testing the calibration solution and warning the operator should a misalignment be detected – this changes the philosophy of calibration from simply being a pre-survey check to being a real-time quality assurance tool. Trajectory files of past survey flights will be processed to determine if they are dynamic enough to be used for calibration.

Also, while the calibration surfaces proposed in this paper were airport runways or the ocean surface, the author believes (as demonstrated in the above proof-of-concept) minor modifications could be performed to adapt the technique to use the sea floor instead. Mud flats, the broad continental shelf or areas with small-to-moderate sand waves all provide a “flat-enough” reference surface. If the sea floor can provide an initialization for the LSA, then a method of automated calibration for a multibeam echosounder is possible.

ACKNOWLEDGEMENTS

The author wishes to acknowledge Dr. David Wells for his relentless feedback in this research and NOAA’s Remote Sensing Division for encouraging his doctoral pursuits.

REFERENCES

- Calder, B. R. and McLeod, A. (2007). Ultraprecise absolute time synchronization for distributed acquisition systems. *IEEE Journal of Oceanic Engineering*, 32(4), 772-785.
- Friess, P. (2006). Toward a rigorous methodology for airborne laser mapping. *International Calibration and Orientation Workshop EuroCOW*. Castelldefels, Spain.
- Gonsalves, M.O. (2010a). Using a dynamic ocean surface to perform a geometric calibration of a bathymetric lidar. *Proceedings of the MTS/IEEE Oceans 2010*. New Jersey: IEEE.
- Gonsalves, M.O. (2010b). *A Comprehensive Uncertainty Analysis and Method of Geometric Calibration for a Circular-Scanning Airborne Lidar*, Mississippi: University of Southern Mississippi.
- Habib, A.F., Kersting, A.P., Ruifang, Z., Al-Durgham, M., Kim, C. and Lee, D.C., 2008, Lidar strip adjustment using conjugate linear features in overlapping strips. *Proceedings of the XXI ISPRS Congress. Part B1.* Publisher: ISPRS, pp. 385-390.
- de Hilster, N. (2008). The MRU and SRF Aligned. *Hydro International*, November 2008, pp. 24-28.
- Hughes Clark, J.E. (2003). A reassessment of vessel coordinate systems: what is it that we are really aligning?, US Hydrographic Conference 2003.
- Lowenstein, C. D. (1965). *Computations for transponder navigation*. Scripps Institute of Oceanography, Report No. MPL-U-2/65.
- McKeown, D. L. (1975). Survey techniques for acoustic positioning arrays. *Journal of The Institute of Navigation*, 22(1), pp. 59-67.
- National Oceanic and Atmospheric Administration. (2010a). *Field Procedures Manual*, Maryland: U.S. Department of Commerce.
- National Oceanic and Atmospheric Administration. (2010b). *NOS Hydrographic Surveys Specifications and Deliverables*, Maryland: U.S. Department of Commerce.
- Schenk, T., 2001, *Modeling and analyzing systematic errors in airborne laser scanners* (Technical Notes in Photogrammetry No. 19), Publisher: Ohio State University.
- Vosselman, G. and Dijkman, S., 2001, 3D building model reconstruction from point clouds and ground plans. *Proceedings of the ISPRS Workshop: Vol. XXXIV-3/W4. Land surface mapping and characterization using laser altimetry.* Editor M.A. Hofton, Publisher: ISPRS – 2001, pp. 37-43.

BIOGRAPHY OF THE AUTHOR

LT Michael O. Gonsalves is a NOAA Corps officer currently assigned to NOAA’s Remote Sensing Division (National Geodetic Survey), stationed at the Joint Airborne Lidar Bathymetry Technical Center of Expertise (JALBTCX) in Southern Mississippi.

He is presently pursuing his doctorate in Marine Science, with an emphasis in Hydrography, at the University of Southern Mississippi.

Article

MODELLING UNCERTAINTY CAUSED BY INTERNAL WAVES ON THE ACCURACY OF MBES

By Travis HAMILTON[1] and Jonathan BEAUDOIN[2] (CANADA)
(1) Ocean Mapping Group, University of New Brunswick
(2) Centre for Coastal and Ocean Mapping, University of New Hampshire

Abstract

A 3D ray tracing model has been developed to estimate the effects of internal waves upon the accuracy of multibeam echosounders (MBES). A case study examines the variability in these effects as a function of survey line direction and also considers the case of improving 2D ray tracing models with wave parameters derived from MBES water column imagery. Results indicate that, under certain circumstances, the effects of internal waves can prove to be a significant source of uncertainty that detracts from the ability to efficiently map the seafloor with wide swath angles.

Résumé

Un modèle de traçage à rayons tridimensionnels a été développé en vue d'évaluer les effets des ondes internes sur l'exactitude des échosondeurs multifaisceaux (MBES). Une étude de cas examine la variabilité sur ces effets comme fonction de la direction des lignes de sondes et traite également de l'amélioration des modèles de traçage à rayons bidimensionnels avec des paramètres d'ondes tirés de l'imagerie MBES des colonnes d'eau. Les résultats indiquent que, dans certaines circonstances, les effets des ondes internes peuvent s'avérer une importante source d'incertitudes qui porte atteinte à la capacité de cartographier de manière efficace le fond marin avec de larges angles de couverture.

Resumen

Se ha desarrollado un modelo de seguimiento de rayos en 3D para estimar los efectos de las olas internas en la exactitud de los sondadores acústicos multihaz (MBES). El estudio de un caso examina la variabilidad en estos efectos como función de la dirección de las líneas de sondas y considera también el caso consistente en mejorar el seguimiento de rayos en 2D con parámetros de olas derivados del tratamiento de imágenes de la columna de agua con MBES. Los resultados indican que, en algunas circunstancias, los efectos de las olas internas pueden resultar ser una fuente significativa de incertidumbre que le resta valor a la capacidad de representar eficazmente el fondo del mar con ángulos de corte anchos.

1. Introduction

One of the main sources of uncertainty for MBES soundings comes from refraction of the acoustic ray path due to variations in sound speed in the water column. Since most of the variability in sound speed occurs in the vertical direction, a vertical profile of the sound speed can be used to correct for refraction effects. If an incorrect or outdated sound speed profile is used then the acoustic ray travels along a different path than what was assumed, resulting in vertical and horizontal biases in the final 3D position of the sounding. The ray path is calculated with a ray tracing algorithm. Although there are different algorithms the key to refraction remains in Snell's Law (equation (1)):

$$\frac{\sin\theta 1}{sound\ speed\ 1} = \frac{\sin\theta 2}{sound\ speed\ 2} \tag{1}$$

where θ_1 is the angle of incidence between the ray and the interface through which it is refracting, and θ_2 is the refracted angle. For ray tracing the interface is between two layers of sound speed (*Sound speed 1* and *Sound speed 2*).

Given that the ocean environment is often generalized as being horizontally stratified, the assumption that sound speed only depends on depth is used for ray tracing (Lurton 2002). This approach greatly simplifies the mathematics in ray tracing models, as well as water column sampling, because it is difficult to measure any deviation from horizontal stratification. This base assumption allows each of the discretely measured layers of speed from a sound speed profile (SSP) to be modeled as a horizontally stratified plane of constant sound speed. With the horizontal stratification assumption, the angle of incidence between a ray and an interface, between two layers of sound speed, will always be relative to the vertical; however, in reality, this is not always the case.

In many areas internal waves occur along the pycnocline ("a layer where density changes most rapidly with depth. It can be associated with either a halocline or a thermocline." (Baum 2004)). This density gradient is often associated with a strong gradient in sound speed (velocline) which acts as a strong refracting layer. Internal waves can introduce a bias into the soundings acquired by a MBES through tilting and vertically oscillating the velocline. Figure 1 is an example of data which is believed to have been collected with the presence of internal waves in the watercolumn. The main objective of this work is to create a mathematical model to predict the uncertainty which is introduced into MBES soundings when internal waves are not accounted for in conventional ray tracing models. A secondary objective is to investigate the potential benefit of manipulating MBES water column imaging to account for the vertical oscillation of the velocline. Note that the uncertainty discussed in this paper is systematic because the uncertainty remains constant for any analysis of the same measurand, for this reason the uncertainty will be referred to as a bias throughout the paper.

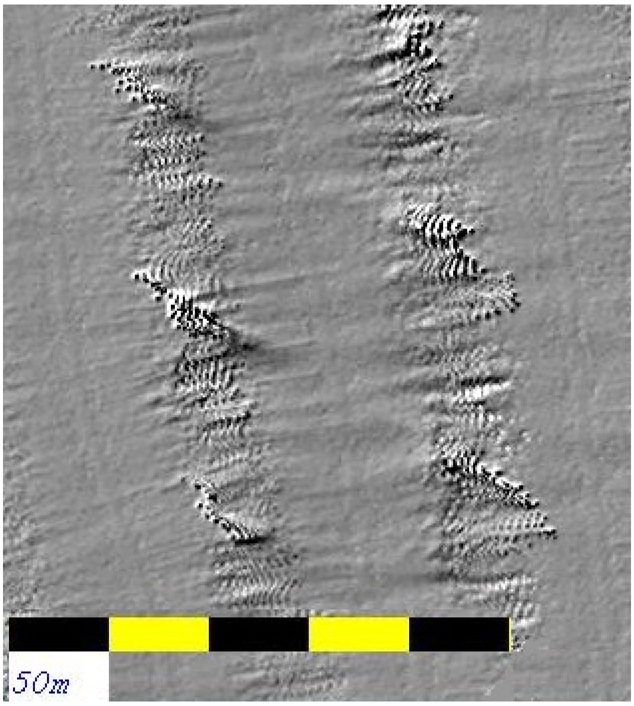

Figure 1: *Gridded MBES data that is believed to have been collected with the presence of internal waves in the watercolumn. Data courtesy of Roger Flood.*

Internal waves and their effect on MBES soundings are discussed in section 2, followed by an outline of the fundamental calculations required to perform the simulation. Finally the model is used in a case study to demonstrate the general behaviour of the bias and

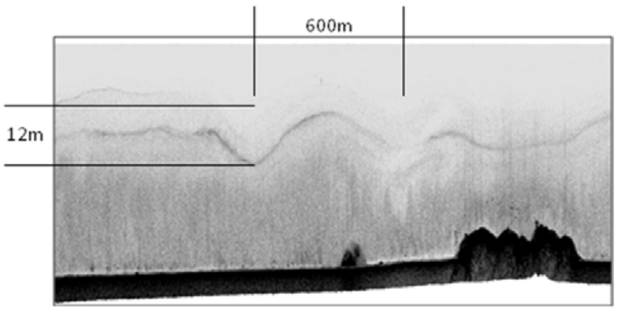

Figure 2: *Along track vertical cross-section of water column scattering intensity showing the presence of an internal wave. (After Hughes Clarke 2006)*

2. Internal waves and their effect on MBES accuracy

An internal wave can be described as a gravity wave which propagates within the volume of any fluid. In the ocean, an internal wave is generated upon the disturbance of the pycnocline. The disturbance can be caused, for example, by flow near a shelf break or over a shoal. Once disturbed, the energy propagates away from the generation point as a wave that travels along the pycnocline (Apel 2004).
A large portion of observed internal waves fall into the category of internal solitary waves which are also referred to as solitons. Solitons occur as groups of oscillations that consist of up to a few dozen cycles. Solitons often have rank-ordered amplitudes and wavelengths, meaning the amplitude and wavelength are both largest on the leading wave and decay with each oscillation (Apel 2004). Typical values for continental shelf internal waves are listed in Table 1.

The shape of a soliton is considered by some to be almost sinusoidal (Sandstrom and Oakey 1994); however they tend to take on a more triangular shape because the wave troughs move faster than the peaks, which cause the gradient to be steeper between the two. This situation is caused by the propagation speed increasing when the isopycnals are displaced downward and decreasing along its upward motion (Sandstrom and Oakey 1994). For the mathematical model discussed in this work the idea of an internal wave taking the shape of a sinusoidal wave is used to facilitate the numerical simulation.
As mentioned in the introduction, internal waves introduce uncertainty through two mechanisms. The first is the vertical oscillation of the velocline; Figure 3 helps to describe the situation. The vertical oscillation of the velocline causes its true depth (dashed line) to differ from its assumed depth (solid line) which was recorded with an SSP. The depth discrepancy causes two effects. The first causes the calculated ray path (red line) to refract at a depth that is different than the true ray path (green line), which alters the ray's path. The second effect causes the two rays (true and calculated) to spend different amounts of time in each layer of sound speed. The overall distance a ray travels is a function of time and sound speed, so the second effect causes the overall length of each ray to be different.

***Table 1**: Typical characteristics of solitons. Adapted from (Apel 2004).*

Characteristic	Symbol	Scale
Packet Length	L (km)	1 – 10
Wave Height	$2\eta_0$ (m)	-15
Upper Layer Thickness	h_1 (m)	20 – 35
Lower Layer Thickness	h_2 (m)	30 – 200
Long Wave Speed	C0 (m/s)	0.5 – 1.0
Maximum Wavelength	λ_{max} (m)	100 – 1000
Crest Length	C_1 (km)	0 - 30

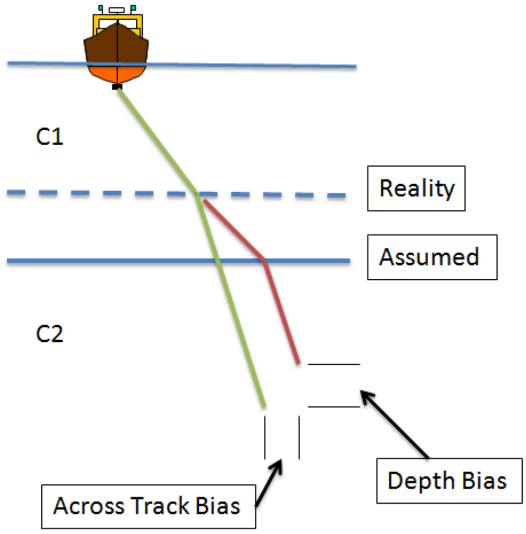

***Figure 3**: Effect of the velocline's vertical oscillation on MBES soundings*

The second mechanism through which internal waves introduce uncertainty into MBES soundings is tilting the velocline. The tilt violates the assumption that all layers of sound speed are horizontally stratified. Every degree of velocline tilt causes one degree of bias in the angle of incidence (Figure 4 (a)). Through Snell's law the incorrect incidence angle causes the refracted angle to be incorrect. It is an angular uncertainty that will cause both an across track (position) and depth uncertainty.
The problem is made even more complex by the fact that the internal wave causes the velocline to tilt about both the along track and across track axis. In the presence of a 2-axis tilt, the ray will no longer be constrained to a 2D plane (green plane in Figure 4 (b)). By ignoring the 3D aspect of the ray path, a bias results in the direction normal to the plane as this component can only be zero in a 2D ray tracing model. Uncertainty is also introduced into the depth and radial components of the ray traced solution as these components absorb the bias resulting from the 2D model's inability to account for the additional travel time associated with refracting out of the plane. One of the goals of this work is to gain an appreciation of the magnitude of the resulting bias; another goal is to gain a better understanding of the conditions under which this effect results in appreciable sounding bias.

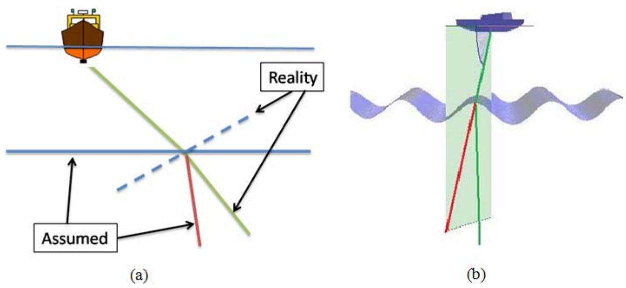

***Figure 4:** **(a)** Effect of across track tilt on refraction. **(b)** Effect of ignoring 3D refraction.*

3. Methods

Software was developed to simulate an estimate of the uncertainty introduced into MBES soundings by internal waves. The simulation requires several inputs to describe the characteristics of the watercolumn. The parameters are:

- the bearing of the survey lines relative to the direction that the internal wave propagates;
- water depth;
- sound speed above and below the velocline;
- the mean depth of the velocline;
- and finally the amplitude and wave length of the internal wave.

The software is currently designed to use equiangular 1° beam spacing with a 130° swath in an attempt to give a typical description of the uncertainty.
The foundation behind the software is that it traces the beam's path in 3D space instead of using the assumption that a beam is constrained by a 2D plane. The coordinate system used for the calculations is a right handed system. The x-axis is aligned with the direction of the internal wave's propagation, the z-axis is pointing down, the y-axis is oriented as to complete the right handed system, the internal wave is infinitely wide along the y-axis, and the origin is at the vessel's position during the first ping. This will be referred to as the internal wave coordinate system (IWCS, shown in Figure 5). The IWCS allows the vector representing the ships track relative to the internal wave to be calculated, simplifying the sounding coordinates by originally calculating them in the IWCS, rather than converting from ship based coordinates.

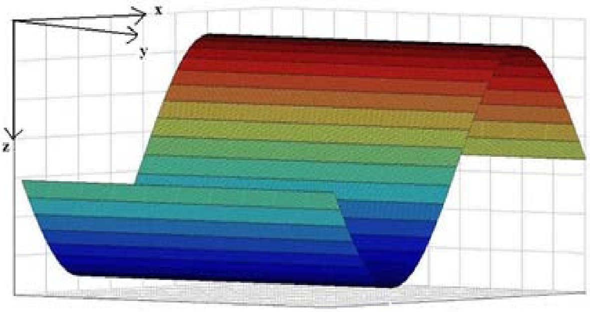

Figure 5: *Internal Wave Coordinate System.*

The simulation numerically models the path of an acoustic ray that travels through a water column which contains an internal wave and experiences three dimensional refraction based on the angle of incidence with the velocline and the sound speed in each layer (of a two layer water mass). Once it passes through the velocline the beam travels through the remainder of the water column until it strikes a synthetic flat seafloor at a user specified depth. The x, y, and z coordinates where the beam strikes the seafloor are used as the "true" coordinates (or solution) for the sounding; these are later compared with the biased solution for the same sounding..

Using the three dimensional Euclidean distance of the two line segments (above and below the velocline) and the corresponding sound speeds in each layer, the two-way travel time (TWTT) is calculated for the synthetic beam. The TWTT is meant to simulate the true time of flight that would have been measured under the specified circumstances. The synthetic TWTT is then used in a traditional 2D ray trace in order to get the coordinate solutions which have been biased by the internal wave (Figure 6). Each biased sounding is plotted onto a surface which represents the difference between the synthetic flat seafloor, and how the flat seafloor would appear if it were imaged through the specified internal wave. The above process repeats for each beam across the swath. The software simulates the vessel traveling over three cycles of the internal wave with sufficient pings in order for the difference surface to show how the pattern of the bias will develop.

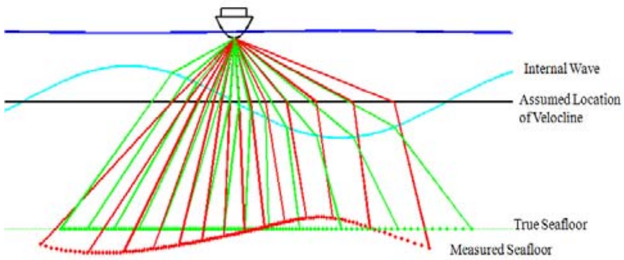

Figure 6 : *True ray paths vs. traditional ray trace*.

The same process is done with an augmented ray trace to evaluate the potential benefit of accounting for the velocline's true depth (*Figure 7*). In order to become augmented, the traditional ray trace is able to account for the true vertical position of the velocline across the entire swath (but does not attempt to account for potential tilting in either the across-track or along-track direction). This is done with the assumption that the depth of the velocline can be successfully imaged across the entire swath allowing for an adjustment in the SSP to replicate the correct depth of the velocline for every receiver beam. The first step in performing the augmented ray trace for a beam is to retrieve the z-coordinate (in IWCS) of the beam's intersection with the internal wave, which is calculated in the simulation. This value replaces the assumed depth of a horizontally stratified velocline (from the SSP). After the value is replaced, a traditional ray trace is performed, producing a sounding which only contains a bias from the tilting velocline and is free from any contamination by the velocline's varying depth.

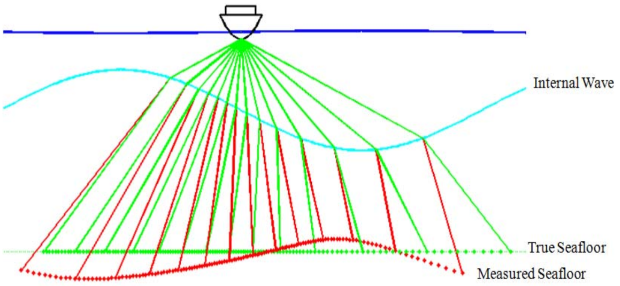

***Figure 7**: True ray paths vs. augmented ray trace.*

a) Three Dimensional Refraction

A velocline that is tilted in the along-track direction can cause a beam to deviate from the 2D plane by which it is assumed to be constrained. It is for this reason that the refraction of each beam must be calculated in 3D space, this requires the definition of the plane that contains: (1) a vector representing the ray direction in the upper layer, (2) the normal to the velocline at the point where the unit ray vector intersects the internal wave, and (3) a vector representing the direction of the refracted ray in the lower layer. The plane defined by these three vectors is referred to as the 3D refraction plane, note that it only differs from the 2D refraction plane by a rotation about the unit ray vector in the upper layer. Snell's law is applied to find the angle of refraction within this plane.
A unit vector representing the refracted ray in the lower layer is easily calculated in a coordinate system whose x-z plane is defined as the 3D refraction plane. A final transformation is thus required to bring the vector back into the IWCS. The following steps must be taken to achieve these results.

The first step in the process is calculating the IWCS coordinates for the point at which the ray intersects the internal wave. This is achieved by setting the x and z values from the unit vector representing the ray direction in the upper layer (B_1) equal to those from the surface representing the internal wave (*IW*) and solving for *U*. Equation (2) defines B_1, where δ is the ray's depression, β is the vessel's azimuth in the IWCS, and *U* is the scalar multiple which represents the length of the ray. Equation (3) defines *IW*, where d_i is the average depth of the internal wave, *A* is the internal wave's amplitude, ω is the angular frequency, and *x* is the x- coordinate in IWCS:

$$B_1 = U * \begin{bmatrix} -\cos\delta * \sin\beta \\ \cos\delta * \cos\beta \\ \sin\delta \end{bmatrix} \tag{2}$$

$$IW = d_i + A * sin(\omega * x) \tag{3}$$

The line *IW* is stretched along the y-axis to create the surface. The result of the substitution is shown with equation (4):

$$B_1\,(z) * U = d_i + A * sin[\omega * (x + B_1(x) * U)] \tag{4}$$

Equation (4) cannot be rearranged to solve for U so the equation is set equal to zero (equation (5)):

$$0 = di + A * sin\,[\omega * (sonar(x) + Beam(x) * U)] - \mathrm{Beam}(z) * U \tag{5}$$

and the bisection method is used to solve for the roots. Once the appropriate value for *U* is determined it is used in equation (2) to solve for the IWCS coordinates of the intersection point.
With the intersection coordinates calculated, the normal (*N*) to the velocline at that point is determined. This is done by taking the cross product of the two tangents to the velocline (tangent in the x direction, tangent in the y direction) at the point of intersection. The tangent in the y direction is always a unit vector running parallel to the y-axis because the surface is stretched along the y-axis, which also means the internal wave can be represented by a line in the x-z plane. The first step in calculating the tangent in the x direction is determining the slope of the line which is in the x-z plane. The slope at a specific value of x (equation (6)) is equal to the Δz which occurs when Δx is 1, allowing the tangent in the x direction to be represented using equation (7). The resulting vector is not of unit length however it is still in the correct direction and will not affect the calculations.

$$slope = A * \cos(\omega * x) * \omega \tag{6}$$

$$tangent\ x = \begin{bmatrix} 1 \\ 0 \\ slope \end{bmatrix} \tag{7}$$

The angle between the beam (*B1*) and the normal is calculated using the dot product in equation (8):

$$\theta_i = cos^{-1}\left[\frac{N \cdot B1}{||N|| * ||B1||}\right] \tag{8}$$

where (θ_i) is the incidence angle. As explained, Snell's law is to calculate the refracted angle (θ_r) within the 3D refraction plane. With this completed it is necessary to construct a new right handed coordinate system that has the incidence ray path as the x-axis, the normal to the refraction plane as the y-axis (calculated as the cross product of *N* and *B1*), and the z-axis defined by the cross product of the x and y axes.

$$B2 = \begin{bmatrix} \cos(\theta_i - \theta_r) \\ 0 \\ \sin(\theta_i - \theta_r) \end{bmatrix} \quad (9)$$

$$B2 = \begin{bmatrix} \cos(\theta_r - \theta_i) \\ 0 \\ -\sin(\theta_r - \theta_i) \end{bmatrix} \quad (10)$$

The final step is to rotate *B2* back into the IWCS, yielding a unit vector which represents the three dimensional direction of the refracted beam in the IWCS, *B3:*

$$B3 = inv(R) * B2 \quad (11)$$

The matrix *R* is the rotation matrix that is composed from the values which represent the axis of the new coordinate system within the IWCS. For example y_x is the y component of the new coordinate system's x axis defined in the internal wave system. The full matrix is represented by equation (12):

$$R = \begin{bmatrix} x_x & y_x & z_x \\ x_y & y_y & z_y \\ x_z & y_z & z_z \end{bmatrix} \quad (12)$$

Once B3 is calculated, the coordinates (in the IWCS) of its intersection with the plane representing the seafloor can be calculated, and are used as the "true" coordinates as previously explained in the Methods section.

b) Visualization of Results

Following the methodology outlined above, it is possible to calculate the 3D bias for a sounding that passes through an internal wave packet. Examination of the bias for all beam angles over the angular sector and over an entire internal wave packet is useful for examining how the bias evolves with beam angle and intersection point with the internal wave. A difference surface resulting from the biased 2D ray trace is useful for visualising the effect of the internal wave. Not surprisingly, an internal wave imprints a wave-like artifact on the synthetic flat seafloor (see Figure 8a). Figure 8b shows how the bias in depth varies as the vessel passes over an internal wave for the nadir ray and the outermost ray of the angular sector. Figure 8c shows the root mean square (RMS) of depth bias as a function of beam angle.

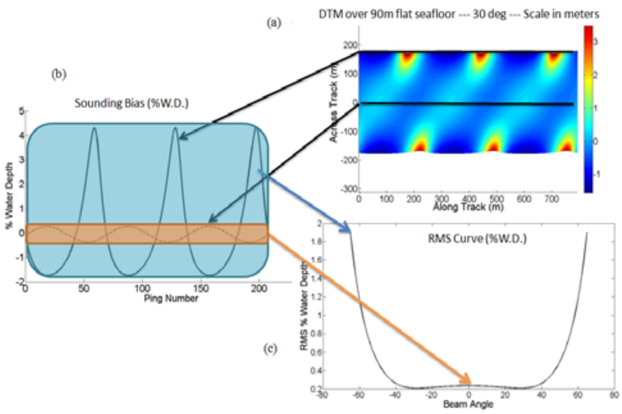

Figure 8: ***(a)*** *Surface representing the difference between the "true" flat seafloor, and the seafloor which has been biased by the internal wave.* ***(b)*** *Cross section of the sounding bias for all soundings by each beam (nadir & outer beam).* ***(c)*** *The depth RMS curve for figure 8 (a).*

The RMS curve is easy-to-understand and can be plotted with several other curves to compare how uncertainty changes with any of the parameters used in an analysis, e.g. amplitude of the internal wave, or depth of the velocline. The same process can be done for the horizontal position with the only difference being that the horizontal bias (Δh) for each sounding is calculated as $\Delta h = (\Delta x^2 + \Delta y^2)^{1/2}$.

4. Case Study

A two week research cruise was conducted by the Bedford Institute of Oceanography (BIO) in August of 1984 to study tidal processes in the Gully, a small canyon-like bathymetric feature located between Sable Island (to the west) and Banquereau Bank (to the east) on the Scotian Shelf (Sandstrom et al. 1988). Internal wave packets were imaged acoustically using a 200 kHz singlebeam echosounder (SBES) and were sampled with a towed undulating CTD. These data provide estimates of internal wave parameters that are useful as a case study in this work. Of particular interest is the internal wave packet observed during a four hour period on August 29th. The SBES water column reflectivity and the towed CTD measurements were able to record, among other things, the geometry of the internal waves as well as the sound speed information for the water column. The sound speed casts were retrieved from the World Ocean Database of 2005 (WOD05), and although it is not with 100% certainty that these casts were from the same project, the metadata indicates that they were taken on the exact date, time and location as the data discussed in Sandstrom et.al (1988). This means even if they are not from the same project they will at least provide similar sound speed values.

The plots and discussions from Sandstrom et al. (1988) provide all the necessary parameters to run through the simulation whereas the casts retrieved from WOD05 provide the speed of sound in the upper and lower layers. Table 2 lists the parameters used.

Parameter	Value
Wave Length	230m
Wave Height	32m
Depth of velocline	32m
Water Depth	90m
Sound speed above velocline	1485m/s
Sound speed below velocline	1459m/s

***Table 2**: Banquereau Bank internal waves*

a) Digital Terrain Model

One of the goals of this research is to help identify when soundings have been collected through an internal wave so that hydrographers may be able to recognize the artifact. In order to achieve this goal the software has the ability to create a difference surface showing how the user-defined flat seafloor would appear if it were imaged through an internal wave as defined by the user parameters. This section presents those images with some qualitative analysis. The colour scales in the images represent the difference between each sounding's depth, and the depth of the flat seafloor.

Figures 9 and 10 (which are two different views of the same figure) are the result of using the Banquereau Bank internal wave parameters while traveling parallel to the direction that the wave propagates, i.e. the crests and troughs of the internal wave are perpendicular to the vessel course. The SSP cast is simulated to have identified the velocline at the average depth of the internal wave, which means the depth bias is equal and opposite at the tops and bottoms of the waves. Essentially it oscillates between the "smile" and "frown" that are synonymous with an incorrect depth of the velocline. In this situation, the depth uncertainty is dominated by the velocline's vertical oscillation. But as seen in figures 11 and 12 (which are two different views of the same figure), this changes as the direction of travel becomes oblique, and the depth uncertainty becomes dominated by tilting. Travelling at 30° relative to the wave's direction of propagation, the depth bias is much larger across the entire swath, reaching values over 3.5m. The oscillating smile and frown remain, but the smiles are much larger than the frowns (3.5m vs. 1.5m). The other interesting quality is how artifacts remain connected across the difference surface, and are aligned with neither the across track or along track axis. Rather they are aligned with the crest on the internal wave and are created by a series of pings. This unique quality presents itself as a good method for a hydrographer to identify the source of the artefact.

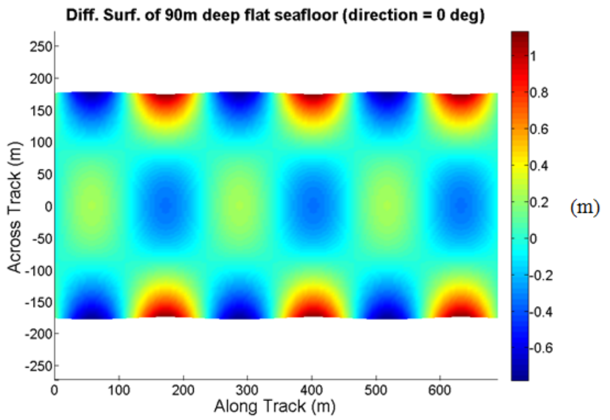

***Figure 9**: Difference surface of 90m deep flat seafloor (direction = 0°).*

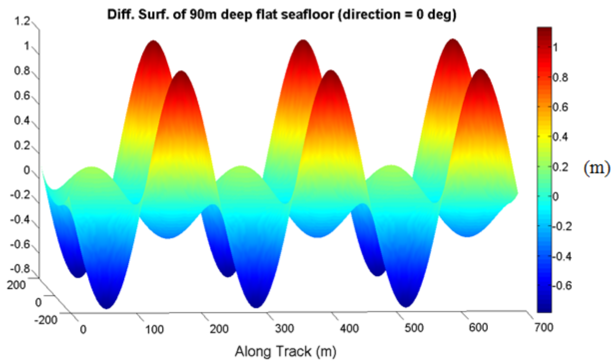

***Figure 10**: Difference surface of 90m deep flat seafloor (direction = 0°).*

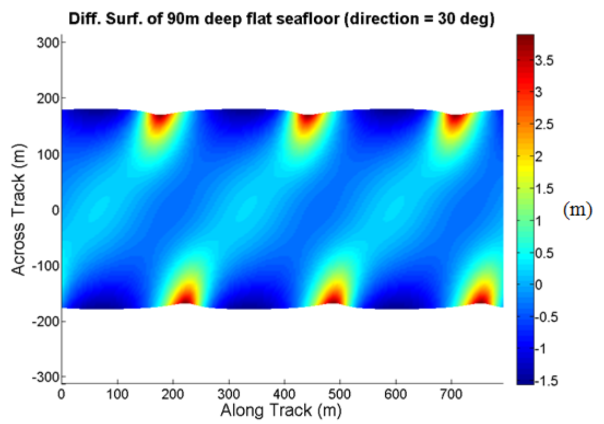

***Figure 11**: Difference surface of 90m deep flat seafloor (direction = 30°).*

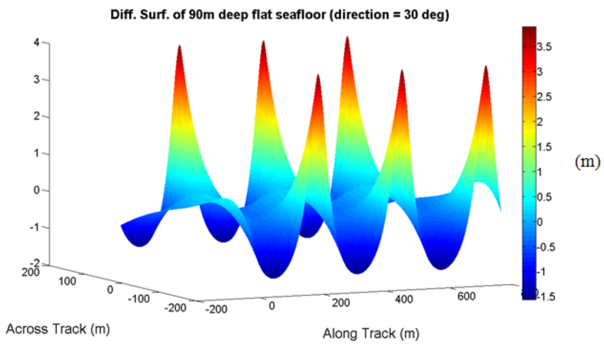

Figure 12: *Difference surface of 90m deep flat seafloor (direction = 30°).*

b) Direction of Travel

In this section the effect of changing the direction of travel relative to the internal wave's direction of propagation will be examined. Figures 13 and 14 are plots of the RMS curves where each colour represents a direction relative to the wave's propagation; the angles in degrees are listed in the legend. The plot for depth RMS also includes the allowable vertical uncertainty reduced to 1-sigma (divide by 1.96) according to the *Internal Hydrographic Organization's standards for hydrographic surveys* (IHO 2008). The allowable uncertainty is taken from Order 1A/1B because they would most likely be the standard used in the 90m water depth of the study area.

It is interesting to note in Figure 13 that the RMS curves for all the directions follow the same general trend. The RMS begins at approximately 0.15% of the water depth (%w.d.) at nadir and grows with the swath angle. Once the direction of travel moves beyond 0° a large portion of the swath (beams past +/- ~40°) has an RMS greater than the allowable uncertainty in 90m of water. The plot also shows that as the direction moves away from being parallel to the wave's propagation, the RMS grows at a greater rate with swath angle. These results mean that if it is possible to plan survey lines to run in the same direction that an internal wave propagates the uncertainty will be minimized (though it is fully realized that this may not always be practical or possible).

There are two important factors to keep in mind when looking at figures 13 and 14. The first is that they represent only the uncertainty created by the internal wave; once all other uncertainties for MBES systems are included the curves will be pushed up, resulting in a reduced usable swath width. The second is how RMS suppresses the maximum uncertainties. While traveling at 75°, the RMS reaches its highest values as it nears 3% w.d. in its outer beams. In this case the bias in the outer beams reaches values which near 12% w.d. (approximately 11m in 90m of water). When travelling at oblique angles over internal waves large discrepancies in the data should be expected.

The horizontal position RMS curves for the range of directions are plotted in Figure 14. The RMS remains relatively the same for all directions, and is within the allowable IHO order 1 A/B horizontal uncertainty of 3.87m (1-sigma). Note that 3.87m is the result of dividing the allowable total horizontal uncertainty (THU), which is expressed in the IHO standard at 95% confidence, by the 2D scaling constant specified in the IHO standard of 2.45 (IHO 2008). It appears as though the horizontal positions are within acceptable limits, however they are being compared to the minimum standards set out by the International Hydrographic Organization, which are meant to be used in the absence of any other guidance and are primarily designed for the production of navigational charts (IHO 2008). It is commonplace for more stringent standards to be set out in a contract, and it is likely that the standards would be considerably higher than the uncertainty introduced in the horizontal positions by internal waves (approx. 8% w.d. for the worst case scenario and 2% w.d. for the RMS of the outer beams).

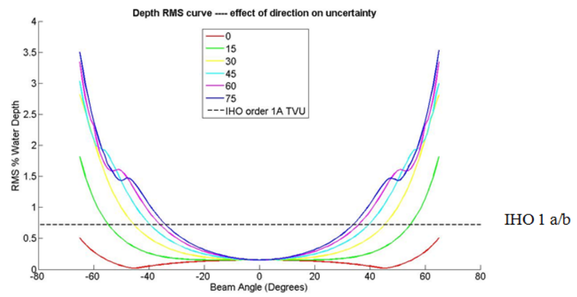

Figure 13: *Depth RMS for different directions at standard*

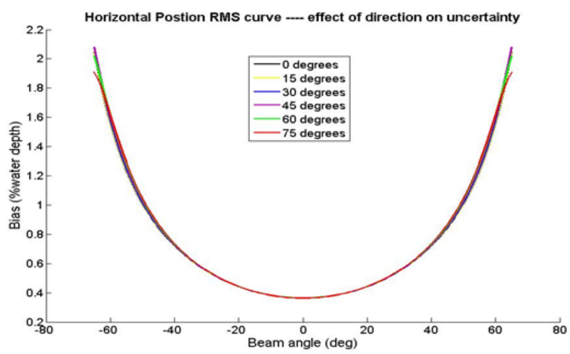

Figure 14: *Horizontal positions RMS for different directions.*

c) Augmented Ray Trace

As explained earlier, the simulator developed in this work has the ability to remove the uncertainty due to the vertical oscillation of the velocline.

The reason for doing this is to assess the potential benefit of adjusting the SSP to account for the varying depth of the velocline for every receiver beam by exploiting water column imaging. This section examines how the simulated Banquereau Bank soundings would improve with such an augmentation.

Both figures 15 and 16 contrast the RMS curves using a traditional 2D ray trace and an augmented 2D ray trace. Figure 15 is travelling parallel to the wave's propagation, whereas Figure 16 is at 30° to the direction of propagation. While travelling parallel to the internal wave propagation the uncertainty is nearly reduced to zero, being less than 0.05% of water depth at the outer beams; this small residual uncertainty is presumably due to the effects of along-track tilting. However while travelling at 30° there is only improvement in the nadir region.

By taking into account the depth of the velocline within the ray trace, the uncertainty for the vertical motion of the velocline is removed, leaving only the portion created by the tilting of the velocline. Through this logic it can be deduced that environments which have a larger fraction of the bias being created by the velocline's vertical displacement stand to have a larger percentage of their bias removed. Considering the previous statement, in terms of the results from the augmented ray trace, this means that while travelling parallel to the direction of propagation, the uncertainty is dominated by the velocline's vertical motion (there is only tilt in the along track direction), and at 30° it is dominated by the tilting (there is tilt in the along-track and across-track directions). For this case it can be concluded that the potential benefit from the augmented ray trace is only significant while travelling parallel to the internal wave's propagation.

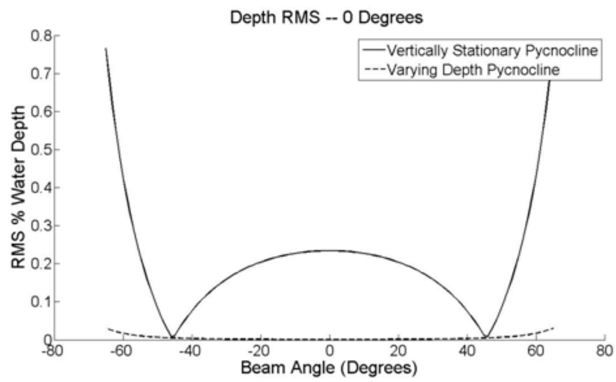

***Figure 15**: Depth RMS improvement by tracking velocline depth (0°).*

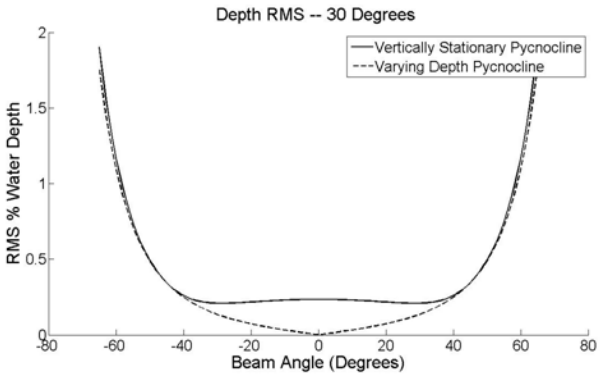

***Figure 16**: Depth RMS improvement by tracking velocline depth (30°).*

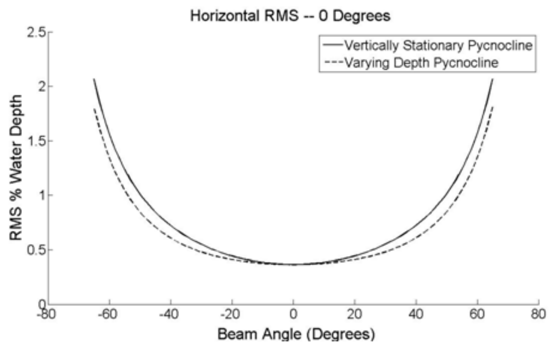

***Figure 17**: Horizontal position RMS improvements by tracking velocline depth.*

Figure 17 shows that there is very little improvement in terms of the horizontal position from using the augmented ray trace. Also, unlike the depth bias, the improvement to the horizontal positions from using the augmented ray trace does not depend significantly on the direction of survey lines relative to internal wave propagation.

d) Sampling the Water Column

The case study has shown that failing to adequately model the effects of an internal wave on ray path propagation can lead to significant biases in MBES soundings. It has also shown that water column imaging methods have limited applicability (though improvements can be made to the augmentation that was applied, e.g. allowing for estimation of the across-track tilt of the velocline on a beam-by-beam basis). Can the problem be addressed instead through increased sound speed profiling?

Sampling equipment does exist that would allow for an increased ability to sample the water column, e.g. ODIM Brooke Ocean Moving Vessel Profiler (MVP) (Furlong et al. 1997).

Internal waves, however, present a unique challenge as the spatial distances over which the water column structure varies can be small compared to what can be realistically sampled using underway sound speed profiling equipment. An MVP's profiling rate (i.e. the maximum number of profiles that can be acquired over a defined time interval) is limited by the winch retrieval speed and maximum desired sampling depth. A downcast of a few tens of metres may take only seconds to complete, but the retrieval may take a few minutes resulting in large distances between samples. For example, a 3 minute profiling interval while travelling at 8 knots would yield a sound speed profile every 740 m. This is quite large when compared with the spatial wavelength of the internal waves observed over Banquereau Bank during the 1984 sampling campaign (~230 m). In this case, an extreme case of aliasing occurs when trying to sample the structure of the internal wave. The above situation is apparent in Figure 18 where the internal wave is plotted in green, roughly to scale for the above situation.

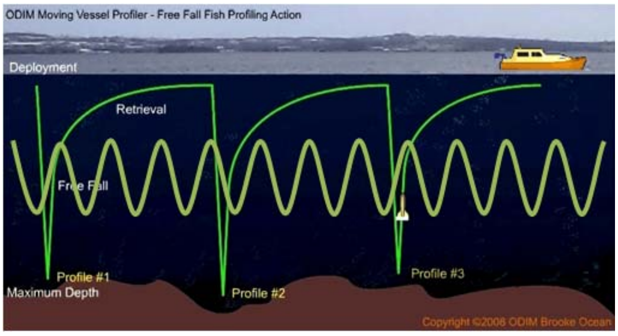

Figure 18: *Sound speed profiles using a MVP over an internal wave.*

Regardless of whether or not there is aliasing, the fact remains that using an SSP requires the assumption that the watercolumn is horizontally stratified. Even if it were possible to have a dense sampling over the internal wave, it would not account for the velocline's tilt, and won't represent the true velocline depth across the entire swath. This should not be misconstrued as saying that there is no advantage to densely sampling the water column. It is only meant to show that in areas with internal waves a hydrographer cannot expect to easily model the oceanographic conditions using sound speed profiles, even with hardware that allows for near continuous sampling of the water column.

5. Conclusions

Under certain conditions, internal waves in the water column can cause the total propagated depth uncertainty of MBES soundings to exceed IHO Order 1A/B specifications for a large portion of a typical MBES angular sector. It has been shown that planning survey lines to run parallel to the direction in which the internal waves propagate significantly reduces their effect. It has also been shown that augmenting traditional 2D ray tracing algorithms with water column imaging has the potential to minimize the uncertainty, however this approach is also limited to the case where survey line direction is parallel to the direction of internal wave propagation. Increasing sound speed acquisition rates can help only in cases where instrumentation can sample often enough to fully capture the nature of the wave.

Without a reliable method for reducing the impact of internal waves on sounding accuracy, perhaps the best approach to dealing with internal waves is a background study of the oceanographic processes at work in the area to be surveyed. With information about the geometry of internal waves, the numerical simulation outlined in this work has potential to assist in creating a more accurate assessment of the expected total propagated uncertainty at the survey design stage. This might allow the hydrographer to estimate parameters such as survey line direction and spacing better. Furthermore, oceanographic background research could also be used to identify periods characterized by low internal wave activity. These "windows of opportunity" would allow the surveyor to work around the problem and avoid high costs associated with reduced line spacing when working in the worst of conditions.

6. Future Work.

The uncertainty discussed in this paper is a systematic uncertainty, meaning that if the true geometry of any specific wave can be identified, the 3D refraction algorithm outlined in this work can be used to correct any erroneous data. The key to this is being able to measure the true geometry of the wave. The potential future of this research is to investigate the possibility of exploiting water column imagery by digitizing the visible impedance contrast caused by the sharp density gradient along the internal wave. The digitized surface should provide a correct depth and incidence angle for each receiver beam ray path. If successful it would provide a method of correcting the artifacts from any phenomena that result in significant tilting or oscillation of the velocline in post processing; however its utility will hinge on willingness to continuously collect water column data.

It should be noted that the results of this work are preliminary. Further research and testing will:

- verify the fidelity of the numerical simulation through field trials
- assess the feasibility and practicality of identifying internal wave propagation direction (if there is only one) and adjusting the direction of survey lines to run parallel to the internal wave propagation

- explore the dependability of multibeam water column imaging to produce images of internal waves which are distinguishable from the surrounding noise in the water column.

References

- Apel, J.R. (2004). Oceanic Internal Waves and Solitons. In *An Atlas of Oceanic Internal Solitary Waves*, Global Ocean Associates, Alexandria, Virginia. 1-40.
- Baum, S.K. (2004). *Glossary of Physical Oceanography and Related Disciplines.* Department of Oceanography, Texas A&M University.
- Furlong, A., Beanlands, B., and Chin-Yee, M. (1997). Moving vessel profiler (MVP) real time near vertical data profiles at 12 knots. In Proc. of Oceans '97 Conference, Halifax, Canada.
- Hughes Clarke, J. (2006). Applications of multibeam water column imaging for hydrographic survey. *The Hydrographic Journal.* April issue.
- International Hydrographic Organization (2008). IHO Standards for Hydrographic Surveys. Special Publication No. 44 5th Edition, Monaco.
- Lurton, X. (2002). *An Introduction to Underwater Acoustics: Principles and Applications*. Praxis Publishing Ltd., United Kingdom.
- Sandstrom, H., J.A. Elliott, and N.A. Cochrane (1988). Observing Groups of Solitary Internal Waves and Turbulence with BATFISH and Echo-Sounder. *Journal of Physical Oceanography,* 19, 987-997.
- Sandstrom, H., and N.S. Oakey (1994). Dissipation in Internal Tides and Solitary Waves. *Journal of Physical Oceanography,* 25, 604-614.

Biographies of the authors

Travis Hamilton has his Bachelor's degree in Geodesy and Geomatics Engineering (2010) from the University of New Brunswick. He was first attracted to the field of hydrographic surveying after being offered an opportunity to work in the Arctic with the Ocean Mapping Group at UNB in 2009.
Currently Travis is working on his Msc in Geodesy and Geomatics Engineering at UNB. The focus of his Msc research is in the estimation of sounding uncertainty from non-horizontal refracting layers.

Jonathan Beaudoin has a PhD (2010) in Geodesy and Geomatics Engineering from the University of New Brunswick and Bachelor's degrees in Geodesy and Geomatics Engineering (2002) and Computer Science (2002), also from UNB.
Having just arrived at CCOM in the Spring of 2010, he plans to carry on in the field of his PhD research, that of estimating sounding uncertainty from measurements of water mass variability. His research plans include an examination of oceanographic databases such as the World Ocean Atlas and the World Ocean Database to see how the data contained in these comprehensive collections can be turned into information that is meaningful to a hydrographic surveyor. Other plans involve assessing how to best acquire, visualize, process and analyse data from high-resolution underway sound speed sampling systems, again, in terms that are meaningful to a hydrographic surveyor.

Article

ECDIS-GNSS COMBINED TO IMPROVE MARINE TRAFFIC SAFETY

By Rosario LA PIRA (ITALY)
Italian Hydrographic Office, Genova, Italy

Abstract

This paper analyses the enhanced GNSS and ECDIS technology in the realm of maritime navigation from the user's perspective taking into account the latest changes in international regulations and standards. It is through this integration that mariners have the possibility to analyze their own ship's position related to the chart information for a safer decision-making process and where the best accuracy of the position data can be properly managed. To obtain the maximum advantage of this enhanced technology a different approach by the mariner is required and a specific training program that provides comprehensive instruction on safe equipment operation must be developed.

Résumé

Le présent article analyse la technologie GNSS et ECDIS améliorée dans le domaine de la navigation maritime, selon la perspective de l'utilisateur et en tenant compte des derniers changements intervenus dans les règles et normes internationales. C'est par cette intégration que les navigateurs ont la possibilité d'analyser la position de leur propre navire par rapport aux informations portées sur la carte en vue d'un processus de prise de décision plus sûr et lorsque la plus grande exactitude des données de position peut être gérée efficacement. Pour retirer le plus grand bénéfice de cette technologie améliorée, une différente approche est requise du navigateur et un programme de formation spécifique fournissant des instructions complètes sur le fonctionnement sûr des équipements doit être développé.

Resumen

Este artículo analiza la tecnología mejorada del GNSS y del ECDIS en el campo de la navegación marítima, desde la perspectiva del usuario, tomando en cuenta los últimos cambios en los reglamentos y las normas internacionales. Es gracias a esta integración que los navegantes tienen la posibilidad de analizar la posición de sus propios buques con respecto a la información de la carta para un proceso de toma de decisiones más seguro y en el que pueda controlarse adecuadamente la mayor exactitud posible de los datos de posición. Para obtener las máximas ventajas de esta tecnología mejorada, se requiere un enfoque diferente por parte del navegante y tiene que desarrollarse un programa de formación específico que proporcione amplias instrucciones sobre el manejo seguro del equipo.

1. Introduction

The International Maritime Organisation (IMO) introduces the issue of maritime safety as follows: Shipping is perhaps the most international of all the world's great industries - and one of the most dangerous. Ship casualties and incidents can result in serious loss of life and pollution of the marine environment as modern ship can carry over 5,000 people and over 500,000 tons of petroleum [1].
Maritime safety is of paramount importance in the new role of Global Navigation Satellite System (GNSS) and Electronic Chart Display and Information System (ECDIS). Increased safety at sea should be considered while taking into account the most critical issue of supplying the master of a vessel and those responsible for the safety of shipping ashore with modern, proven tools to make marine navigation and communications more reliable thereby reducing errors, especially those with the potential to cause equipment damage, pollution harm to the marine environment, injury and loss of life.

Maritime safety in this case means to address the particular needs of enhancing the prevention of collisions and groundings. According to statistics, the number of ship collisions and groundings has not appreciably changed over the last ten years despite the growing technology.

The European Maritime Safety Agency (EMSA) statistics show that 626 vessels were involved in 540 accidents (sinkings, collisions, groundings, fires/explosions and other significant accidents) in and around European Union (EU) waters during 2009 [2].

The majority of vessels in the 2009 EMSA survey were involved in collisions and contacts (around 47%) and groundings (around 28%), while sinkings accounted for around 4% of the total and fires and explosions for around 11% (other causes 10%).

It is acknowledged that there is evidence to show that the great majority of accidents have a human error component, and also that seafarers often make mistakes under difficult circumstances (eg. bad weather, geographical/infrastructure restrictions, fatigue, task overload, training shortcomings, etc.).

There are numerous examples of collisions and groundings that might have been avoided had there been suitable input into the navigation decision-making process.

In recent years, the enhanced GNSS has dramatically changed the way mariners, surveyors and other professional engineers measure positional coordinates.

For the scope of navigation, this development should not be considered independently, but should be viewed from a broader perspective of enhanced navigation as a result of the simultaneous improvements of existing and new navigational tools, in particular electronic tools.

Today, mariners as well as those ashore can use enhanced information derived from GNSS in a reliably and efficient way through the extensive electronic navigational and communication technologies and services available or in development, such as ECDIS, Automatic Identification System (AIS), Automatic Radar Plotting Aids (ARPA), Integrated Bridge Systems/ Integrated Navigation Systems (IBS/INS), Vessel Traffic Services (VTS), Long Range Identification and Tracking (LRIT) systems, Global Maritime Distress and Safety System (GMDSS) and the Marine Electronic Highway (MEH).

All these technologies and equipment/system needs to be connected with an Electronic Position Fixing System (EPFS) such as GNSS to perform the concerning navigational tasks they are used for. Fundamental Navigational tasks necessary to support the mariner to conduct navigation safely such as “Route monitoring”, “Collision avoidance”, “Navigation control data”, “Navigation status and data display” and “Alert management”.

This paper will discuss the enhanced GNSS technology in the realm of maritime navigation from the user’s perspective through the integration of the other navigation systems used in the decision-making process and taking into account the latest changes in international regulations and standards already in force and those under consideration.

2. GNSS maritime requirements

Since the earliest days of navigation, seafarers have sought to keep track of their direction and position.
Since the beginning an important part of IMO regulations have dealt with ship positioning and the related equipments.

The first step of IMO in radionavigation positioning occurred with the International Convention for the Safety of Life at Sea (SOLAS-1948), which required all ships over 1600 tons gross tonnage engaged on international voyages, to carry Radio Direction Finder apparatus. In 1968 the amendments to the 1960 SOLAS Convention, added requirements to carry radar. In 1988 IMO adopted an amendment which allowed ships the option to carry radionavigation equipment instead of the Radio Direction Finder. On 1st September 1984, new requirements for shipborne navigational equipment came into force, requiring large ships, especially tankers, to be fitted with ARPA.

In July 2002, new requirements for the carriage of navigation equipment come into effect following a complete revision of Chapter V of the SOLAS 1974 Convention (current situation).

After 1st July 2002, the radio direction-finding apparatus is not required anymore. With the carriage requirements currently in force all ships constructed on or after 1st July 2002 shall be fitted with a receiver for a GNSS or a terrestrial radio navigation system, or other means, suitable for use at all times throughout the intended voyage to establish and update the ship's position by automatic means. It is the first time a GNSS receiver is in the SOLAS convention.

a) GNSS minimum requirements

IMO resolutions A.953(23) and A.915(22) specified the maritime navigation requirements for GNSS. The first of these resolutions establishes operational requirements relevant to GNSS-1 (the first generation GNSS) (*Table 1*), whereas the second resolution is interpreted as being a living document specifying top-level requirements more appropriate to a future GNSS-2 (the second generation GNSS) (*Table 2*).

The IMO resolutions contain the internationally adopted maritime requirements for general navigation. These requirements are applicable to all radio-navigation systems. The maritime use of radio-navigation systems pass through the IMO recognition. The recognition by IMO of a radio-navigation system would mean that the Organization recognizes that the system is capable of providing adequate position information within its coverage area and that the carriage of receiving equipment for use with the system satisfies the relevant requirements of the 1974 SOLAS Convention.

Current first generation GNSS (GNSS-1) such as GPS and GLONASS systems have been recognized as a component of the World Wide Radio-navigation System (WWRNS) for navigational use in waters other than harbour entrances and approaches and restricted waters.

Area	Absolute horizontal Accuracy (95%)	Signal Availability	Continuity	Warning (non-availability)	Update Rate
Ocean	≤ 100 m	> 99.8% over 30 days	N/A	ASAP by Maritime Safety Information (MSI) System	< 10 s < 2 s*
harbour entrances-approaches and coastal waters with a low volume of traffic and/or less significant degree of risk	≤ 10 m	> 99.5% over 2 years	≥ 99.85% over 3 hours	< 10 s	< 10 s < 2 s*
harbour entrances-approaches and coastal waters with a high volume of traffic and/or significant degree of risk	≤ 10 m	> 99.8% over 2 years	≥ 99.97% over 3 hours	< 10 s	< 10 s < 2 s*

* If the computed position data is used for AIS, graphical display or for direct control of the ship

Table 1:
Operational requirements for a world-wide radio-navigation system (GNSS-1)

	System level parameters				Service level parameters			
	Absolute Accuracy	Integrity			Availability % per 30 days	Continuity % over 3 hours	Coverage	Fix interval* (sec)
	Horizontal (m)	Alert limit (m)	Time to alarm* (sec)	Integrity risk (per 3 hours)				
Ocean	10	25	10	10^{-5}	99.8	N/A**	Global	1
Coastal	10	25	10	10^{-5}	99.8	N/A**	Global	1
Port approach and restricted waters	10	25	10	10^{-5}	99.8	99.97	Regional	1
Port	1	2.5	10	10^{-5}	99.8	99.97	Local	1
Inland wa-terways	10	25	10	10^{-5}	99.8	99.97	Regional	1

*More stringent requirements may be necessary for ships operating above 30 knots.
** Continuity is not relevant to ocean and coastal navigation.

Table 2:
Future GNSS minimum maritime user requirements for general navigation (GNSS-2)

Future GNSS(s) are expected to improve, replace or supplement the current systems, which have short-comings in regard to integrity, availability, control and system life expectancy. Early identification of maritime user requirements has been developed to ensure that these requirements are considered in the development of future GNSS(s). These IMO requirements should be incorporated in GNSS plans to be accepted for maritime use. The second generation GNSS will meet the maritime user's operational requirements for general navigation, including navigation in harbour entrances and approaches and restricted waters. Furthermore the shipborne GNSS equipment should meet performance standards adopted by IMO.

The developing European Galileo have already considered these second generation GNSS requirements in order to make possible for the mariners broader and enhanced safety critical applications. Actual assessment of the Galileo navigation service requirements, as laid down in the most recent issues of the GALILEO reference documents, indicates that the IMO requirements for Oceanic, Coastal, Port approach and restricted waters operations as stated in resolution A.915(22), can be met by the GALILEO stand-alone system using the Safety Of Life service.

3. GNSS and the navigation system

The navigation system includes the GNSS and the Chart System. In order to specify the overall navigation system requirements and performance of a vessel it is necessary to consider all possible contributions to the errors in navigation.
In the navigation system context of GNSS used in the maritime environment, the sources of error affecting overall navigation performance include the GNSS signal, the user receiver, the charts and the equipment and crew (e.g., human factors) controlling the navigation of the vessel.

Therefore in determining the requirements of a GNSS used in the maritime environment, it is necessary to understand these contributing factors. The most important new equipment that needs input of GNSS data is the ECDIS.

ECDIS, as defined by IMO, is the navigation information system which with adequate back-up arrangements can be accepted as complying with the up-to-date chart required by the 1974 IMO SOLAS Convention (regulations V/19 and V/27), by displaying selected chart information derived from electronic navigational charts (ENCs) with positional information from navigation sensors to assist the mariner in route planning and route monitoring, and if required display additional navigation -related information. The electronic chart navigation with ECDIS and real-time GNSS positioning with improved performance (accuracy, integrity, availability, continuity, coverage and fix interval) is a relatively new technology that is considered to be the most important advancement in maritime navigation since the advent of radar some 60 years ago. IMO adopted, on 23th November 1995, the first performance standards for ECDIS, by resolution A.817(19), recently amended on 5th December 2006, with resolution MSC232(82). However, the introduction of new real-time electronic navigation has not been an easy process since the first type approved ECDIS occurred in 1999. It is not just an electronic representation of a paper nautical chart on a colour display with its own ship's position plotted on it, but it represents a new, more powerful navigation aid that significantly improves safety.

ECDIS reduces the navigational workload compared to using the paper chart. It is capable of continuously plotting the ship's position to enable the mariner to execute in a convenient and timely manner all route planning, route monitoring and positioning currently performed on paper charts.

The most important improvement is surely the real time positioning. With ECDIS plus GNSS the mariner knows for the first time where he is and not where he was a few minutes before. This represents a notable change because it allows some most effective and immediate evaluations on the route monitoring activities. At the same time it reduces the Officer Of the Watch (OOW) workload to determine and to plot the ship's position on the paper chart, leaving him increased lookout capability and more time for other evaluations and activity related to the safety of the ship.

Also of great benefit is the new ability to monitor in real time the effective movement of the ship, the Course Over Ground (COG) and Speed Over Ground (SOG), on the chart feature and in comparison to the true course steered (heading) and the speed log. It makes possible the continuous evaluation of the angular difference between COG and heading (sum of leeway and drift angle). A very important feature during route monitoring in narrow channel with bad whether as shown in ***figure 1***.

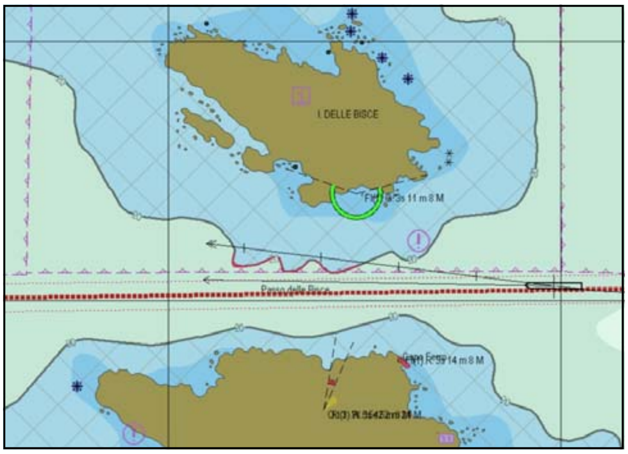

Figure 1: *COG and SOG real-time monitoring*

Moreover the GNSS integration on ECDIS makes possible the automatic generation of an alarm if, within a specified time set by the mariner, the own ship crosses the safety contour or the boundary of a prohibited area or of a geographical area for which special conditions exist.

It is in this context that mariners have the possibility to analyze in an efficient way their own ship's position related to the chart information for a safer decision-making process and where the best accuracy of the position data can be properly managed. This means that navigational risks could be reduced when using ECDIS compared to traditional paper charts.

It is for this reason that IMO has recently approved an amendment to SOLAS regulation V/19, introducing for the first time a mandatory carriage requirement for ECDIS. With the adoption of this amendment at the 86th session of the Maritime Safety Committee (MSC), in June 2009, ECDIS is no more only a mariner optional alternative to the adequate and up-to-date folio of paper nautical charts requirement.

The new ECDIS carriage mandatory requirement will have a phased implementation period from 2012 to 2018 depending on class of ship and tonnage (Table 3).

Furthermore IMO has already agreed a carriage requirement for ECDIS on board all High-Speed Craft (HSC) from 1st July 2008 with a two years transition period for HSC constructed before (full mandate from 1st July 2010).

ECDIS are widely expected to improve safety at sea and make life easier for the navigator. Hardware, software and standards capable of supporting ECDIS have been available for some time, but to be of use they need chart and positional information.

Ship class	Gross Tonnage (KGT*)	New Construction on or after	Existing ship not later first survey on or after
Passenger	KGT≥0.5	1 July 2012	1 July 2014
Tanker	KGT≥3	1 July 2012	1 July 2015
Cargo	KGT≥10	1 July 2013	
	3≤KGT≤10	1 July 2014	
	KGT≥50		1 July 2016
	20≤KGT≤50		1 July 2017
	10≤KGT≤20		1 July 2018

*expressed in Kilo Gross Tonnage

Table 3 **: *ECDIS mandatory carriage requirement***

Both these two kinds of information are the fundamental elements that make ECDIS a safe and reliable tool. Furthermore ECDIS performances are strongly dependent on their availability, reliability and quality. These make the real difference for the mariners using ECDIS compared to paper chart for route monitoring activities and make ECDIS together with new enhanced GNSS a more powerful navigation aid that significantly improves safety.

a) ECDIS chart information

The chart information to be used in ECDIS are the latest edition ENC, as corrected by official updates, issued by or on the authority of a Government, government-authorized Hydrographic Office or other relevant government institution, and conforming to IHO standards (now S-57 and in future S-100).
The provision of chart information is a responsibility and obligation of the coastal State, so it is an issue that clearly the international rules put at the maximum level of importance. They can be derived from the previous United Nations General Assembly resolution (A/RES/53/32 -1988),

This is currently an IMO obligation under regulation 9 of the revised chapter V of the SOLAS (1974) Convention, which entered into force on 1st July 2002. Regulation related to the provision on Hydrographic services under which it is clearly stated that Contracting Governments undertake to arrange for the collection and compilation of hydrographic data and the publication, dissemination and updating of all nautical information necessary for safe navigation.

In May 2010, the IHO submitted a report to the 56th meeting of the IMO Sub Committee on the Safety of Navigation (NAV56) that provides an evaluation of ENC coverage, in comparison with corresponding paper charts, for international voyages based on available data as of the 16 April 2010 [3]. An extract of this evaluation is provided in *table 4* with the following related IHO consideration.

ENCs type	May 2010
Small scale ENCs (planning charts)	~100%
Medium scale ENCs (coastal charts)	84%
Large scale ENCs (top 800 ports)	91%

***Table 4 : Comparison of ENCs with corresponding paper* charts for international voyages**

The IHO is continuously monitoring the situation to ensure that ENCs for vessels engaged on international voyages is given the highest priority for ENC production. The IHO is aware that at the end of 2010 some small gaps will remain in Africa, Arctic routes and the Caribbean. However, in most cases, and especially in any areas frequented by significant levels of international traffic, these gaps are planned to be filled as soon as possible.

The IHO is aware that some ports used by certain classes of vessel, and in particular by cruise ships, may be of relatively low use and therefore not reflected in the busiest international routes. The IHO has been in contact with Cruise Lines International Association (CLIA) and the International Chamber of Shipping (ICS) on this matter to try and identify any such ports.

b) ECDIS positional information

Noting that the collection and dissemination of accurate and up-to-date chart information is vital to safe navigation it is also evident that this accuracy will become useless if the positional information are not of the same reliability.

The positioning requirements for ECDIS are clearly identified on the IMO Performance Standard for ECDIS (Resolution MSC232(82)). The ECDIS requirements related to positioning clearly identify the operational need to carry out the route monitoring activities in a simple and reliable manner. ECDIS is connected to the ship's position fixing system, to the gyro compass and to the speed and distance measuring device. The ship's position required is to be derived from a continuous positioning system of an accuracy consistent with the requirements of safe navigation. Whenever possible it is also required that a second independent positioning source, preferably of a different type, should be provided. In such cases ECDIS is able to identify and display discrepancies between the two sources.

Because of the fundamental importance of the position data input, ECDIS has the requirement to provide to the user an alarm when the input from position sources is lost. Furthermore it also has to repeat, as an indication, any alarm or indication passed to it from position sources.

The collection and use of positioning data is a responsibility of the mariner. It is the mariners that assess what is the safe distance from dangerous chart features and the safe under-keel clearance through a quantitative estimation of the overall related accuracy.

If ECDIS relies on GPS input only, as it is a single position fixing system without integrity information, the exclusive use of this violates the most important rule of navigation: never rely on a single source of position fixing and try always to evaluate a quality indicator through LOP redundancy. A GPS ship's position as displayed on an ECDIS or plotted on paper chart can and should be cross-referenced using a separate independent positioning system, such as radar, terrestrial electronic position-fixing systems, visual, depth sounder etc. This is nowadays much more needed for GPS because of the absence of integrity information, often absent also on DGPS .

What are the requirements for position fixing for route monitoring?

The standard method of position fixing during route monitoring close to hazard such as in coastal, restricted water and harbour approach navigation has always been by visual compass bearing while maintaining an appropriate Dead Reckoning (DR) and Estimated Position (EP) outlook. Furthermore there should be also available a backup method of fixing (usually Radar and radio-navigation), independent from the primary, which makes possible for the mariner to cross-check and monitor the standard method. Currently, most often the primary position fixing method is GNSS with visual and Radar ranges as secondary. This is particularly true in restricted visibility conditions. The mariner should always have an indicator of the reliability of the ship's position that give trust of the route made good. This old rule still works nowadays and it is its violation that most often is the cause of groundings and marine casualties.

It should also be noted that current GNSS providers do not accept liability for the service they provide. In 2007, the IMO Sub-Committee on Safety of Navigation (NAV) agreed that there was a need to provide an internationally agreed alternative system for complementing the existing satellite navigation, positioning and timing services to support e-navigation and recognised that potential back-up systems could be made available.

The new challenge for the future will be to provide the mariner "assured positioning data" to fuel all the mandatory shipborne equipments and systems as it happens for chart information (***figure 2***). The key to success on navigation safety is first of all the quality of all the concern data throughout skilled and well trained mariners.

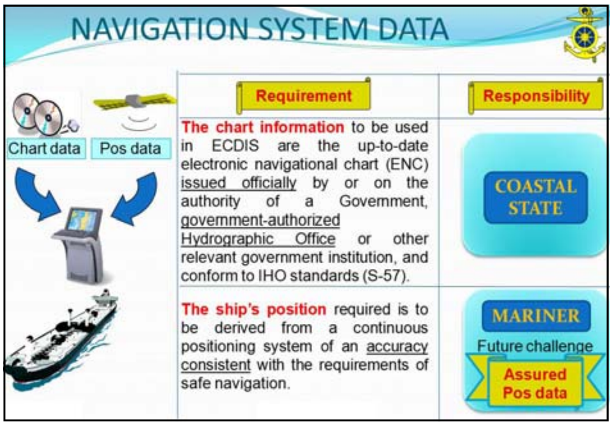

Figure 2: ECDIS+GNSS Data Requirement and Responsibility

This has been true for the past and will be true for the future besides the bridge navigation aids that make it possible for the mariners to use it better.

An important milestone towards this future challenge has been achieved recently on 12th July 2010 when the European Satellite Services Provider (ESSP SAS) of European Geostationary Navigation Overlay Service (EGNOS)' Safety-of Life Service (SoL) received a certificate of Air Navigation Service Provider according to the Single European Sky Regulation 2096/2005. The certification confirms that ESSP complies with safety criteria for operations and is a prerequisite for the company to provide navigation services to airspace users. It assessed compliance with the European Safety Requirements, and with the International Civil Aviation Organization Standards. By the end of 2010, after a successful operational period, the European Commission will be able to declare the EGNOS' SoL available to the aviation community, enabling the publication of precision approach procedures with vertical and lateral navigation guidance (APV) based on EGNOS. At that time, European air navigation service providers will be able to implement satellite-based precision approaches without needing ground equipment on the airport, and with performances similar to those of the instrument landing system (ILS Category I) currently used in the world[4].

This is an important milestone towards the "assured positioning data" that will involve in the near future also the IMO community for the provision to maritime users of the EGNOS' SoL in pan-European region and of the GALILEO' SoL and similar developing new second generation GNSS worldwide.

The GALILEO' SoL has been designed specifically for safety critical users, for example maritime, aviation and trains, whose applications or operations require stringent performance levels.
This service will provide high-level performance globally to satisfy the user community needs and to increase safety especially in areas where services provided by traditional ground infrastructure are not available.

The Safety of Life service will be provided globally according to the performances indicated in table 5. These specifications include two levels (critical level and not-critical level) to cover two conditions of risk exposure and are applicable to many applications in different transport domains, for example air, land, maritime, rail [5].

		GALILEO Safety-Of-Life Service	
Type of Receiver	Carriers	Three Frequencies	
	Computes Integrity	Yes	
	Ionospheric correction	Based on dual-frequency measurements	
Coverage		Global	
		Critical level	Non-critical level
Accuracy (95%)		H: 4 m V: 8 m	H: 220 m
Integrity	Alarm Limit	H: 12 V 20 m	H: 556 m
	Time-To-Alarm	6 seconds	10 seconds
	Integrity risk	3.5×10^{-7} / 150 s	10^{-7}/hour
Continuity Risk		10^{-5}/15 s	10^{-4}/hour - 10^{-8}/hour
Certification/Liability		Yes	
Availability of integrity		99.5%	
Availability of accuracy		99.8 %	

***Table 5* : Service Performances for the Galileo Safety of Life Service**

4. The issue of quality of data

The issue of the dissemination of data quality information has not been a big concern in the past for hydrography because of the implicit protection related to two natural barriers.

The first was the much better positioning accuracy available for hydrographic surveys compared to the one available to mariners. The second was on the means the surveyed data final product reaches the mariner end users, that was a printed paper chart with a scale of reduction. The power to control and to choose the scale of the printed chart, with its implicit limitation, makes it possible for Hydrographic Offices to include all the position errors in the graphic uncertainty (0.2 mm). The scale of the paper chart limits also the accuracy to which the mariner could plot geographic position on the chart (a plottable difference is considered to be 0.3 mm). In a common coastal purpose chart with a scale of 1:100.000 it means that the graphic uncertainty produces a positional uncertainty of 20 m and a mariner plottable difference of 30 m.

a) The positioning barrier

The first barrier has been removed in the last years with the advent of GNSS and DGNSS and the consequent availability to the mariners of the same order of position accuracy of the hydrographic surveyors. This situation will be much more real in the near future with the enhancement of GNSS performances that will be delivered to the maritime navigation users. Nevertheless, the speed up of positioning accuracy has created a gap with some old surveys that need some years before updating.

In many parts of the world, even the most recent data available may have been gathered when survey methods were less sophisticated than they are now and the achievable accuracy currently available with GPS was not possible. In these areas, GPS positions available to the navigator may be more accurate than the charted detail.

This deficiency may not be limited to sparsely surveyed waters of developing nations, but may also apply to the coastal waters of major industrial states. Fortunately, new survey technologies have improved the precision to which modern hydrographic surveys can be conducted and it is required that positions of shoreline constructions in Berthing cells should be one dimension more precise than the shipborne GPS-Position.

However, in some areas of the world there are still charts that are based on old surveys for which there is no determined geodetic datum or the datum is imprecise. Therefore in such areas, paper charts (and thus raster navigational charts - RNC) are not compatible with GNSS navigation, and it will take some time to resolve this problem. This makes it extremely difficult to accurately plot the ship's position obtained by the GNSS in relation to surrounding shoals and other dangers on such charts. The difference in the plotted position can often be significant and could lead to an accident, casualties and is a risk in restricted waters.

This has led to a specific IMO recommendation to the mariners to cross-check position using relative references such as visual or radar fixing or ECDIS radar overlay to provide for the immediate detection of datum inconsistencies in electronic charts, and immediately alert on potential positional shifts required for particular charts (SN.1/Circ.255 dated 24th July 2006 - Additional guidance on chart datums and the accuracy of positions on charts).

b) The chart scale barrier

The barrier of the paper chart scale was removed with the advent of the Electronic Chart era. With ECDIS the mariner can change the scale of the video representation of the Electronic Navigational Chart (ENC) without any limitation choosing to zoom-in and zoom-out as he wishes.

One of the most innovative aspects of digital cartography is represented by the fact, that for a vector database (ENC), it would seem to overcome the concept of representation scale ratio, since hydrographic data are stored in absolute coordinates and therefore always in real scale 1:1. The protection of the carefully selected Hydrographic Office paper chart scale has been removed and subsequently also the user plottable limited difference.

It would seem therefore improper to speak of scale of an Electronic Navigational Chart. Nevertheless this reference cannot be removed because it is no longer connected to the printed ratio of reduction but to the related content and accuracy it has been produced for.

The concept of scale still works as ENC compilation scale refers to the scale at which the ENC was designed to be displayed and is related to the chart's navigational purpose. The concept of scale remains for ENCs also because of cartographic generalization of depth areas.

It is important for the mariner to know that if he overzooms an ENC of a data compilation scale he will not get more data detail and better positional accuracy. This risk to overrate is increased in term of accuracy due to the fact that most ENCs have been produced by digitizing paper charts which were themselves designed to be used individually rather than as part of a database. ***Figures 3 and 4*** put in evidence this risk – looking at the rocks close to P.ta delle Formiche in overscale the mariner performing route monitoring with DGPS could wrongly evaluate to pass between two of them; evaluation that for sure he will not realize in 1:1 scale display [6]. The greater scale of representation gives expectation of grater detail and accuracy that instead should be experienced with a greater ENC compilation scale if available inside ECDIS storage.

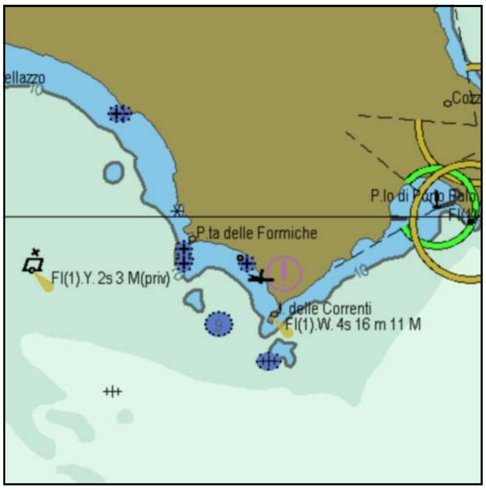

Figure 3*: display scale = compilation scale*

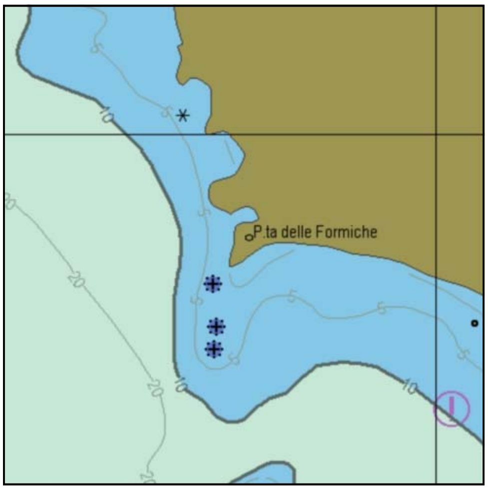

Figure 4*: display scale (1:20,000) > compilation scale (1:90,000)*

As required by IMO Performance Standards, ECDIS should warn the mariner with an overscale indication whenever he selects a display scale that is larger than the ENC compilation scale. This is a new conceptual skill required for the mariner who is an ECDIS plus GNSS user.

c) Chart data quality indicator

ECDIS combines chart and navigational information in a powerful way that, by removing these two important barriers, gives the mariner a new aid with more accuracy expectation that is not always true.

As a result, there is evidence that enhanced navigation systems (e.g. GNSS and DGNSS) may offer comparable or more accurate positioning than the one provided by the ENC data. For this reason the IHO introduced a mandatory data quality indicator in the ENC, which allows a quantitative estimate of the accuracy of important chart features, to be used in combination with estimates of position accuracy from satellite navigation in assessing safe distance from hazards, in order that the mariner may be informed of the quality of the information he uses. This is another important new safety skill required of the marine user of future integrated navigation systems using GNSS and ECDIS.

A chart data quality indicator by zones of confidence (M_QUAL - CATZOC) will cover the entire ENC (although not all data will be assessed initially). ZOC provide a simple and logical mean of displaying to the mariner the confidence that the national charting authority places on any particular selection of bathymetric data. It seeks to classify areas for navigation by identifying the various levels of confidence that can be placed in the underlying data using a combination of the following criteria:

- position accuracy,
- depth accuracy, and
- sea floor coverage (certainty of significant feature detection).

Under this concept there are six possible ZOCs value. ZOCs A1, A2, and B are generated from modern and future surveys with, critically, ZOCs A1 and A2 requiring a full area search. ZOCs C and D reflect low accuracy and poor quality data whilst ZOC U represents data which is un-assessed. ZOCs are designed to be depicted on the ECDIS electronic displays as a ready available symbol. The depth and position accuracy specified for each ZOC refer to the errors of the final depicted soundings and include not only survey errors but also any other errors introduced in the chart production process.

An example of a ECDIS displayed S-52 symbol for CATZOC in comparison with the corresponding quality information data provided to the mariners with source diagrams in paper charts are provided on **figure 5 and 6** respectively.

Figure 5*: example of CATZOC symbol displayed on ECDIS and window for supplementary related information*

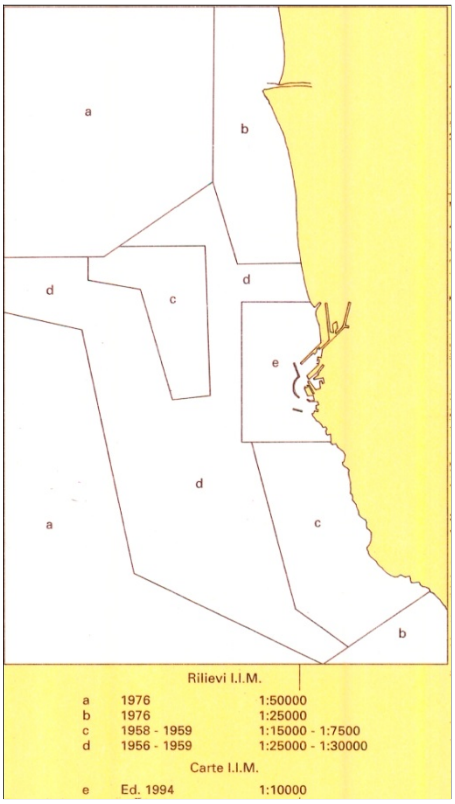

Figure 6*: example of quality information provided on source diagram on paper chart*

Furthermore in this contest the IHO is now looking to determine whether the existing ENC data quality indicators will be appropriate or whether new indicators will need to be developed. The IHO is in fact investigating how to improve the way the quality of survey data could be better presented to the mariner.

5. ECDIS and GNSS functional status

ENC data for ECDIS are compiled for a variety of navigational purposes such as overview, general, coastal, approach, harbour and berthing (defined in the IHO ENC Product Specification, S-57 Appendix B.1). It is the responsibility of the coastal Hydrographic Offices to optimize and produce the ENC data that is most appropriate to the requirements of safe navigation in the area.

The future second generation GNSS receiver equipment should indicate to the user whether its performance is outside the bounds of requirements for general navigation in the ocean, coastal, port approach and restricted waters, and inland waterway phases of the voyage as specified in IMO resolutions.

As outlined above ECDIS and GNSS involved in the navigation system require some new important mariner skills related to the correct evaluation of quality of data. This evaluation is not an easy process and is of fundamental importance in electronic chart real-time positioning.

There is the need for a similar navigational status indicator both for the ENC and for the GNSS data. A future solution could be to make it possible for ECDIS to provide a functional status green, yellow or red light to warn the mariner performing the route monitoring of the overall navigation system situation related to the current type of navigation (coastal, approach, harbour, etc.), according to *Table 6*.

FUNCIONAL STATUS	ENC	Positioning	
		GNSS	Other requirement
GREEN	Appropriate navigational purpose/scale for navigation available and up-to-date	Performance met the requirement for the navigational purpose	None
YELLOW	As above	Only accuracy performance met the requirement for the navigational purpose	Alternative appropriate positioning method required as integrity monitoring. Ship's position should be cross-referenced using a separate independent positioning system, such as visual, Radar, terrestrial electronic position-fixing systems, depth sounder etc
	As above	Performance not met for the navigational purpose	Appropriate positioning method required other than GNSS
RED	Appropriate navigational purpose/scale for navigation not available or not up-to date	Not applicable for ECDIS – refer to up-to-date paper nautical chart.	

Table 6*: *ECDIS +GNSS functional status

6. The e-Navigation strategy

The rapid improvement of these new technologies and the consequent impact on maritime navigation resulted in the IMO considering in 2005 the need to develop a broad strategic vision. A new vision for incorporating the use of new technologies in a structured way and ensuring that their use is compliant with the various navigational communication technologies and services that are already available, with the aim of developing an overarching accurate, secure and cost-effective system with the potential to provide global coverage for ships of all sizes. In December 2008, the IMO Maritime Safety Committee approved the strategy for the development and implementation of e-Navigation along with a time frame and the framework for its implementation process. IMO also requested the participation of other international organizations (IHO, IALA, etc.) in the implementation of e-Navigation.

This need has been summarized by a new concept of "e-Navigation", where "e" stands for "enhanced-navigation" since the electronic navigation has already been used in the maritime navigation for some years. What is new is the proper reliable and efficient integration of these electronic system and the related profit use of the related information technology.

The concept has been well summarized in the definition of e-Navigation as the harmonized collection, integration, exchange, presentation and analysis of marine information on board and ashore by electronic means to enhance berth to berth navigation and related services for safety and security at sea and protection of the marine environment.

It is in this context that the new perspective and advantage of the GNSS information should be analyzed in light of the new requirements related to safety of navigation. Some of the most important requirements are:

- Information shall be automatically checked for validity and plausibility.
- Data failing these checks will trigger an alarm and should not be used by the system.
- The integrity of information should be monitored and verified automatically before being used.
- e-Navigation systems must have sufficient integrity and/or redundancy commensurate with the safety, security and environmental protection requirements.
- All navigation related information should be made available to the user in an effective manner via an integrated system.

7. Improvement of ECDIS related standard of training for seafarers

The enhanced ECDIS technology and its integration with other navigation systems used in the decision-making process has been considered in the last years by IMO in relation also to the requirements of minimum standard for seafarers training.

IMO, recognizing the importance of establishing detailed mandatory standards of competence necessary to ensure that all seafarers shall be properly educated and trained, skilled and competent to perform their duties, recently approved an important revision to the International Convention on Standards of Training, Certification and Watchkeeping for Seafarers (the STCW Convention), and its associated Code. The amendments, to be known as "The Manila amendments to the STCW Convention and Code" have been adopted at a Diplomatic Conference in Manila, the Philippines, in june 2010 and are set to enter into force on 1 January 2012.

Amongst the amendments adopted, there are a number of important changes to each chapter of the Convention and Code, including new requirements relating to ECDIS use and its integration with other navigation systems. Some of the most important ECDIS new specification of minimum standard of competence for officers in charge of a navigational watch and for masters and chief mates are summarized on **table 7 and 8** respectively [7].

(FOR MORE DETAILS SEE FULL SIZE TABLES OVER PAGE)

Competence	Knowledge, understanding and proficiency	Methods for demonstrating competence	Criteria for evaluating competence
Use of ECDIS to maintain the safety of navigation	*Navigation using ECDIS* Knowledge of the capability and limitations of ECDIS operations, including: .1 a thorough understanding of Electronic Navigational Chart (ENC) data, data accuracy, presentation rules, display options and other chart data formats .2 the dangers of over-reliance .3 familiarity with the functions of ECDIS required by performance standards in force Proficiency in operation, interpretation, and analysis of information obtained from ECDIS, including: .1 use of functions that are integrated with other navigation systems in various installations, including proper functioning and adjustment to desired settings .2 safe monitoring and adjustment of information, including own position, sea area display, mode and orientation, chart data displayed, route monitoring, user-created information layers, contacts (when interfaced with AIS and/or radar tracking) and radar overlay functions (when interfaced) .3 confirmation of vessel position by alternative means .4 efficient use of settings to ensure conformance to operational procedures, including alarm parameters for anti-grounding, proximity to contacts and special areas, completeness of chart data and chart update status, and backup arrangements .5 adjustment of settings and values to suit the present conditions .6 situational awareness while using ECDIS including safe water and proximity of hazards, set and drift, chart data and scale selection, suitability of route, contact detection and management, and integrity of sensors	Examination and assessment of evidence obtained from one or more of the following: .1 approved training ship experience .2 approved ECDIS simulator training	Monitors information on ECDIS in a manner that contributes to safe navigation. Information obtained from ECDIS (including radar overlay and/or radar tracking functions, when fitted) is correctly interpreted and analysed, taking into account the limitations of the equipment, all connected sensors (including radar and AIS where interfaced), and prevailing circumstances and conditions. Safety of navigation is maintained through adjustments made to the ship's course and speed through ECDIS-controlled track-keeping functions (when fitted) Communication is clear, concise and acknowledged at all times in a seamanlike manner

Table 7: Specification of minimum standard of competence for officers in charge of a navigational watch on ships of 500 gross tonnage or more – function: Navigation at the operational level

Competence	Knowledge, understanding and proficiency	Methods for demonstrating competence	Criteria for evaluating competence
Maintain the safety of navigation through the use of ECDIS and associated navigation systems to assist command decision making	Management of operational procedures, system files and data, including: .1 manage procurement, licensing and updating of chart data and system software to conform to established procedures .2 system and information updating, including the ability to update ECDIS system version in accordance with vendor's product development .3 create and maintain system configuration and backup files .4 create and maintain log files in accordance with established procedures .5 create and maintain route plan files in accordance with established procedures .6 use ECDIS log-book and track history functions for inspection of system functions, alarm settings and user responses Use ECDIS playback functionality for passage review, route planning and review of system functions	Assessment of evidence obtained from one of the following: .1 approved in-service experience .2 approved training ship experience .3 approved ECDIS simulator training	Operational procedures for using ECDIS are established, applied, and monitored Actions taken to minimize risk to safety of navigation

Table 8: Specification of minimum standard of competence for masters and chief mates on ships of 500 gross tonnage or more - Function: Navigation at the management level

Furthermore, with the "The Manila amendments to the STCW Convention and Code", IMO approved a new recommendation guidance regarding the use of simulator specifically related on "training and assessment in the operational use of electronic chart display and information systems (ECDIS)".

Competence	**Knowledge, understanding and proficiency**	**Methods for demonstrating competence**	**Criteria for evaluating competence**
Use of ECDIS to maintain the safety of navigation	*Navigation using ECDIS* Knowledge of the capability and limitations of ECDIS operations, including: .1 a thorough understanding of Electronic Navigational Chart (ENC) data, data accuracy, presentation rules, display options and other chart data formats .2 the dangers of over-reliance .3 familiarity with the functions of ECDIS required by performance standards in force Proficiency in operation, interpretation, and analysis of information obtained from ECDIS, including: .1 use of functions that are integrated with other navigation systems in various installations, including proper functioning and adjustment to desired settings .2 safe monitoring and adjustment of information, including own position, sea area display, mode and orientation, chart data displayed, route monitoring, user-created information layers, contacts (when interfaced with AIS and/or radar tracking) and radar overlay functions (when interfaced) .3 confirmation of vessel position by alternative means .4 efficient use of settings to ensure conformance to operational procedures, including alarm parameters for anti-grounding, proximity to contacts and special areas, completeness of chart data and chart update status, and backup arrangements .5 adjustment of settings and values to suit the present conditions .6 situational awareness while using ECDIS including safe water and proximity of hazards, set and drift, chart data and scale selection, suitability of route, contact detection and management, and integrity of sensors	Examination and assessment of evidence obtained from one or more of the following: .1 approved training ship experience .2 approved ECDIS simulator training	Monitors information on ECDIS in a manner that contributes to safe navigation. Information obtained from ECDIS (including radar overlay and/or radar tracking functions, when fitted) is correctly interpreted and analysed, taking into account the limitations of the equipment, all connected sensors (including radar and AIS where interfaced), and prevailing circumstances and conditions. Safety of navigation is maintained through adjustments made to the ship's course and speed through ECDIS-controlled track-keeping functions (when fitted) Communication is clear, concise and acknowledged at all times in a seamanlike manner

Table 7

Specification of minimum standard of competence for officers in charge of a navigational watch on ships of 500 gross tonnage or more – function: Navigation at the operational level

Competence	Knowledge, understanding and proficiency	Methods for demonstrating competence	Criteria for evaluating competence
Maintain the safety of navigation through the use of ECDIS and associated navigation systems to assist command decision making	Management of operational procedures, system files and data, including: .1 manage procurement, licensing and updating of chart data and system software to conform to established procedures .2 system and information updating, including the ability to update ECDIS system version in accordance with vendor's product development .3 create and maintain system configuration and backup files .4 create and maintain log files in accordance with established procedures .5 create and maintain route plan files in accordance with established procedures .6 use ECDIS log-book and track history functions for inspection of system functions, alarm settings and user responses Use ECDIS playback functionality for passage review, route planning and review of system functions	Assessment of evidence obtained from one of the following: .1 approved in-service experience .2 approved training ship experience .3 approved ECDIS simulator training	Operational procedures for using ECDIS are established, applied, and monitored Actions taken to minimize risk to safety of navigation

Table 8

Specification of minimum standard of competence for masters and chief mates on ships of 500 gross tonnage or more - Function: Navigation at the management level

IMO has also taken steps to revise and update the existing model courses 1.27 "Operational use of ECDIS" which provide guidance on the implementation of the training and assessment provisions of the amended STCW Convention and Code.

8. Conclusion

ECDIS and GNSS are giving the mariner a powerful tool to increase operational performance and safety of the route monitoring activities. Furthermore it enables the mariner to safely conduct transits in confined and crowded waters that were previously not always possible. To make this integration reliable and successful the user has to know very well the capabilities and all kind of limitations related to the information provided such as ENC and GNSS data first and other sensor data supplied (AIS, ARPA, Radar, etc.). To obtain the maximum advantage and benefit from real-time navigation with ECDIS and GNSS positioning, a different approach by the mariner is required and a specific training program that provides comprehensive instruction on safe equipment operation as well as capabilities and limitations shall be developed. This training program should use available modern, innovative instruction methodologies, including the use of simulators with integrated bridge systems, such as ECDIS, GNSS, ARPA and AIS. The accuracy of GNSS positioning and the advantages of electronic charts will be worthless without this mutual system integration. This integration must occur in order to meet the user needs, in terms of coverage, accuracy and reliability for electronic charts and accuracy, integrity, reliability and system redundancy for position fixing systems. It is for these reasons that IMO has recently amended the STCW related to the ECDIS training. During the implementation of the IMO model course for ECDIS training it is very important to highlight the importance of GNSS integrated with chart data in ECDIS. There are some specific basis for training already available (STCW, Model course, others) where is possible to properly address the correct integrated use of GNSS and ECDIS and where also future improvements can be introduced.

It is important to be aware that in some areas chart accuracy is lower than that available from GNSS. Operationally, this discrepancy in accuracy requires the mariner to be alert to the danger of placing overconfidence in his position in relation to objects critical to navigation, which are likely to be located on charts to an accuracy inconsistent with that of the GNSS. In the future of legally recognized real-time positioning in restricted waters, with enhanced GNSS and ECDIS, there is an urgent need, in some areas of the world, to revise charts to an accuracy consistent with GNSS and to common horizontal and vertical datums. International bodies such as IMO and IHO are therefore giving high priority to this issue.

Biography of the Author

Captain Rosario LA PIRA is the Head of the Survey and Production Department of the Italian HO. He is a Category A FIG/IHO Hydrographer that served for 13 years on board of various Italian Navy Ships, as Navigation Officer, Hydrographic surveyor, Executive Officer and Commanding Officer. He also served for several years on the Italian HO as Head of the Electronic Chart and Paper Chart Offices and has been actively involved in various IMO, IHO, EC and RTCM Committees and Working Groups dealing with electronic chart. He drafted the requirements for the Italian Navy ECDIS and the ECS national requirements and performance standards for the Italian pleasure and fishing boats. Recently he was employed as Professor of navigation at the Italian Naval Academy in Livorno, primarily involved in radionavigation, Electronic Chart and ship manoeuvring and as a member of the full Marine casualty or incident safety investigation board of Direzione Marittima Livorno – Italian Coastguard. He is the author of the Italian Naval Academy book "La Cartografia Elettronica".

References

1. *Introduction to IMO*, IMO web site – http:www.imo.org
2. *Annual Maritime Accidents Review*, EMSA (2009)
3. *Development of an e-Navigation strategy implementation plan - Evaluation of Availability of Electronic Navigational Chart,* doc. NAV 56/8/7 submitted by IHO to IMO Sub-Committee on Safety of Navigation (NAV), 56th session:, July 2010
4. *ESA News*, ESA Navigation web site - http://www.esa.int/esaNA/egnos.html
5. *Galileo Mission High Level Definition Document (HLD),* EU 2002
6. *La Cartografia Elettronica.* R. La Pira (2008). Poligrafico Accademia Navale, Livorno
7. *The Manila Amendments to the Seafarers' Training, Certification and Watchkeeping (STCW) Code,* IMO, Manila Conference Resolution 2, Manila, the Philippines, 21-25 June 2010
8. *International Convention for the Safety of Life at Sea,* IMO, SOLAS,1974
9. *Revised Maritime Policy and Requirements for a Future Global Navigation Satellite System (GNSS)*, IMO, Resolution A.915(22), 29 November 2001
10. *World Wide Radionavigation System*, IMO, Resolution A.953(23), 5 December 2003
11. *Revised performance standards for electronic chart display and information systems (ECDIS),* IMO, Resolution MSC.232(82), , 05 December 2006
12. *Report to the Maritime Safety Committee,* IMO Sub-Committee on Safety of Navigation (NAV), 53rd session:, August 2007

13. *IHO Specification for Chart Content and Display aspect of ECDIS*, IHO Special Publication n° 52 (IHO S-52), 5th edition, 1996, Monaco.
14. *IHO transfer Standard for digital Hydrographic data*, IHO Special Publication n° 57 (IHO S-57), edition 3.1.1, November 2000, Monaco.

Note

RENAISSANCE OF CARTOGRAPHY IN EQUATORIAL GUINEA.

By Laurent LOUVART (France)

Groupe Hydrographique de l'Atlantique (GHA) du SHOM.

Abstract

This Note refers to the different steps followed to build hydrographic capability in Equatorial Guinea. Acknowledging the intense maritime traffic in the area, the modernization of the precarious cartographic situation was a must and it was transformed in an Equatorial Guinea government challenge and ambition. France, an International Hydrographic Organization Member State, conducted hydrographic surveys and other operations with its Naval Hydrographic and Oceanographic Service (SHOM) and resurrected the cartographic activities opening an opportunity for a national sustainable hydrographic development to allow Equatorial Guinea to comply with international regulations aimed at providing information, products and services to ensure safety to navigation. It is just the start and some initiatives are still to progress.

Résumé

Cette note se réfère aux différentes étapes suivies pour la création de capacités hydrographiques en Guinée équatoriale. Compte tenu de l'intense trafic maritime de la zone, la modernisation de la situation cartographique précaire qui était indispensable est aujourd'hui devenue un défi et une ambition du gouvernement de Guinée équatoriale. La France, Etat membre de l'Organisation hydrographique internationale, a exécuté des levés hydrographiques et d'autres opérations dans le cadre de son Service hydrographique et océanographique de la Marine (SHOM) et a ressuscité les activités hydrographiques, ouvrant ainsi la voie à la possibilité d'un développement hydrographique national durable pour que la Guinée équatoriale puisse se conformer aux règles internationales visant à fournir des informations, des produits et des services en vue d'assurer la sécurité de la navigation. Ce n'est là qu'un début et d'autres initiatives doivent encore être prises.

Resumen

Esta Nota se refiere a las diferentes etapas seguidas para crear capacidad hidrografica en Guinea Ecuatorial. Siendo consciente del intenso trafico maritime en el area, la modernizacion de la precaria situacion cartografica constituyo un hecho y se transformo en un desafio y ambision del gobierno de Guinea Ecuatorial. Francia, un Estado Miembro de la Organizacion Hidrografica Internacional, llevo a cabo levantamientos hidrograficos y otras operaciones con su Servicio hidrografico y Oceanografico de la Marina (SHOM) y resucito las actividades cartograficas, abriendo una oportunidad para un desarrollo sustentable de la hidrografia en Guinea Ecuatorial a fin de cumplir con las normas internacionales tendientes a proporcionar informacion, productos y servicios que procuren seguridad de la navegacion. Es solo el comienzo y aun se debe progresar otras inicitivas.

Increasing requirements

In the maritime field, Equatorial Guinea is poised to become one of the major crossing points in Central Africa for the circulation of manufactured goods and for support for the oil industry.

At the present time traffic is estimated to be in the region of 300 000 tonnes of merchandise per year. The existing ports are close to saturation. Among the many projects under way in Equatorial Guinea, transport is currently the subject of extensive plans for modernisation. Engineering companies and equipment manufacturers are gradually replacing the insufficient, unsuitable or dilapidated constructions with new, more modern infrastructures. In this way the government is realising its maritime ambitions.

Natural assets

The volcanic landscape of the isle of Bioko and the sheer seabed naturally endow Malabo and Luba with deepwater ports, capable of accepting ships with deep draught (16 metres). Extension of the current wharves and the creation of new ones gained from the sea will enable the acceleration in goods traffic to be matched and will anticipate the imminent arrival of 3rd generation container ships with a capacity of 11000 TEU.

Fig. 1 *– Extension of the port of Malabo*

Compliance with international obligations

Alerted by the International Hydrographic Organisation (IHO) to the dilapidated nature of its charts, Equatorial Guinea has gradually become aware of the need to synchronise its cartography with its coastal developments. Especially since the stakes are high and of a diverse nature: safety of navigation, development of the coastal belt, national sovereignty, actions of the state at sea….

Fig. 2 *– In addition to endangering human life, the perils of the sea*

Although it has not yet signed up to the International Hydrographic Organisation, Equatorial Guinea has, however, signed the SOLAS (Safety Of Life At Sea) and Law of the Sea (Montego Bay) conventions. It is also a member of the International Maritime Organisation (IMO). Consequently it has an obligation to provide all of the nautical information that is essential for operating at sea in complete safety and to communicate this information to the regional maritime community.

Enlightened decisions

Development in a country like Equatorial Guinea means having up-to-date information in order to be able, in the main, to judge the relevance and cost of the work envisaged. Some shore zones would be able to accept deep-draught ships but would, for example, be too enclosed to accommodate a container port or a road network up the hills. Other regions would have sufficient space to create an airport hub, but would be disadvantaged by the regular and inexorable enlargement of the rivers that provide access to it.

The coastal strip is also the site for numerous human activities, often mutually exclusive but sometimes complementary. Only well-thought-out management of the space, and good coordination of the various parties involved, will enable collateral damage to be minimised and the necessary consensus to be achieved. A part of the enormous tourist potential of Equatorial Guinea might thus be exploited without waiting for the post-oil period.

In order to do this, there needs to be a national master scheme established long before the final decisions have to be taken, that would take account of these constraints associated with the environment. It is essential that such planning should be based on recent, accurate and detailed cartography, relying on modern technologies (space imagery, GPS positioning, multibeam echo sounders …).

Act of empowerment

Detailed knowledge of one's territory is also an act of empowerment for which the chart constitutes an indispensable tool in the practice and maintenance of sovereignty. The international maritime boundaries shown on marine charts are a physical reflection of the political, military and economic legitimacy of the actions of Equatorial Guinea at sea. The naval forces responsible for assistance at sea, protection of oil platforms, and policing fishing and the fight against illegal immigration are among the first navigators to be served.

Taking stock

The latest systematic hydrographic surveys of Equatorial Guinea date from the middle of the 1960s, before independence. A task historically undertaken by Spain, marine cartography of the waters and coast has long been abandoned in favour of activities deemed more essential for the development of the country.

Practically no hydrographic data from equipment manufacturers or oil companies have reached the Equatorial Guinea authorities. And yet information relating to ports, and the positions and movements of platforms, are essential items for the safety of navigation. No up-to-date chart of the area has been produced since the middle of the 1980s. After numerous alternations between discovery and neglect, it is now time to renovate this essential tool for the development of the country.

In 2003, a number of French experts were authorised by the IHO to help Equatorial Guinea in taking stock of these matters. Many proposals were then made to progressively update the charts. Successive deployments of French navy specialist ships chartered by SHOM (the French navy's Hydrographic and Oceanographic service) in Equatorial Guinea in 2009 and 2010 are now the most visible reflection of this.

From Land…..

The visit by the French hydrographic ship *La Pérouse* in 2009 therefore initiated a long series of work. Aerial photographs taken over the principal ports of Equatorial Guinea: Malabo, Luba and Bata, have revealed notable differences from the old maps and have enabled the land parts of the navy chart to be updated.

Fig. 3 – ***Aerial photographs of Malabo***

... to offshore

The *Laplace* took up the baton this year by conducting measurements of the seabed at those areas which are most necessary and critical for navigation. The descriptions of the buoys, lights and, more generally, all aids to maritime navigation have been checked, augmented and updated. The wharves and access channels taken by ships have been minutely explored in order to check that they are free from dangers or obstacles to navigation. All of the data acquired in this way will form the geographic reference baseline for creating future marine charts, and also for all Equatorial Guinea projects.

Fig. 4 – ***The hydrographic ship Laplace at anchor at Corisco***

Towards hydrographic autonomy

Through this work, SHOM is laying the foundation of a fruitful collaboration between France and Equatorial Guinea and resurrecting cartography activities in this region. This confirms the maritime vocation of the region that has ten times more sea area than land, and where 75% of imports and exports are made by shipping. Because of the intensification of maritime traffic and the development of new ports, the creation and development of hydrographic capabilities reporting to the port authorities is of prime importance

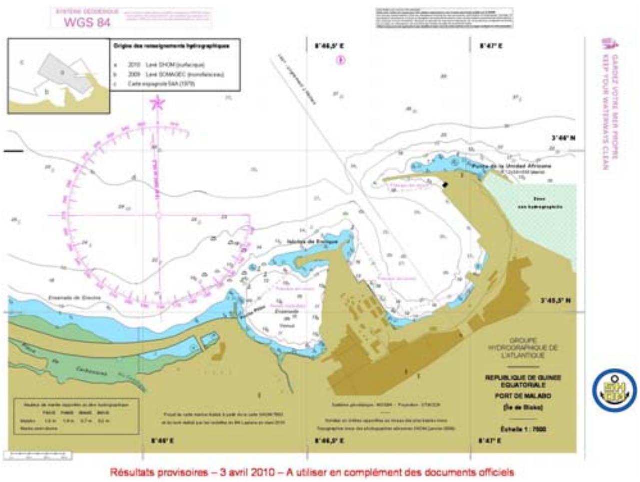

Fig. 5 – *Project for the future chart of Malabo*

In parallel with the work performed by SHOM, Equatorial Guinea might consider the creation of a national hydrographic committee, uniting the representatives of the various ministries concerned with maritime matters.

Such a committee could gather together the port authorities and the ministries for defence, the environment, fishing, transport, the merchant navy and all other organisations involved. The committee could be the focal point for centralisation and distribution of data for the maritime safety agency (RSM) and for initiating activities concerned with safety at sea. For SHOM and the IHO, the committee would provide a permanent preferred point of contact for these matters.

At the present time there is no organisation for RSM (Maritime Safety Agency) and GMSDS (Global Maritime Safety and Distress System). The current method imposes on ship captains the need to keep up-to-date personal logbooks each time that they enter territorial waters and ports, and then to pass such data among all ships. Maritime navigation is therefore based on rather unreliable methods of distributing nautical information. Equatorial Guinea must try to centralise the data and retransmit them to SHOM at Brest, coordinator for the NAVAREA II zone, extending over the eastern Atlantic (fig. 7). In turn, SHOM would redistribute the data via the INMARSAT satellites to ships passing through the zone. With regard to the distribution of coastal recommendations, a VHF radio network must be set up soon in Nigeria, and this will augment this essential facility for navigational safety.

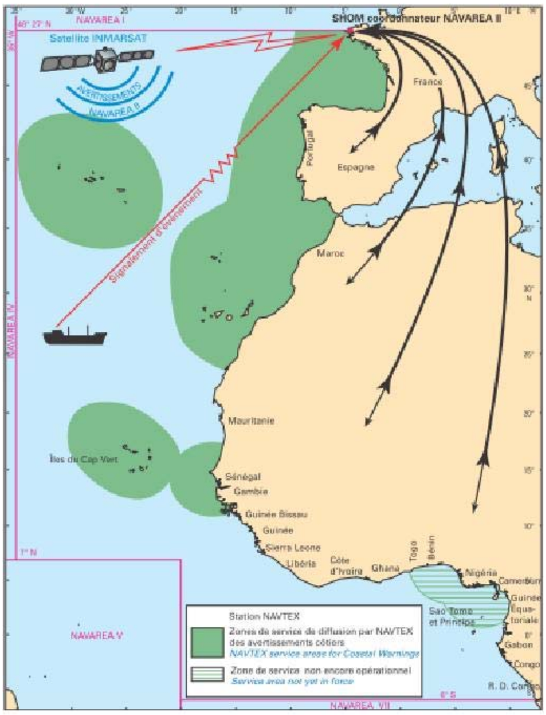

Fig. 6 –NAVAREA zone coordinated by France

France strongly encourages Equatorial Guinea to equip itself with its own hydrographic capabilities. In addition to regional collaboration with Nigeria, Cameroon and Gabon, Equatorial Guinea should proceed autonomously to collect nautical data and to group the material at a focal point charged with distributing urgent information to navigators; to generate its own marine charts and to keep them up-to-date. With the facilities at Equatorial Guinea's disposal and the willingness to do it, this objective could be achieved within a few years.

Note

TIDE ANALYSIS FROM BATHYMETRIC SOUNDINGS

A Method for Extracting Tidal Amplitude and Phase Errors from Overlapping Soundings

By Alex OSBORNE (UK)

Abstract

This paper describes a method for identifying phase and amplitude tide errors in bathymetric soundings. It is applicable to bathymetric surveys where tide is measured and then used to reduce raw soundings to datum (as opposed to absolute depth measured using kinematic GPS).

The problem of tide inaccuracy is briefly explained, along with a description of some of the key concepts which should be understood. The processing method is then explained and demonstrated using a real-world example. The optimum tide curve for this example dataset is identified based on analysis of the soundings.

Resumé

Le présent article décrit une méthode d'identification des erreurs de phase et des erreurs d'amplitude de la marée dans les sondes bathymétriques. Elle est applicable aux levés bathymétriques lorsque la marée est mesurée et sert ensuite à réduire les sondes brutes au zéro des cartes (par opposition aux profondeurs mesurées à l'aide du GPS cinématique).

Le problème de l'inexactitude de la marée est brièvement expliqué, en même temps qu'une description de certains des concepts clés qui devraient être compris. La méthode de traitement est ensuite expliquée et démontrée à l'aide d'un exemple du monde réel. La courbe de marée optimale pour l'ensemble des données de cet exemple est identifiée à partir d'une analyse des sondes.

Resumen

Este artículo describe un método para identificar errores de fase y amplitud de las mareas en las sondas batimétricas. Se aplica a los levantamientos batimétricos en los que se mide la marea, y se utiliza después para reducir las sondas sin procesar al cero hidrográfico (a diferencia de la profundidad absoluta medida usando un GPS cinemático).

Se explica brevemente el problema de la inexactitud de las mareas, junto con una descripción de algunos de los conceptos clave que deberían entenderse. El método de procesado se explica y se demuestra entonces utilizando un ejemplo del mundo real. Se identifica la curva de mareas óptima para la colección de datos de este ejemplo basándose en el análisis de las sondas.

Introduction

So-called ‘tide busts’ are a common problem during bathymetric surveys, and result from uncertainty as to the level of the tide in a given place at a particular time. This may be due to a lack of measured tide information and consequent use of predictions as a substitute. Alternatively, observed tide levels may be available but only at some distance away, leading to inaccuracies when applied to the survey area. During processing, tide error manifests itself as a difference in apparent seabed level measured in the same place at different times.

This paper describes a method developed by the author for analysing overlapping soundings in order to identify amplitude and phase errors in the tide corrections. It has only been used to date with multibeam soundings, but it seems reasonable to think that it could also be applied to singlebeam soundings, given enough overlapping data.

This method is not applicable to all situations. It requires soundings which overlap at various times during the tide cycle and are restricted to a limited geographical area (i.e. a fairly consistent tidal regime). An initial tide curve is required as a starting point. This may be a prediction or an interpolation.

Concepts

Some ideas and terms are used here which are not in mainstream usage. These are briefly described as follows.

- *Sounding group*

A group of depth soundings acquired at roughly the same time and place, which can therefore be represented by single time and depth values. Similar to gridded depth values except that multiple groups can fall within in single grid cell if the same area was crossed more than once during a survey.

- *Standard deviation matrix*

A matrix containing standard deviation values, where each represents the average of the standard deviations calculated from all individual cells in a grid. The standard deviation for each cell is calculated from the depths of the sounding groups within it. Therefore, broadly speaking the lower the number, the better the agreement between the overlapping soundings. The horizontal and vertical axes represent varying phase delay and amplitude scale factor. The lowest value in the matrix therefore represents the combination of phase delay and amplitude scale factor which results in the lowest average standard deviation across the entire grid, and therefore the minimum depth discrepancy between overlapping soundings. The concept is illustrated below in ***Figure 1***.

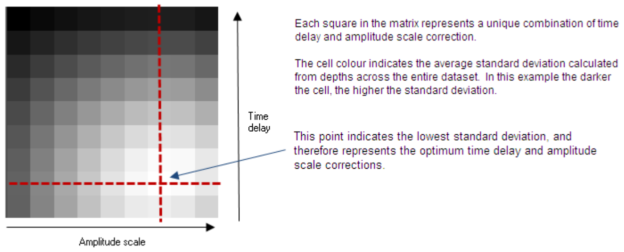

Figure 1 *- theoretical SD matrix before adjustment*

- *Cross-comparison plot*

A plot of ‘apparent tide error’ against time, where each point plotted represents the apparent depth error of a sounding group, based on a comparison against another sounding group in the same grid cell. Every sounding group is compared against every other group in the same cell, and each comparison results in two points on the cross-comparison plot. It is assumed that the error is equal i.e. if one group is a metre deeper than another, it is half a metre too deep and the other is half a metre too shallow. Although this is a slightly simplistic assumption, the trend is still visible if enough comparisons are made and plotted together.

Some other terms which are fairly basic and widely understood within the survey industry are still worth mentioning here because they are so central to the subject at hand:

- *Phase and amplitude*

Phase is a relative measure referring to the position of the tide curve on the x (time) axis. A phase shift applied to a tide curve moves it left or right. Amplitude refers to the height difference between low and high water. An amplitude scale factor applied to the tide curve has the effect of stretching it if greater than one, or compressing it if less than one. See ***Figure 2*** for an illustration.

- *Raw/reduced soundings*

Raw soundings are individual depth observations, uncorrected for tide. Reduced soundings are individual depth observations with tide subtracted, thus reduced to a vertical reference level (datum).

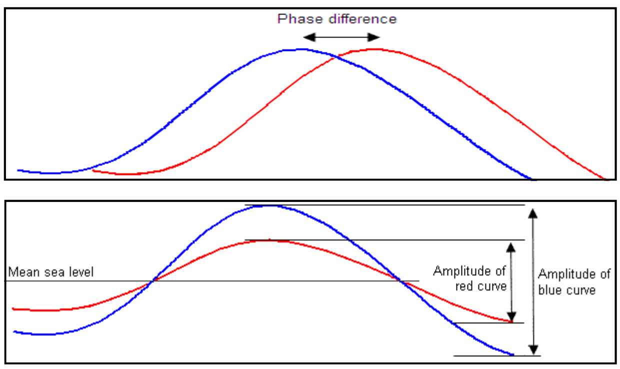

Figure 2 *-(a) Phase difference (b)- Amplitude difference*

A Note about Standard Deviation

Different measures of standard deviation are used in this analysis, depending on the purpose.

The standard deviation as calculated from *sounding groups* only represents areas of overlapping data, by definition. In areas which have been covered only by a single swath, there will rarely – if ever - be more than one sounding group in each cell, and therefore no meaningful comparison can be made. The standard deviation as calculated from *individual soundings* is calculated wherever there are multiple soundings in a grid cell.

The value calculated from sounding groups is a more pure measure of any change when tide adjustments are applied. The value calculated from individual soundings, however, is unbiased and better represents the whole dataset.

Whenever standard deviations are mentioned, it will be specified what the value actually represents.

Method

A co-tidal approach is used, based on the premise that the change in tidal regime between locations can be described in terms of phase and amplitude differences. This idea is well established and used by such authorities as the British Admiralty.

Given enough overlapping data, some number-crunching power in the form of a computer and a method that is suitably selective in its use of data in order to process it quickly and efficiently, it is possible to apply multiple phase and amplitude corrections to a dataset and analyse the results from each. When this is done systematically, and given suitable input data (i.e. meeting the criteria given above in the introduction) a pattern emerges in the standard deviations calculated from overlapping soundings recorded at different states of tide.

Processing starts by reducing the number of points to be processed, using a variation of a gridding technique. Groups of soundings are formed, whereby each group contains soundings from the same time and place (see '*Concepts*', above). The standard deviation for each cell is then calculated from the depths of each group, wherever there is more than one. The average is then calculated from the individual standard deviations, and this value is taken as being representative of the dataset as a whole.

This process is repeated multiple times, with phase delay and/or amplitude scale systematically altered each time, and applied to the tide curve. Each combination of phase delay and amplitude scale results in a unique standard deviation value. The results are then plotted as a standard deviation matrix, the lowest value of which indicates the optimum combination of phase delay and amplitude scale.

The optimum phase and amplitude corrections are applied to the tide curve. The process can then be repeated as required, with increasingly fine adjustments. When the optimum phase and amplitude have been identified and applied, the matrix will have the lowest standard deviation at its centre, as illustrated below in ***Figure 3***.

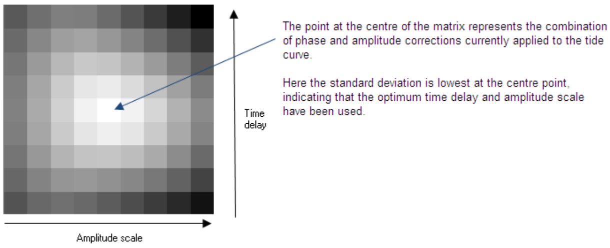

Figure 3- *theoretical SD matrix after adjustment*

Once the apparent tide phase and amplitude errors have been identified, the adjusted tide curve is used to reduce the raw soundings. The corrected soundings should exhibit less scatter than those reduced using the original tide curve.

The process is best illustrated using a real-world example.

Case study

A site survey was carried out in the Dutch sector of the North Sea in around 30m of water. Parallel survey lines were run with overlapping edges and some lines were run in a perpendicular direction, resulting in overlapping soundings which were recorded at quite different states of tide. Around thirty-four million soundings were recorded using a single-head multibeam echosounder over a period of about nine hours. Weather conditions were somewhat marginal and the effects of motion were visible in the dataset. Acquisition started and ended, coincidentally, at around low tide.

Predicted tide corrections were used for initial processing. Since the site was offshore and not particularly close to any one source of predictions, four tide curves were entered into the survey software, which used interpolation to estimate the tide height at the required place and time. There is a considerable amount of uncertainty when this sort of method is used since a simple interpolation can only be based on the assumption of linear (or at least regular) change in tide height over distance.

The tide stations in the vicinity of the survey area are listed in Table 1.

The tide stations in the vicinity of the survey area are listed in ***Table 1***.

Station	Latitude	Longitude	Distance from site (km)
Hoek van Holland	51° 59' N	4° 7' E	20
Scheveningen	52° 6' N	4° 15' E	22
Europlatform	52° N	3° 17' E	47
IJmuiden	52° 28' N	4° 35' E	58

Table 1

Analysis and Adjustment of the Original Tide Curve

The method just described was used to analyse and optimise the tide correction, using the interpolated tide curve as the starting point. An increment of 0.1 amplitude scale and 10 minutes phase delay was used to create the first standard deviation matrix shown in ***Figure 4a***. The total range covered, with four steps each way, was amplitude 0.6 to 1.4 (representing a vertical compression or stretch of 40%) and phase delay +/-40 minutes.

Given the step sizes of 10 minutes and 0.1 amplitude scale, it was not possible to be very specific at this point about the optimum correction, but it was evidently somewhere in the region of +30 minutes delay, and 0.90 scale factor. These corrections were applied and the process was repeated, this time with increments of only 2 minutes delay and 0.02 amplitude scale. After a further iteration, the second matrix shown in ***Figure 4b*** was produced, using 1 minute and 0.01 scale increments. The optimum phase and amplitude corrections are found to be +25 minutes and ×0.93, respectively.

Standard deviation is shown in centimetres for clarity due to the small numbers involved, and limited space for zeros.

Time delay (mins) \ Amplitude scale	0.6	0.7	0.8	0.9	1.0	1.1	1.2	1.3	1.4
40	12.4	9.8	7.7	7.1	8.0	9.7	11.9	14.5	17.3
30	11.9	9.0	6.4	5.0	5.6	7.4	9.9	12.7	15.7
20	12.0	9.1	6.6	5.2	5.5	7.3	9.7	12.5	15.4
10	12.7	10.2	8.4	7.7	8.0	9.4	11.5	14.0	16.8
0	13.9	12.0	11.2	11.3	11.8	12.7	14.4	16.7	19.3
-10	15.6	14.4	14.4	15.1	16.0	17.1	18.4	20.1	22.3
-20	17.6	17.2	17.8	19.0	20.3	21.8	23.3	24.9	26.6
-30	19.8	20.0	21.3	22.9	24.7	26.5	28.4	30.4	32.4
-40	22.1	22.9	24.6	26.6	28.8	31.0	33.3	35.6	38.0

Figure 4 a *- actual SD matrix before adjustment*

Time delay (mins) \ Amplitude scale	0.89	0.90	0.91	0.92	0.93	0.94	0.95	0.96	0.97
29	4.97	4.90	4.86	4.84	4.84	4.86	4.91	4.97	5.06
28	4.90	4.83	4.78	4.75	4.75	4.77	4.81	4.87	4.96
27	4.85	4.77	4.72	4.69	4.69	4.70	4.74	4.80	4.88
26	4.82	4.74	4.68	4.65	4.64	4.65	4.69	4.74	4.82
25	4.81	4.73	4.67	4.64	4.62	4.63	4.67	4.72	4.79
24	4.83	4.75	4.69	4.65	4.63	4.64	4.67	4.72	4.79
23	4.87	4.79	4.73	4.69	4.67	4.68	4.70	4.75	4.82
22	4.94	4.86	4.79	4.75	4.73	4.74	4.76	4.81	4.88
21	5.03	4.95	4.88	4.85	4.83	4.83	4.85	4.90	4.97

Figure 4 b *- actual SD matrix after adjustment.*

Based on these results, applying a phase delay of 25 minutes and an amplitude scale of 0.93 should result in a significant reduction in depth mismatches between overlapping soundings.

It would not be advisable to apply this sort of adjustment without checking carefully that it was really correct, and not just best-fitting some other non-systematic error(s) in one place whilst making things worse in another. The validity of the correction should be checked by analysing what effect it has across the entire dataset.

There are various ways in which the 'before' and 'after' cases can be compared. Four checks will be demonstrated before moving on to a comparison of results using tide curves from the different stations in the vicinity of the site.

F,igure 5 below, shows cross-comparison plots (see '*Concepts*', above) before and after tide adjustment, each with a third order polynomial trend line shown in red. The fact that the apparent error is almost symmetrical around zero in the second plot indicates that the time-varying component has been largely removed.

The plots were generated using comparisons only between sounding groups with a standard deviation below 0.2m, as calculated from the soundings within them, and a time difference of at least three hours. (Although the trend is much the same when less strict criteria are used, there is more noise.)

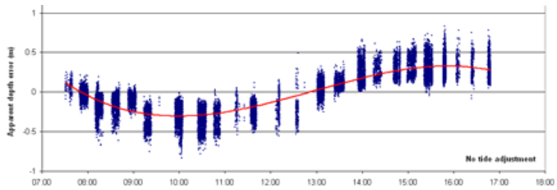

Figure 5a *- cross-comparison plot before adjustment*

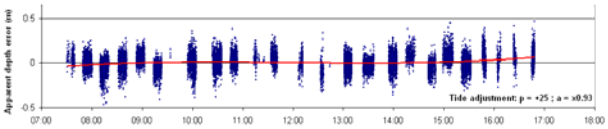

Figure 5b

Figure 6 comprises two difference plots showing the effects of the tide adjustment.

The first plot shows the change in standard deviation, calculated from all soundings within 2.5m grid cells. Green indicates a decrease in standard deviation, and therefore a reduction in depth mismatches between soundings. Red indicates the opposite. An improvement is seen across most of the survey area, which demonstrates that the tide adjustment has had the intended result.

The second plot shows change in depth. Red indicates a depth increase, and green indicates a depth decrease. The fact that there are roughly equal amounts of red and green shows that there the overall depth has not been significantly affected by the adjustment.

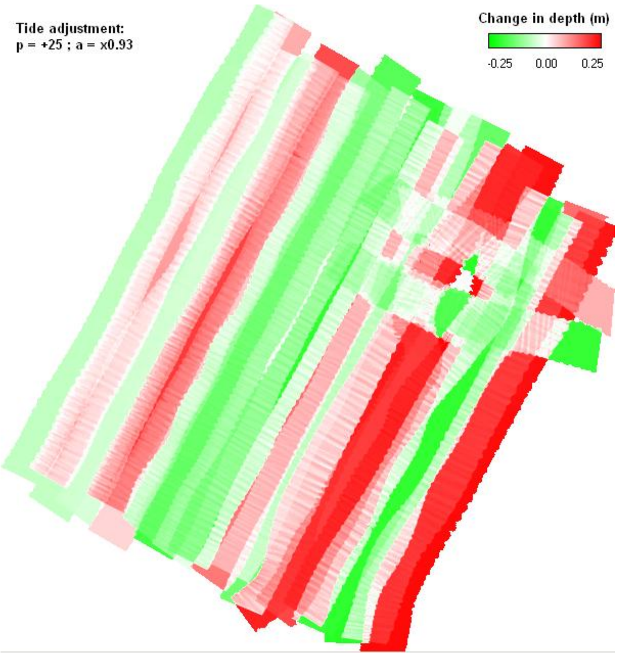

Figure 6b *- depth change*

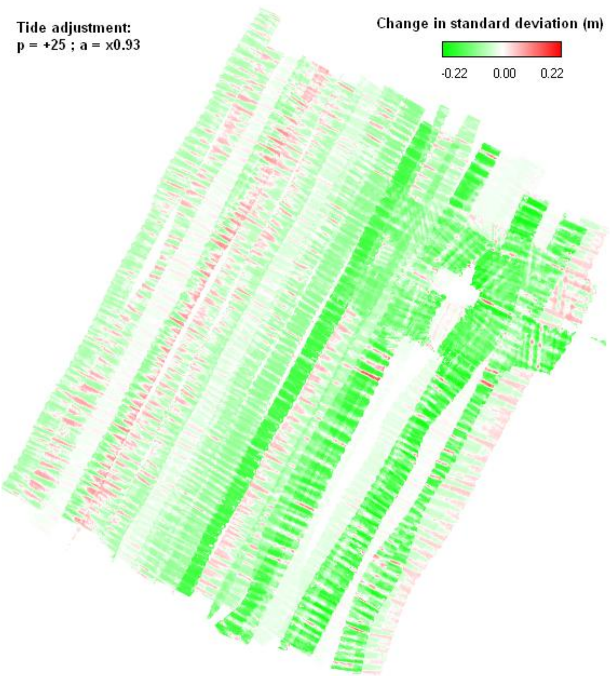

***Figure 6a**- SD change.*

A comparison of illuminated gridded bathymetry also indicates a noticeable and consistent improvement. A before/after comparison of the southern part of the site is shown in ***Figure 7***. The NNE/SSW striping is much more pronounced in the upper image. Where it remains in the lower image, this may have as much to do with increased noise at the swath edges as with tide error.

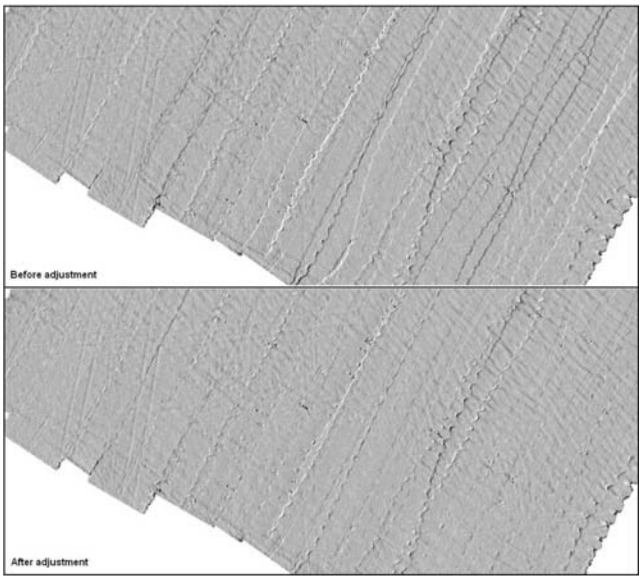

Figure 7 *- illuminated bathymetry.*

Comparison of Available Tide Curves

Having hopefully optimised the tidal corrections using the original interpolated tide curve as a starting point, the question remains as to how any of the predicted tide curves from the four closest stations, without any interpolation, would compare.

To investigate this, the same process as was used for the original tide curve was repeated in turn for each of the individual tide stations, yielding results summarised below in ***Table 2.*** Standard deviations are shown for sounding groups and individual soundings, since both are relevant and results may differ. Note that phase adjustments are given in terms of phase delay, so a negative number indicates a shift to the left on the time axis.

Station	Phase delay (minutes)	Amplitude scale	Standard deviation (from sounding groups)[1]		Standard deviation (from individual soundings)[2]	
			Before	After	Before	After
Original interpolation	+25	0.93	0.111	0.046	0.125	0.087
Hoek van Holland	-3	0.95	0.048	0.044	0.088	0.086
Scheveningen	-21	0.92	0.099	0.047	0.118	0.087
Europlatform	+63	1.15	0.224	0.056	0.209	0.091
IJmuiden	-75	1.04	0.222	0.057	0.208	0.093

It is clear from this comparison that the tide curve from Hoek van Holland is the best on all counts. It requires less adjustment than any of the others to produce a best fit. Furthermore, it results in the lowest standard deviations both before and after adjustment. Although this might not have been originally anticipated, the tide from Hoek van Holland appears to match the actual tide at the site better than the interpolation used originally.

The histograms shown in ***Figure 8*** bear this out. Europlatform and IJmuiden have not been included here since the statistics indicate that the degree of fit from these curves is noticeably worse than the other three. They are also significantly further from the site than Hoek van Holland and Scheveningen. Standard deviation as shown in the histograms is calculated from all soundings in 2.5m grid cells.

When an illuminated plot of the gridded soundings as reduced using the adjusted Hoek van Holland tide is compared with the equivalent plot using the adjusted interpolation, there is a visible improvement in one area of the site, where striping is slightly reduced. This will not be demonstrated here as a side-by-side comparison of illuminated bathymetry since the difference is very subtle and may not be visible in a reproduced image. The end result is that using the adjusted Hoek van Holland tide curve does appear from a visual inspection to produce the best result.
The adjusted Hoek van Holland tide curve, as found to best fit the data, is shown below in ***Figure 9*** along with the interpolation which was used originally.

[1] From sounding groups within 5m grid cells
[2] From all soundings within 2.5m grid cells

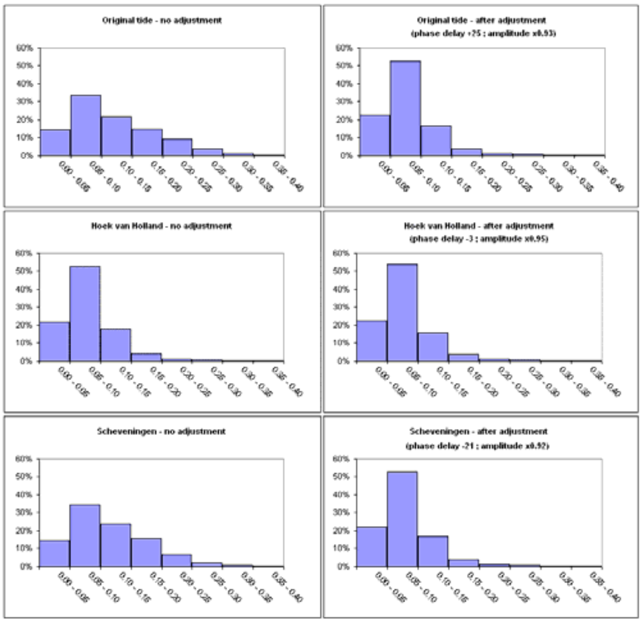

Figure 8 *- histograms showing frequency distribution of standard deviations from three sets of tidal corrections.*

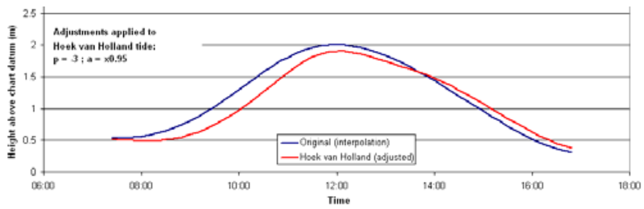

Figure 9 *- comparison of original and optimised tide* curves.

Conclusions

It has been demonstrated that it is possible to measure apparent phase and amplitude errors from overlapping bathymetric soundings, given suitable source data. Correcting the observed errors can significantly reduce depth discrepancies in the reduced soundings.
As well as improving the appearance (and hopefully absolute accuracy) of the final product, a useful insight can be gained into the actual tidal regime at the survey location. At the site shown in the example, the tide curve from Hoek van Holland was found to fit the soundings significantly better than any other that was tried. This would not have been apparent or expected based purely on proximity, since the site is roughly equidistant from Hoek van Holland and Scheveningen.

Biography of the Author

Alex Osborne, BSc (Hons), MSc graduated from Plymouth University in 2000 with an MSc in Hydrography and works worldwide as a freelance hydrographic surveyor, mainly on offshore projects.
(alexosbornesurvey@gmail.com)

Page intentionally left blank